A Role for Sirtuins in Maintaining Mammalian Lifespan and Healthspan

by

William J. Giblin, Jr.

A dissertation submitted in partial fulfillment
of the requirements for the degree of
Doctor of Philosophy
(Human Genetics)
in the University of Michigan
2017

Doctoral Committee:

Associate Professor David B. Lombard, Co-Chair
Associate Professor JoAnn M. Sekiguchi, Co-Chair
Associate Professor Yali Dou
Assistant Professor Shigeki Iwase
Associate Professor Sundeep Kalantry

William J. Giblin, Jr.

wgiblin@umich.edu

ORCID iD: 0000-0001-5247-7802

DEDICATION

I dedicate this thesis to Sgt. Timothy R. Giblin and Roy E. Wareham. Thank you for your strength and sacrifice.

ACKNOWLEDGEMENTS

I have many people to thank who have helped and supported me during my graduate career. First, I'd like to thank my thesis advisor, Dr. David Lombard. Dave is a great mentor, and I have felt he has always treated me as colleague. He has great optimism and is always excited about almost every result, big or small, positive or negative – you can learn from every experiment. This was a nice counter to my less-than-optimistic perspective on many experiments I've presented at lab meetings. Dave has also been invested in my career development, in that he would always arrange for me to meet, host, or lunch with the many, many speakers he has invited to the university, which allowed me to network, but also to gain outside perspective about my research. Second, I'd like to thank my second committee co-chair, Dr. JoAnn Sekiguchi. I have known JoAnn for several years, and when I'm complimented on my technical capabilities at the research bench, I often credit her, as she was my first mentor in an academic research lab. Her mentorship laid the groundwork for me to be able to become an independent research scientist.

I also want to thank the other members of my thesis committee, Dr. Yali Dou, Dr. Shigeki Iwase, and Dr. Sundeep Kalantry for their useful suggestions, patience, support and at times, collaborations during these years. I would also like to acknowledge the Human Genetics faculty and administrative staff, in particular, Karen Grahl, who is the

first point of contact when students have a problem or issue, and Susan Kellogg for all her help. I also thank Reynetta Fath, who organizes the Geriatrics Seminars and Symposia. I also must thank the entire Lombard lab, past and present for your friendship, support and tolerance. I would like to specifically thank a very talented undergraduate, Michelle Azar, who has worked with me since I started my work in the Lombard lab, and will be attending graduate school next year.

I have made many, many friends during my extended stay in Michigan. I'd like to thank all of you, in no particular order: Sandy, Jennie, Cheryl, Scout, Betsy, Chris, Huira, Mary, Andrew, Carie, Brain, Lauren, Gonzalo, Matt, Adam, Heather, Nicole, Surinder, Martina, Donna, Mike, Tamar, Andrej, Kylie, Bernadette, Ali, Michelle, Jessica, Angela, Emmalee, Bebo, Haya, and probably others (sorry). Thanks for your support.

I also must thank my family. I have a very large extended family, so suffice it to say, thank you for your love and support.

I am grateful for my funding throughout the years as well. I have been supported by the Human Genetics Training Grant T32-GM07544, the Biomedical Research Training in the Biology of Aging Award T32-AG000114, and the Rackham Merit Fellowship.

TABLE OF CONTENTS

LIST OF FIGURES

LIST OF TABLES

LIST OF ABBREVIATIONS

AD, Alzheimer's disease; **ADP-ribosyltransferase**, adenosine diphosphate ribosyltransferase; **AMPK**, 5' adenosine monophosphate-activated protein kinase; **APC**, adenomatous polyposis coli; **aPKC**, atypical protein kinase C; **APOE**, apolipoprotein E ; **ARNTL**, aryl hydrocarbon receptor nuclear translocator-like; **ATP**, adenosine triphosphate; **BAT**, brown adipose tissue; **BER**, base excision repair; **BMAL1**, ARNTL; **BRASTO**, brain-specific SIRT1-overexpressing; **BRCA1**, breast cancer 1; **BSA**, bovine serum albumin; **cDNA**, complementary DNA; **CaMKKβ** Ca^{2+}/calmodulin-dependent protein kinase kinase; **CH**, cardiac hypertrophy; **ChIP**, chromatin immunoprecipitation; **CLOCK**, circadian locomotor output cycles kaput; **CNS**, central nervous system; **CPS1**, carbamoyl phosphate synthetase 1; **CR**, calorie restriction, caloric restriction or restricted; **CtIP**, C-terminal binding protein (CtBP)-interacting protein; **CVD**, cardiovascular disease**; DCFDA**, dichlorofluorescin diacetate; **DMEM**, Dulbecco's modified eagle medium; **DMH/LH**, dorsomedial and lateral hypothalamic nuclei; **DNA**, deoxyribonucleic acid; **DNA-PKcs**, DNA-dependent protein kinase catalytic subunit; **DSB**, double strand break; **DTT**, dithiothreitol; **ECM**, extracellular matrix; **EDTA**, ethylenediaminetetraacetic acid; **EGTA**, ethylene glycol-bis(β-aminoethyl ether)-N,N,N',N'-tetraacetic acid; **ERK**, extracellular signal-regulated kinase; **ES cell**, embryonic stem cell; **FACS**, fluorescent activated cell sorter; **FACT**, facilitates

chromatin transcription; **FBS**, fetal bovine serum; **FITC**, fluorescein isothiocyanate; **FOXO**, forkhead box protein O; **GLUT**, glucose transporter; **GCN5 (KAT2A)**, general control nonrepressed protein 5 (lysine acetyltransferase 2A); **GDH**, glutamate dehydrogenase; **H#K#Ac**, Histone # lysine # acetylation; **HD**, Huntington's disease; **HFD**, high-fat diet; **HIF-1α**, hypoxia-inducible factor 1 alpha; **HMGCS2**, 3-hydroxy-3-methylglutaryl CoA synthase 2; **HSCs**, hematopoietic stem cells; **HSP70**, heat shock protein 70; **H&E**, heamatoxylin and eosin; **H_2O_2**, hydrogen peroxide; **HAT**, histone acetyltransferase; **HDAC**, histone deacetylase; **HMGB1**, high-mobility group protein B1; **HP1**, heterochromatin protein 1; **HR**, homologous recombination; **HREs**, responsive elements; **IDH2**, isocitrate dehydrogenase 2; **IGF-1**, insulin-like growth factor-1; **IIS**, insulin and IGF-1 signaling; **IHC**, immunohistochemistry; **iMEF**, immortalized MEF; **IP**, immunoprecipitation; **KAP1**, KRAB-associated protein 1; **KD**, knockdown; **KO**, knockout; **LDHA**, lactate dehydrogenase A; **LDL**, low density lipoprotein; **LIF**, leukemia inhibitory factor; **LINE-1**, long interspersed nuclear element-1; **LFS**, Li-Fraumeni syndrome; **MBP**, myelin basic protein; **MCD**, malonyl-CoA decarboxylase; **MDM2**, mouse double minute 2 homolog; **MMP**, matrix metalloproteinase; **mtDNA**, mitochondrial DNA; **mTOR**, mechanistic target of rapamycin; **mTORC1**, mechanistic target of rapamycin complex 1; **MEF**, mouse embryonic fibroblast; **mRNA**, messenger RNA; **MSR**, major satellite repeat; **NAC**, N-acteyl cysteine; **NK cells**, natural killer cells; **NLS**, nuclear localization signal; **NRF1**, nuclear respiratory factor 1; **NAD^+**, nicotinamide adenine dinucleotide; **NADPH**, nicotinamide adenine dinucleotide phosphate; **NAM**, nicotinamide; **NAMPT**, nicotinamide phosphoribosyltransferase; **NF-κB**, nuclear factor kappa-light-chain-enhancer of activated B cells; **NICD**, NOTCH intracellular domain;

NMN, nicotinamide mononucleotide; **NR**, nicotinamide riboside; **OD**, optical density; **OE**, overexpression; **OSCC**, oral squamous cell carcinoma; **OTC**, ornithine transcarbamoylase; **PAR3**, partitioning defective 3; **PARP1**, poly[ADP-ribose] polymerase 1; **PBS**, phosphate buffered saline; **PCR**, polymerase chain reaction; **PDC**, pyruvate dehydrogenase complex; **PDH**, phosphate dehydrogenase; **PDK1**, pyruvate dehydrogenase kinase 1; **PDP1**, pyruvate dehydrogenase phosphatase catalytic unit 1; **PFA**, paraformaldehyde; **PFK1**, phosphofructokinase 1; **PMSF**, phenylmethylsulfonyl fluoride; **PVDF**, polyvinyl difluoride; **PD**, Parkinson's disease; **PDC**, pyruvate dehydrogenase complex; **PDK1**, 3-phosphoinositide dependent protein kinase-1; **PEPCK**, phosphoenolpyruvate carboxykinase; **PER2**, period circadian protein homolog 2; **PGC-1α**, PPARγ coactivator 1 alpha; **PPARα**, peroxisome proliferator-activated receptor alpha; **PPARγ**, peroxisome proliferator-activated receptor gamma; **PS**, pulsatile shear; **PTM**, post-translational modification; **RARβ**, retinoic acid receptor beta; **rDNA**, ribosomal DNA; **RNA**, ribonucleic acid; **rRNA**, ribosomal RNA; **RT-PCR**, real-time polymerase chain reaction **rDNA**, ribosomal DNA; **RELA/p65**, V-rel avian reticuloendotheliosis viral oncogene homolog A; **ROS**, reactive oxygen species; **RSV**, resveratrol; **SCN**, suprachiasmatic nucleus; **SCID**, severe combined immunodeficiency; **SD**, standard deviation; **SDS**, sodium dodecyl sulfate; **SEM**, standard error of the mean; **shRNA**, short hairpin RNA; **siRNA**, small interfering RNA; **SSC**, saline-sodium citrate; **ssDNA**, single strand DNA; **SSRP1**, structure specific recognition protein 1; **SIR**, silent information regulator; **SIRT**, sirtuin; **SNP**, single nucleotide polymorphism; **SOD1**, superoxide dismutase 1; **SOD2**, superoxide dismutase 2; **SREBPs**, sterol regulatory element-binding proteins; **STACs**, sirtuin-activating compounds; **TBS**, tris-buffered

saline; **TCA**, tricarboxyl acid; **TEB**, triton extraction buffer; **TF**, transcription factor; **TPE**, telomere position effect; **TSA**, trichostatin A; **T2D**, type 2 diabetes; **TCA**, tricarboxylic acid cycle; **TFAM**, transcription factor A, mitochondrial; **TNFα**, tumor necrosis factor alpha; **TR4**, testicular receptor 4; **TSC2**, tuberous sclerosis complex 2; **UTP**, uridine 5'-triphosphate; **UTR**, untranslated region; **UV**, ultraviolet; **VHL**, von Hippel-Lindau; **WCE**, whole cell extract; **WT**, wild type**; UCP2**, uncoupling protein 2; **WAT**, white adipose tissue; **XPA**, xeroderma pigmentosum group A

ABSTRACT

A Role for Sirtuins in Maintaining Mammalian Lifespan and Healthspan

by

William J. Giblin, Jr.

Epigenetic alterations are a conserved feature of biological aging in diverse organisms, and have been designated as a “hallmark of aging”. Chromatin organization – in particular, diminished heterochromatinization of repetitive regions – is progressively lost during cellular and organismal aging. Experimentally, work in *S. cerevisiae* has revealed an age-associated loss of chromatin structure, and elucidated its deleterious impacts on gene expression and genomic stability. The first example of age-associated heterochromatin perturbation in mammals was identified in a seminal study 25 years ago. This work focused on the Major Satellite Repeats (MSRs), pericentromeric repeats in the mouse that ensure proper chromosomal segregation and maintenance of euploidy. This study showed that MSR repression is lost during aging specifically in mouse myocardium. The mechanistic basis for this effect has never been elucidated.

I have found that MSR derepression is not associated with decreases in levels of the canonical repressive marks – DNA methylation, H3K9me3, or H3K56me3 – at the

MSRs. Instead, levels of the activating marks, acH3K9 and acH4K16, targets of the SIRT1 deacetylase, increase during aging in the heart. These findings have led to the hypothesis that loss of SIRT1 activity contributes to derepression of MSR loci in aged myocardium. Consistent with this hypothesis, I have found that *Sirt1* deletion results in increased MSR expression in heart tissue. I then present data that suggests that SIRT1 activity maintains chromatin structure and transcriptional silencing at the MSRs, using aged muscle-specific SIRT1 overexpressors.

Melanoma is the most lethal skin cancer, with an estimated 73,870 new melanoma cases occurring in the US in 2015. I have found that SIRT5 is critical in melanoma cell survival. SIRT5 removes succinyl, malonyl, and glutaryl modifications from lysines on diverse protein targets, primarily in the mitochondrial matrix, thereby regulating multiple metabolic pathways. In 10/10 human melanoma cell lines tested, SIRT5 knockdown resulted in rapid loss of proliferative potential and cell death. Likewise, I have found that SIRT5 loss impeded melanoma xenograft formation in mice, and SIRT5 knockdown results in increased apoptotic cell death, which can be partially rescued by overexpressing anti-apoptotic BCL2. Lastly, via metabolomics, SIRT5 regulates glucose and glutamine metabolism in melanoma.

CHAPTER 1

Sirtuins as Guardians of Mammalian Lifespan and Healthspan

Abstract

The seven mammalian sirtuins (SIRT1-SIRT7) are NAD^+-dependent enzymes involved in a broad range of cellular pathways relevant to energy metabolism, cellular stress responses, genomic stability, and tumorigenesis. While SIRT1 has been at the forefront of sirtuin research, functional insights regarding SIRT2-SIRT7 are rapidly accumulating. There is now a large literature demonstrating that mammalian sirtuins suppress a variety of age-associated pathologies to promote healthspan. Also, new evidence reveals that increased expression of SIRT1 or SIRT6 extends mouse lifespan. Pharmacologic targeting of sirtuins – either directly with specific activators, or indirectly with interventions to boost cellular NAD^+ levels – has been proposed as one means of treating or preventing age-associated disease. In this chapter, I summarize the interactions between sirtuins and the common diseases of aging, such as cardiovascular disease and cancer.

Introduction

Until recently, a common point of view emerging from evolutionary biology was that aging was much too complex a phenomenon to be amenable to simple genetic or pharmacologic intervention. Proof that eukaryotes possess regulatory pathways that profoundly influence lifespan emerged when it was shown, initially in *C. elegans* but then in other invertebrates and subsequently in mice, that single gene alterations can dramatically extend lifespan (Guarente and Kenyon, 2000). A large body of evidence generated in model organisms has now conclusively shown that modulation of specific signaling pathways – e.g. insulin/insulin-like growth factor-1 (IGF-1) signaling (IIS), mechanistic target of rapamycin (mTOR), and sirtuins – can extend lifespan in a manner that is conserved across distantly-related organisms (Lopez-Otin et al., 2013). In mammals, the aging process can be slowed by interventions that concomitantly reduce the onset and pace of degenerative, neoplastic, metabolic and other age-related diseases (Lombard and Miller, 2014). Thus, these interventions not only extend lifespan, but more importantly, prolong healthspan, defined as the period of life free from major disease (Gems, 2011). Therefore, a deep understanding of these pathways and how they regulate the aging process may permit development of therapeutics with beneficial effects against a wide spectrum of age-associated degenerative diseases.

This chapter focuses on the evolutionarily conserved sirtuin genes, and discusses their ability to affect mammalian healthspan and lifespan. As a consequence of their NAD^+

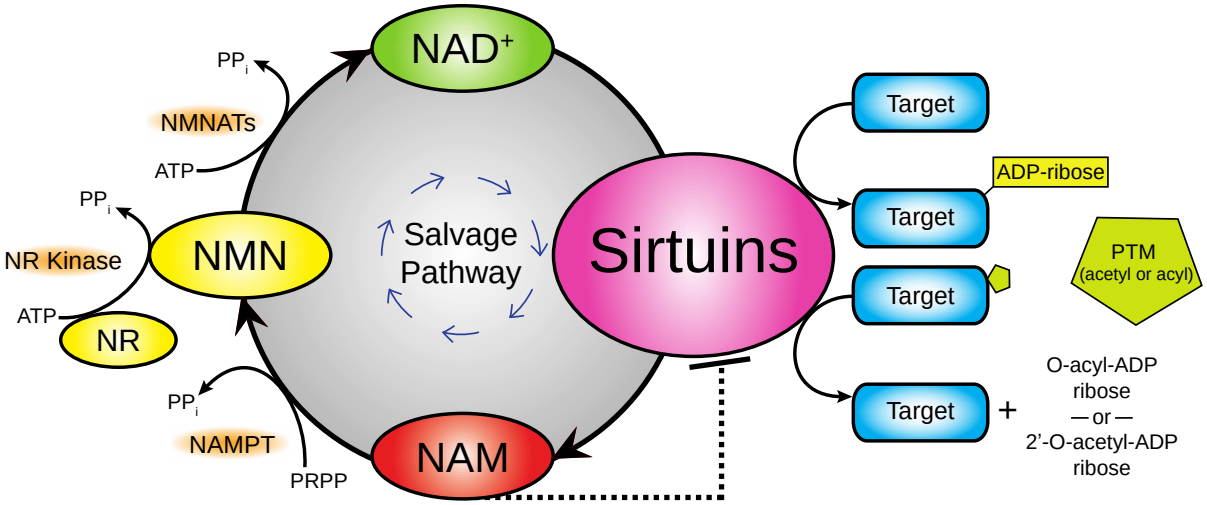

Figure 1.1 Sirtuins are NAD$^+$ dependent enzymes. The salvage pathway uses ATP to convert NMN back to NAD$^+$ via the catalytic activity of nicotinamide mononucleotide adenylyltransferases (NMNATs). Sirtuin activity consumes nicotinamide adenine dinucleotide (NAD$^+$) and produces downstream effectors that are involved in diverse cellular pathways. Products of the deacetylase (or deacylase) reaction are indicated. Nicotinamide (NAM) is a by-product of the reaction and is a non-competitive sirtuin inhibitor. Nicotinamide phosphoribosyltransferase (NAMPT) converts NAM into the NAD$^+$ precursor nicotinamide mononucleotide (NMN). NR, nicotinamide riboside; ADP-ribose, adenosine diphosphate ribose; PTM, post-translational modification.

dependence, sirtuins have evolved as sensors and responders to environmental stressors to modulate diverse cellular processes such as genome maintenance, cell proliferation, and energy expenditure and storage (Figure 1.1).

Sirtuin-driven Lifespan Extension in Invertebrates

SIR2 was first identified in yeast as a gene whose loss-of-function conferred meiotic sterility, due to loss of transcriptional repression of the silent mating-type loci (Klar et al., 1979). Subsequent screens in yeast also identified *SIR2* and other phenotypically similar mutants, which have come to define the four yeast *SIR* genes (Haber and

George, 1979; Rine and Herskowitz, 1987; Rine et al., 1979; Shore et al., 1984). These enzymes comprise the SIR complex that maintains transcriptional silencing at the mating-type loci, telomeres, and the ribosomal DNA (rDNA) arrays (Kueng et al., 2013). Sir2p, an NAD^+-dependent histone deacetylase (HDAC) (Imai et al., 2000), is the only yeast Sir protein whose activity is required for silencing at all three of these loci, while the other *SIR* genes are critical for silencing only at mating-type loci and telomeres.

Initial studies revealed that a specific mutation in one of the *S. cerevisiae SIR* genes, *Sir4-4.2,* increases replicative lifespan, defined as the number of times an individual yeast mother cell divides (Kennedy et al., 1995). Later work showed that this mutation allows relocalization of the SIR complex (containing SIR2, SIR3, and SIR4) from telomeres to the nucleolar rDNA (Kennedy et al., 1997). This focused attention on the only evolutionarily conserved member of this complex, *SIR2*. Modest *SIR2* overexpression on its own increases replicative lifespan in yeast by 30%, whereas *sir2* deletion shortens it by 50% (Kaeberlein et al., 1999). Initial investigation into the mechanism of this pro-longevity effect revealed that Sir2p protects yeast cells from a toxic accumulation of self-replicating extrachromosomal rDNA circles (ERCs) (Kaeberlein et al., 1999; Sinclair and Guarente, 1997). Deleting the gene encoding the replication fork-blocking protein, Fob1p, enhances replicative lifespan by attenuating recombination at the rDNA arrays (Defossez et al., 1999; Kaeberlein et al., 1999). This rescues the shortened lifespan of Sir2p-deficient yeast cells.

Data from subsequent studies suggest that additional distinct mechanisms by which Sir2p contributes to yeast replicative lifespan may exist. For example, Sir2p facilitates asymmetrical partitioning of oxidized proteins, misfolded protein aggregates, and dysfunctional mitochondria by maintaining the polarity machinery responsible for retention of damaged macromolecules in mother cells (Higuchi et al., 2013; Liu et al., 2010). Sir2p may also promote yeast replicative lifespan through an epigenetic mechanism involving the heterochromatic regions adjacent to telomeres. At the telomere-euchromatin boundary, Sir2p opposes the activity of the Sas2p histone acetyltransferase to maintain silencing, by regulating histone H4 lysine 16 acetylation (H4K16Ac) (Suka et al., 2002). Derepression of subtelomeric silencing via a mutation mimicking constitutive H4K16 acetylation reduces yeast lifespan (Dang et al., 2009). Indeed, Sir2p expression levels steadily decline over the yeast lifespan, concomitant with an increase in H4K16Ac. Altogether, these studies have cast Sir2p in multiple, distinct roles in promoting yeast replicative lifespan: first, by stabilizing the rDNA array; second, by protecting daughter cells from inheriting damaged proteins and dysfunctional mitochondria; and third, by maintaining transcriptional silencing at subtelomeric regions.

Chromatin organization – in particular, diminished heterochromatinization of repetitive regions – is progressively lost during cellular and organismal aging. Experimentally, work in *S. cerevisiae* has revealed an age-associated loss of chromatin structure, and elucidated its deleterious impacts on gene expression and genomic stability. These studies prompted investigations into whether *SIR2*-like genes exist and show analogous functions in higher eukaryotes. For example, in mice, pericentromeric heterochromatin,

comprising of major satellite repeat (MSR) sequences that help to ensure proper chromosomal segregation and maintenance of euploidy, remains transcriptionally silent. Mammalian SIRT1 and H1K26ac, a SIRT1 target, has been implicated in maintaining MSR silencing (Oberdoerffer et al., 2008). According to this model, tested in mouse stem cells, increased DNA damage causes SIRT1 to relocalize from MSR loci to the damaged sites to facilitate repair, which allows transcription within the MSR regions. Over 25 years ago, a seminal study, focused on MSRs silencing, identified the first example of age-associated heterochromatin perturbation in mammals (Gaubatz and Cutler, 1990). This study showed that MSR repression is lost during aging specifically in mouse myocardium. The mechanistic basis for this effect has never been elucidated.

SIR2 homologues have been identified in diverse species, and are present in both eukaryotes and prokaryotes. Collectively, these Sir2p-like proteins are termed sirtuins, and are of ancient evolutionary origin (Frye, 2000). *Caenorhabditis elegans* and *Drosophila melanogaster* have been used as experimental tools to elucidate the roles sirtuins may play in promoting longevity and to some extent disease susceptibility in multicellular organisms. The *C. elegans* genome encodes four sirtuin genes, *SIR-2.1* though *SIR-2.4,* that are homologous to mammalian SIRT1 (SIR-2.1), SIRT4 (SIR-2.2/2.3) and SIRT6/SIRT7 (SIR-2.4) (Frye, 2000). Overexpression of the SIRT1 homologue, SIR-2.1, modestly extends mean lifespan in worms (by 10-15%), an effect that is dependent upon DAF-16. DAF-16 is the single worm forkhead box O (FOXO) transcription factor homologue, a major target of the IIS cascade (Berdichevsky et al., 2006; Mouchiroud et al., 2013; Rizki et al., 2011; Tissenbaum and Guarente, 2001,

2002; Viswanathan and Guarente, 2011). Independent of IIS signaling through DAF-16, pure synthetic ascaroside administration increases worm lifespan and stress resistance in a SIR-2.1-dependent manner. *C. elegans* ascarosides are secreted molecules that control developmental timing and various social behaviors in this organism. Inhibition of sensory neurons abolishes this phenotype, linking sensing of endogenous small molecules to sirtuin-dependent longevity and stress resistance (Ludewig et al., 2013). Also, studies of the *C. elegans* SIRT6/SIRT7 homologue SIR-2.4 have revealed that this protein promotes DAF-16 function in response to stress, and is required for resistance to cellular dysfunction induced by expression of a poly-glutamine tract-containing protein (Chiang et al., 2012).

The *Drosophila melanogaster* genome encodes five sirtuins, corresponding to mammalian SIRT1 (dSir2), SIRT2, SIRT4 SIRT6, and SIRT7 (Frye, 2000). Overexpression of dSIR2, in the nervous system, the fat body or whole organism increases longevity (Banerjee et al., 2012; Hoffmann et al., 2013; Rogina and Helfand, 2004). Importantly, one prominent report could not reproduce the pro-longevity effects of either *C. elegans* or *D. melanogaster* sirtuins (Burnett et al., 2011). Differing husbandry conditions and/or genetic backgrounds may explain the discrepancies between laboratories.

Sirtuin Enzymatic Activity

Mammalian sirtuins have varied enzymatic activities, working as NAD^+-dependent deacetylases/deacylases (SIRT1, SIRT2, SIRT3, SIRT5, SIRT6, SIRT7), and ADP-ribosyltransferases (SIRT4, SIRT6) (Figure 1.1). They function as cellular stress sensors to modify histones and a plethora of other proteins – including transcription factors – to modulate diverse cellular processes (Imai et al., 2000; Jiang et al., 2013; Lin et al., 2009). Although the seven mammalian sirtuins share a fairly conserved NAD^+-binding catalytic domain, the amino and carboxy regions that flank this domain are highly divergent. Sirtuins differ in expression pattern, catalytic activity, biological function and subcellular localization (Figure 1.2, Table 1.1), residing predominantly in the nucleus (SIRT1, SIRT6, and SIRT7), cytosol (SIRT2), or mitochondrial matrix (SIRT3, SIRT4, and SIRT5) (Canto et al., 2013). Among the mammalian sirtuins, only SIRT6 and SIRT7 are homologous to one another across their entire coding sequences (Frye, 2000). In this section we briefly review the salient enzymatic features of each sirtuin and the subcellular context in which they reside.

The best-characterized sirtuin, SIRT1, deacetylates a variety of proteins to modulate many cellular processes such as metabolism and cellular stress responses (Rahman and Islam, 2011). SIRT1 also possesses deacylase activity *in vitro*, though the *in vivo* significance of this activity is not known (Feldman et al., 2013). SIRT1 possesses two nuclear export and two nuclear localization signals, allowing it to translocate to the cytosol in certain transformed cell lines (Byles et al., 2010; Jin et al., 2007), adult cardiomyocytes (Tanno et al., 2007) and neurons (Hisahara et al., 2008; Li et al., 2008); however, the biological relevance of this shuttling is not fully understood

.Cytosolic SIRT2 deacetylates α-tubulin and has been found in the nucleus during the mitotic G2/M transition, where it localizes to chromatin and deacetylates H4K16Ac (Vaquero et al., 2006). In this regard, SIRT2 has been identified as a regulator of mitotic exit in mammalian cells (Harting and Knoll, 2010). Also, SIRT2 deacetylase activity regulates chromatin dynamics and gene expression, by opposing autoacetylation of the histone acetyltransferase p300 *in vivo* (Black et al., 2008). SIRT2 also activates the NADPH-generating enzyme, glucose-6-phosphate dehydrogenase (G6PD) by deacetylating lysine 403, which lies within its $NADP^+$ binding domain (Wang et al., 2014).

Sirtuin	Subcellular localization	Enzymatic Acitivity	Confirmed Histone Substrates	Examples of Major Nonhistone Interactors and Substrates
1	**Nuclear** / Cytoplasmic	Deacetylase	H1K26, H3K9, H3K14, H4K16	p300, SUV39H1, EZH2, p53, FOXOs, NF-kB, c-Fos, c-Jun, c-MYC, HIF-1a, Ku70, NBS1, PARP1, PGC-1a, many others
2	Nuclear / **Cytosolic**	Deacetylase	H3K56, H4K16	TUBA, PEPCK1, FOXOs, PAR3, p300, p53, p65, NF-kB, c-MYC, CDH1, CDC20, PGC-1a
3	**Mitochondrial**	Deacetylase	--	LCAD, HMGCS2, SOD2, IDH2, p53, Ku70, ACS2, ALDH2, NDUFA9 SDHA, GDH, many others
4	**Mitochondrial**	Deacetylase / ADP-ribosyltransferase	--	MCD, GDH, IDE, ANT2, ANT3
5	**Mitochondrial** /Cytosolic	Deacetylase (?) / Demalonylase / Desuccinylase / Deglutarylase	--	CPS1, HMGCS2, SOD1, PDC, SDH, many others
6	**Nuclear Chromatin** / Cytoplasmic	Deacetylase / Deacylase / ADP-ribosyltransferase	H3K9, H3K56	c-MYC, CtIP, GCN5, c-Jun, DNA-PK, PARP, HIF-1a, TNFa
7	**Nucleolar**	Deacetylase	H3K18	c-MYC, p53, GABPb1

Table 1.1 Sirtuin subcellular localization, enzymatic activities and known histone substrates. Also, examples of major non-histone interacting partners or substrates are indicated:

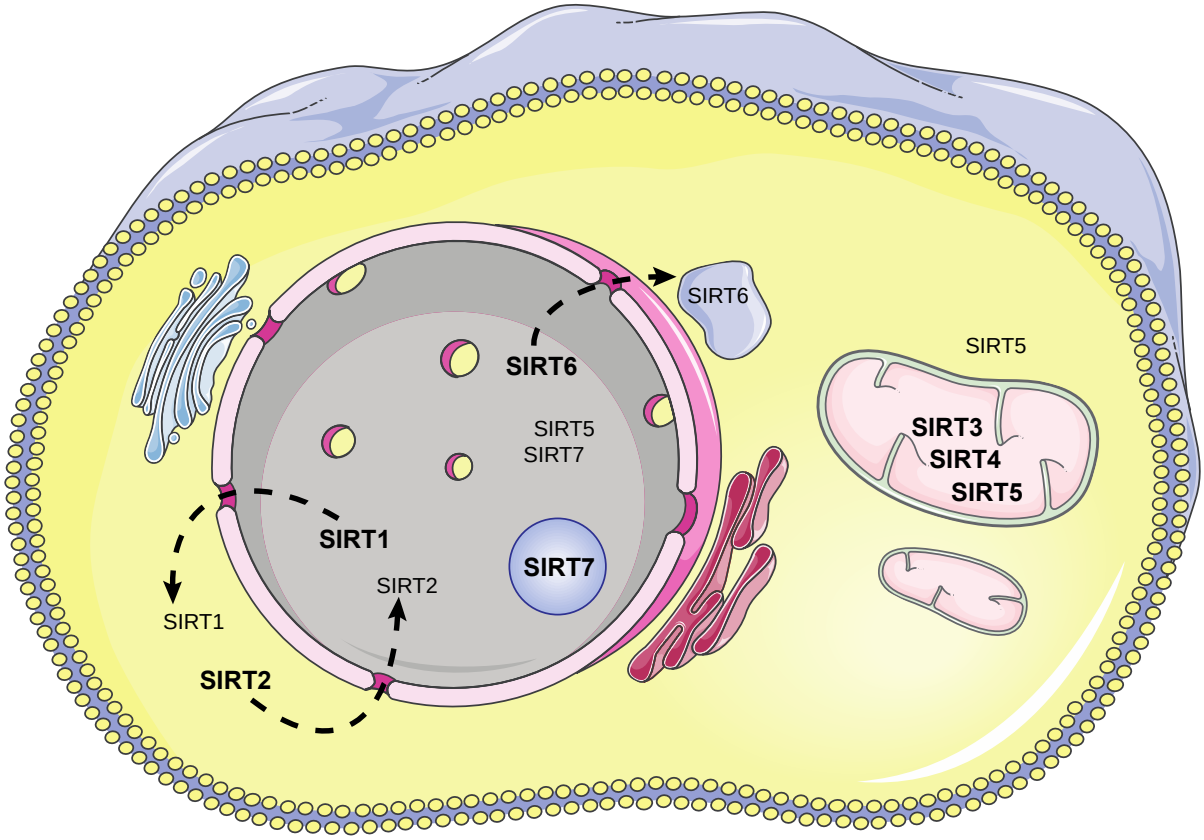

Figure 1.2 Sirtuin subcellular localization. SIRT1 is localized to the nucleus and can shuttle to the cytoplasm under certain conditions. SIRT2 is a cytosolic protein present in the nucleus during the G2/M transition of the cell cycle. SIRT3, SIRT4 and SIRT5 are primarily mitochondrial sirtuins. SIRT5 has been detected outside the mitochondria where it deacylates specific targets. SIRT6 is chromatin-bound in the nucleus, but has been found associated with cytoplasmic stress granules. SIRT7 is nucleolar and associates with ribosomal DNA, but also regulates extra-nucleolar nuclear processes.

The SIRT2-G6PD interaction is further enhanced upon oxidative stress, and results in activation of the pentose phosphate pathway, which supplies the cell with increased NADPH levels to maintain redox homeostasis.

SIRT3 is the principle mitochondrial deacetylase that plays essential roles in mitochondrial functions: ATP production, reactive oxygen species (ROS) management,

β-oxidation, ketogenesis and cell death among other processes (Brenmoehl and Hoeflich, 2013; Lombard et al., 2007; Lombard and Zwaans, 2014).

SIRT4 and SIRT5 are also present mainly in the mitochondrial matrix; a recent proteomic analysis identified a number of extra-mitochondrial SIRT5 targets, as well as an extra-mitochondrial fraction of SIRT5 (Park et al., 2013). Initially, SIRT4 was found to be an ADP-ribosyltransferase (Haigis et al., 2006); however Laurent *et al.* recently reported that SIRT4 deacetylates and inhibits malonyl-CoA decarboxylase (MCD), an enzyme that generates acetyl-CoA from malonyl-CoA to regulate fatty acid synthesis (Laurent et al., 2013). Likewise, initial characterization of SIRT5 found that it deacetylates and activates carbamoyl phosphate synthetase 1 (CPS1), to promote urea cycle function. Subsequent mass spectrometry-based analyses have revealed that the major biochemical function of SIRT5 is to remove newly-discovered, negatively-charged PTMs (*i.e*. succinyl, malonyl, and glutaryl moieties) from lysine residues, including those on CPS1 (Du et al., 2011; Nakagawa et al., 2009; Park et al., 2013; Peng et al., 2011; Rardin et al., 2013; Tan et al., 2014).

Nuclear SIRT6 deacetylates H3K9Ac and H3K56Ac (Michishita et al., 2008; Michishita et al., 2009; Yang et al., 2009), the DNA repair factor CtIP (Kaidi et al., 2010), and the acetyltransferase GCN5 (Dominy et al., 2012). The presence of long-chain fatty acids stimulates SIRT6 function (Feldman et al., 2013), hinting at a distinct means of coupling SIRT6 function to nutrient status independent of NAD^+ levels. SIRT6 also activates poly[ADP-ribose] polymerase 1 (PARP1) via mono-ADP-ribosylation (Mao et al.,

2011b), and promotes secretion of the pro-inflammatory cytokine tumor necrosis factor alpha (TNFα) via deacylation (Jiang et al., 2013). SIRT6 and its invertebrate homologue SIR-2.4 promote formation of cytoplasmic stress granules, and associate with these structures (Jedrusik-Bode et al., 2013; Michishita et al., 2005; Simeoni et al., 2013). SIRT6 regulates hepatic circadian gene expression by directly interacting with the circadian control proteins, CLOCK (circadian locomotor output cycles kaput) and BMAL (or ARNTL for aryl hydrocarbon receptor nuclear translocator-like) to modulate their recruitment to chromatin. SIRT6 also restricts sterol regulatory element binding protein 1 (SREBP-1)-mediated transcription of target genes, thereby controlling circadian-dependent metabolism, including fatty acid synthesis and β-oxidation (Masri et al., 2014).

SIRT7 is mainly localized to the nucleolus, where it associates with RNA polymerase I and nucleolar transcription activator upstream-binding factor 1, and occupies the promoters of ribosomal DNA (rDNA) loci (Ford et al., 2006). The c-MYC transcription factor interacts with and targets SIRT7 to the rDNA promoters. By reducing ribosomal protein expression, SIRT7 mitigates ER stress brought about by the unfolded protein response (Shin et al., 2013). By interacting with the transcription factor ELK4, SIRT7 suppresses transcription of target genes by deacetylating H3K18Ac at specific gene promoters (Barber et al., 2012). SIRT7 is also responsible for the reduction in genome-wide H3K18 acetylation associated with oncogenic transformation. SIRT7 protects the testicular receptor 4 (TR4) transcription factor from ubiquitin-mediated degradation by binding to components of the E3 ubiquitin ligase complex (Yoshizawa et al., 2014).

SIRT7 also localizes outside the nucleolus. *In vivo* and mass spectrometry analyses have demonstrated that SIRT7 can directly deacetylate GA repeat binding protein, beta 1 (GABPβ1) on three lysine resides, K69, K340 and K369. GABPβ1 along with its alpha subunit (GABPα) comprises a heterotetrameric complex that stimulates transcription of target mitochondrial genes. Deacetylation of these residues is required for GABPα/GABPβ□complex formation and subsequent transcriptional activation. This complex governs mitochondrial function, and SIRT7, through GABPβ1 signaling, is a nuclear regulator of mitochondrial activity (Ryu et al., 2014). Therefore, SIRT7 may be a clinically relevant target in treating or preventing mitochondrial disease.

Sirtuin enzymatic activity requires and consumes NAD^+, synthesized *de novo* or regenerated through the salvage pathway, to produce the noncompetitive feedback inhibitor nicotinamide (NAM), 2'-O-acetyl-ADP-ribose (or the corresponding acyl derivative), and the modified substrate (Tanner et al., 2000) (Figure 1.1). Thus, the requirement of sirtuins for NAD^+ distinguishes them from other classes of mammalian deacetylases, linking their enzymatic activity to the cellular nutritional and redox milieu and metabolic state of the organism (Bordone and Guarente, 2005).

Sirtuins and Mammalian Longevity

Several groups have generated sirtuin knockout and overexpressor mouse models (Finkel et al., 2009). In this section, we review currently existing data showing that overexpression of two mammalian sirtuins, SIRT1 and SIRT6, can extend mammalian

lifespan. SIRT2 overexpression also extends longevity in the context of a mutant with defective chromosomal segregation.

SIRT1

The closest mammalian homologue of yeast Sir2p is SIRT1. Multiple groups have investigated whether elevated SIRT1 expression can increase mammalian lifespan. Initial characterization of transgenic mice overexpressing SIRT1 in multiple tissues from an ectopic promoter revealed improvements in several metabolic parameters, somewhat resembling the benefits of calorie restriction (reduced caloric intake without malnutrition) (Bordone et al., 2007). Subsequent characterization of transgenic mouse strains modestly overexpressing SIRT1 – from a bacterial artificial chromosome containing the SIRT1 genomic locus and its putative regulatory elements – revealed that SIRT1 protects against hepatosteatosis and preserves hepatic insulin sensitivity in a diabetic mouse model and in mice fed a high-fat diet (HFD) (Banks et al., 2008; Pfluger et al., 2008). Overexpressing SIRT1 in the brain rescues the age-related decline in circadian rhythm adaptation by regulating expression of the central circadian clock genes, BMAL1 and PER2 (period circadian protein homolog 2) in the suprachiasmatic nucleus (SCN) (Chang and Guarente, 2013). Given that mutations in genes controlling the circadian rhythm are associated with features of premature aging, and SIRT1, BMAL1 and PER2 expression all decrease in the SCN with age, it will be important to determine if maintaining SIRT1 expression in this region of the brain is critical for promoting longevity in mammals (Chang and Guarente, 2013; Masri and Sassone-Corsi, 2014).

Later studies demonstrated that SIRT1 overexpression in most tissues does not extend mouse lifespan (Herranz et al., 2010; Jeong et al., 2012). However, Herranz, *et al.* reported that *Sirt1* transgenic mice were healthier in some respects than littermate controls. Improved maintenance of glucose homeostasis, wound healing, and neuromuscular function, as well as delayed bone loss, and a reduced incidence of carcinomas and sarcomas, were observed in SIRT1 overexpressing mice (Herranz et al., 2010). The inability of global SIRT1 overexpression to extend longevity has been ascribed to its failure to protect against age-associated lymphoma, a major cause of death in many inbred mouse strains (Herranz et al., 2010).

However, more recently, using a brain-specific SIRT1 overexpressing mouse line (BRASTO mice), Satoh *et al.* demonstrated a median lifespan extension of 11%, and a delay in the incidence of cancer-related death in both sexes (Satoh et al., 2013). Increased SIRT1 expression specifically in the dorsomedial and lateral hypothalamic nuclei (DMH/LH) extends lifespan of both male and female mice by upregulating expression of the orexin type 2 receptor, through deacetylation of the transcription factor Nk2 homeobox 1 (Figure 1.3). DMH/LH SIRT1 overexpression increases physical activity and whole-body oxygen consumption, maintains healthy mitochondrial morphology in skeletal muscle of aged animals, and promotes body temperature maintenance. Based

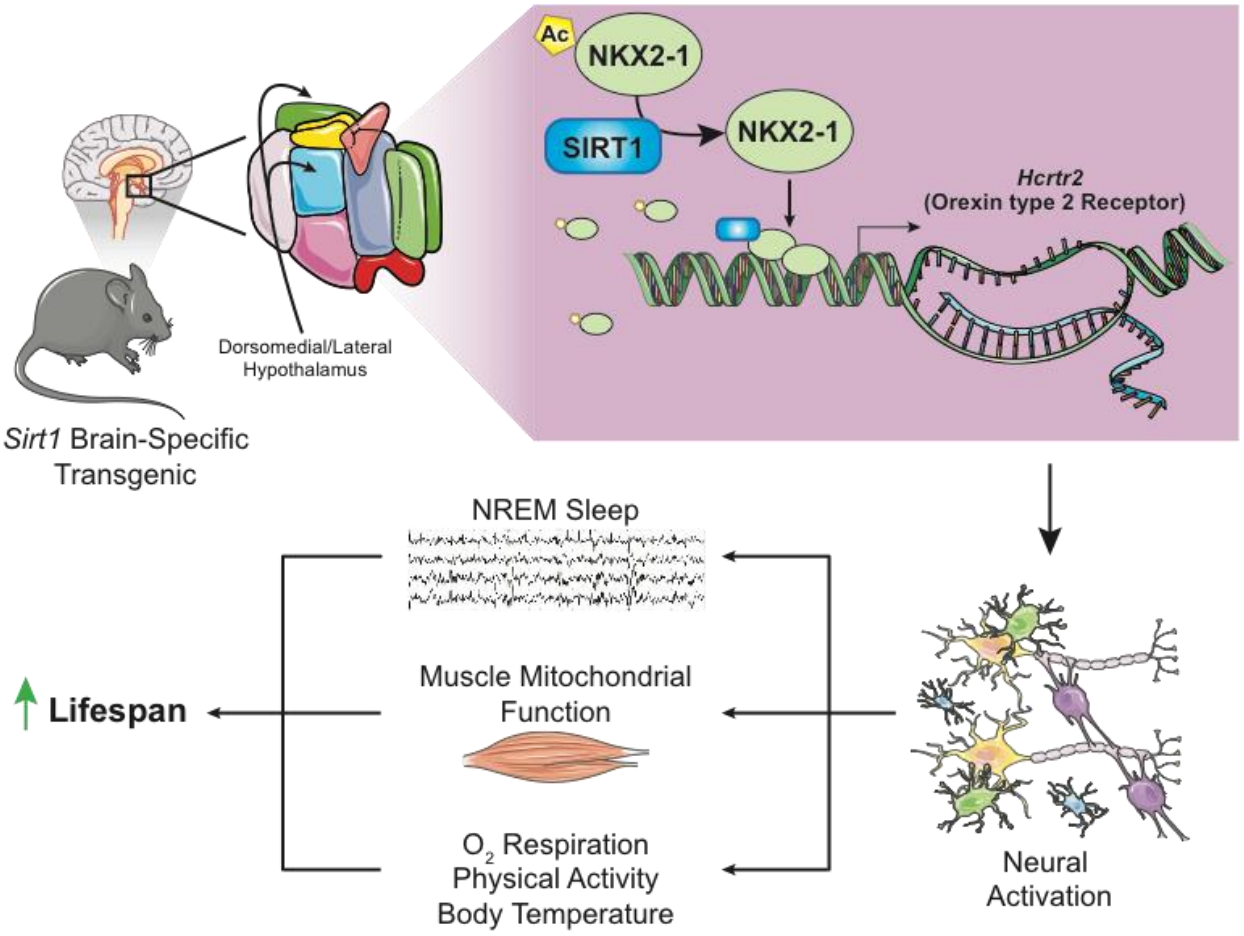

Figure 1.3 Lifespan extension in brain-specific *Sirt1* transgenic mice. When overexpressed in the dorsomedial and lateral hypothalamic nuclei of mice (DMH/LH), SIRT1 extends lifespan of both male and female mice by upregulating expression of *Hcrtr2*, the gene encoding the orexin type 2 receptor (OX2R), through deacetylation and activation of the Nk2 homeobox 1 transcription factor (NKX2-1). Increased neural activation results in better quality of sleep, and preservation of youthful mitochondrial morphology and function.

on characterization of a second independently derived BRASTO transgenic line in which no lifespan extension was observed, Satoh *et al.* hypothesize that relative differences in SIRT1 overexpression levels in specific regions of the brain may be required for increased longevity. In this regard, dose-dependent effects of sirtuin expression have been previously documented, both in invertebrates and in mammals. For example, in the mouse heart, a 7.5-fold increase in SIRT1 expression protects against cardiac

dysfunction, apoptosis and oxidative stress, but an approximately 12.5-fold increase in SIRT1 levels causes hypertrophy and impairs cardiac function (Alcendor et al., 2007).

Notably, Zhang *et al.* have reported a progressive age-dependent hypothalamic activation of nuclear factor kappa-light-chain-enhancer of activated B cells (NF-κB), associated with an increase in expression of pro-inflammatory markers in the aging brain (Zhang et al., 2013). Suppression of hypothalamic NF-κB activity extends mouse lifespan. Given that SIRT1 is an inhibitor of NF-κB transcriptional output (Yeung et al., 2004), it is possible that the pro-longevity function of hypothalamic SIRT1 may occur in part via suppression of NF-κB signaling.

Global deletion of *Sirt1* in inbred 129/Sv mice causes late prenatal or early postnatal lethality. Homozygous null embryos are developmentally delayed, with a subset displaying exencephaly (Cheng et al., 2003; McBurney et al., 2003). However, in a genetically outbred strain, or an FVB background, SIRT1 nullizygosity is compatible with adult viability (McBurney et al., 2003; Satoh et al., 2010). *Sirt1* knockout mice are runted, sterile and show a significantly reduced lifespan (Boily et al., 2009; Li et al., 2008; Mercken et al., 2014a). Together these results highlight the importance of SIRT1 activity for normal mammalian development and physiologic homeostasis.

SIRT2

BUBR1 is a protein kinase involved in the spindle assembly checkpoint, and ensures proper chromosomal segregation by inhibiting anaphase until correct alignment of sister

chromosomes occurs (Bolanos-Garcia and Blundell, 2011; Elowe, 2011). BUBR1 protein levels decline as a function of age, and mice carrying hypomorphic alleles (designated *BubR1*$^{H/H}$) are predisposed to aneuploidy and display premature aging phenotypes, such as postnatal developmental delay, impaired would healing, cataracts and shortened lifespan (Baker et al., 2004; Hartman et al., 2007; Matsumoto et al., 2007). Transgenic overexpression of BUBR1 rescues these progeroid phenotypes, maintains genomic integrity, and extends lifespan in wild-type mice (Baker et al., 2013).

Using biochemical and mass spectrometry approaches, North *et al.* demonstrated that lysine 668 (K668) in BUBR1 is a SIRT2 target. By acetylating K668, the acetyltransferase cyclic-AMP response element binding protein (CREB) binding protein (CBP) promotes BUBR1 ubiquitylation and subsequent degradation. SIRT2 stabilizes BUBR1 protein by counteracting CBP-mediated K668 acetylation; conversely inhibiting SIRT2 activity or reducing its levels diminishes BUBR1 protein levels.

Crossing *Sirt2* transgenic mice (*Sirt2tg*) to *BubR1*$^{H/H}$ animals on the C57BL/6J background resulted in a 58% increase in median lifespan and a 21% increase in maximal lifespan compared to *BubR1*$^{H/H}$ mice in analyses of combined sexes (North et al., 2014). When sexes were analyzed independently, SIRT2 increased male median lifespan by 123% but showed no effect in females. In *Sirt2tg-BubR1*$^{H/H}$ tissues, BUBR1 protein levels were restored, demonstrating that SIRT2 can promote BUBR1 stability *in vivo.* *BubR1*$^{H/H}$ mice die of cardiac dysfunction, while SIRT2 overexpression ameliorates their cardiac phenotypes. Also, *in vivo* supplementation with the NAD^+

precursor NMN rescues the age-dependent decline of NAD^+ in heart tissue, and elevates BUBR1 protein levels in testes from aged wild-type mice to the level observed in young mice.

The phenotypes associated with *BubR1*$^{H/H}$ mice are not reported to be sex specific (Baker et al, 2004). However male mice in general may be more susceptible to cardiac pathology than females (Du, 2004), which may partly account for the observed sex bias for SIRT2-dependent lifespan extension. These results are clinically relevant since mutations in *BUB1B*, the human ortholog of *BubR1,* are associated with Mosaic variegated aneuploidy (MVA), a syndrome characterized by progeria-like phenotypes, short stature and shortened lifespan (Callier et al., 2005; Garcia-Castillo et al., 2008; Wijshake et al., 2012). Given that BUBR1 protein levels decrease with age, and SIRT2 overexpression is able to mitigate this defect, SIRT2 overexpression might be predicted to extend lifespan in wild-type mice, and merits closer examination as a potential therapeutic for human disease.

SIRT6

In two independent *Sirt6* transgenic mouse strains, whole-body SIRT6 overexpression extends median lifespan of males by 14.5% and 9.9% respectively (Figure 1.4) (Kanfi et al., 2012). In contrast, no significant increase in lifespan is observed in female transgenics. Sexually dimorphic effects of pro-longevity interventions have commonly

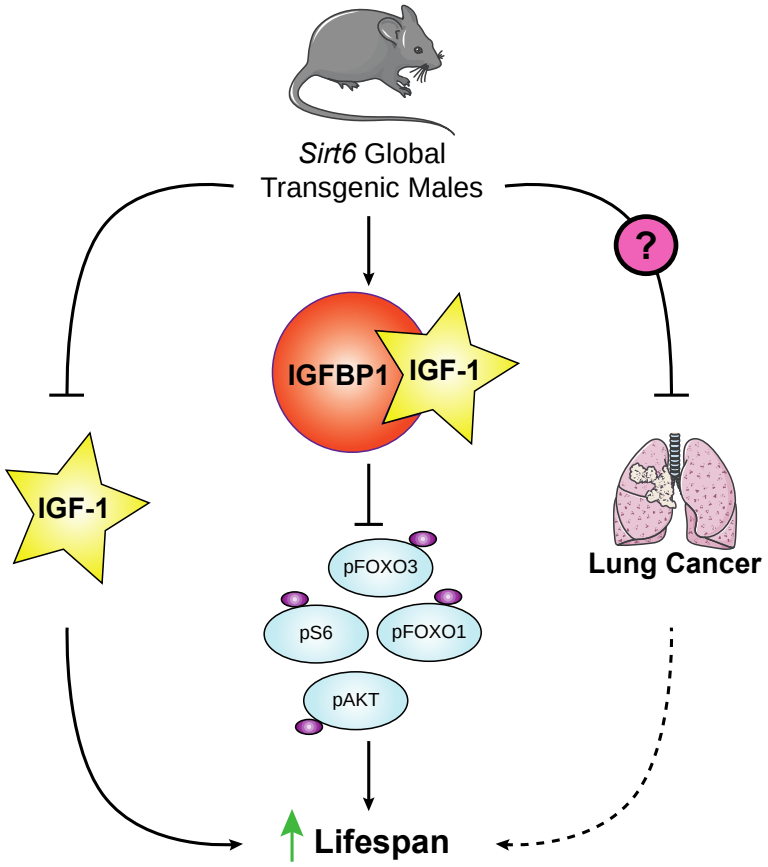

Figure 1.4 Global SIRT6 overexpression increases the lifespan of male mice. In male mice, global SIRT6 overexpression increases lifespan by inhibition of the insulin-like growth factor 1 (IGF-1) signaling cascade. Phosphorylation of downstream IGF-1 signaling effectors are affected as indicated: phosphorylated AKT, (pAKT), phosphorylated forkhead box protein O1 and O3A (pFOXO1 and pFOXO3A), and phosphorylated S6 kinase (pS6). IGFBP1 (IGF-1 binding protein 1) binds to IGF-1 to limit the amount available to bind to receptor molecules. Relative protection against lung cancer was observed in male SIRT6 transgenics, potentially due to reduced IGF-1 signaling.

been observed in studies of lifespan extension by small molecules in mice (*e.g.* (Harrison et al., 2009; Strong et al., 2008)). In the case of SIRT6, these differences may result from discrepant effects of SIRT6 overexpression on IIS. In male *Sirt6* transgenic mice, lower serum IGF-1 levels and reduced downstream signaling are present, an effect associated with longevity in many other model organisms (Fontana et

al., 2010). Further analyses by Kanfi *et al.* reveal that male *Sirt6* transgenics are relatively protected against lung tumors, and show a trend towards maintenance of glucose tolerance with age. Protection against other phenotypic characteristics of aging such as osteopenia and adrenal cortical hyperplasia was not observed upon detailed pathological analysis (Kanfi et al., 2012).

Germline deletion of *Sirt6* in inbred 129/Sv-strain mice causes severe growth retardation, along with progressive, lethal hypoglycemia (Mostoslavsky et al., 2006). SIRT6-deficient mice display a degenerative phenotype, lymphopenia, and genomic instability; although a subset of germline knockout mice on an outbred 129/Sv-C57BL/6 genetic background can survive up to 1 year if supplemented with glucose early in life (Xiao et al., 2010). SIRT6 inhibits expression of GLUT1, which is responsible for transporting glucose across the plasma membrane in mammalian cells. In *Sirt6* knockout mouse retinas, GLUT1 is upregulated, several glutamate receptor genes are downregulated, and an increase in apoptosis occurs. *Sirt6* knockout retinas are less responsive to photostimulation, indicating that SIRT6 is required for normal retinal function (Silberman et al., 2014).

These initial results reveal that specific mammalian sirtuins can exert pro-longevity effects, similar to their invertebrate homologues. One important caveat is that disease-specific interventions can extend lifespan, if those diseases are a prevalent cause of death in the population (Lombard and Miller, 2014). In this regard, the generality of the positive effects of SIRT1 and SIRT6 on lifespan needs to be assessed in other mouse

genetic backgrounds. SIRT1 and SIRT6 expression may indeed slow aging in mammals, however in order to conclusively demonstrate that these sirtuins are *bona fide* anti-aging factors, many more studies are required to comprehensively assess the impact of increased levels of these and other sirtuins on longevity and diverse age-sensitive traits.

Sirtuins as Modulators of Responses to Caloric Restriction

Dietary or caloric restriction (CR) is the only known environmental intervention that robustly and reliably extends lifespan across phyla, including mammals. CR can extend rodent lifespan up to 50%, while suppressing diverse age-associated conditions such as cancer, autoimmune disease, T2D, neurodegeneration, and many others (Speakman and Mitchell, 2011). Mechanisms underlying this effect are still unclear. Since most individuals find that a long-term reduction in caloric intake is difficult to maintain, a great deal of current aging research focuses on elucidating the mechanisms of the pro-health effects of CR, using yeast, flies, worms and rodent models. Several physiological pathways have been proposed to regulate CR-dependent lifespan extension and healthspan maintenance, including IIS, mTOR signaling, AMPK signaling, and sirtuins (Guarente, 2013). Given that sirtuin catalytic activity is NAD^+-dependent, and NAD^+ levels rise upon nutrient stress in certain tissues, upregulation of specific sirtuin functions has been proposed to represent a means to reap some beneficial effects of CR (Guarente, 2013).

Little direct evidence linking CR to sirtuin activation exists in the context of invertebrate models. Also, conflicting results have been obtained regarding roles for these proteins in the response to CR. Reduction of glucose in growth medium extends the replicative lifespan of *S. cerevisiae* in a strain-specific manner, though there is controversy as to whether this phenotype is Sir2p-dependent. The use of inconsistent glucose concentrations by different laboratories has further complicated the interpretation of discrepant results in this area (Kaeberlein and Powers, 2007; Lamming et al., 2005; Lin et al., 2000). Longo and Kennedy have detailed the controversies surrounding the involvement of yeast sirtuins in the CR response (Longo and Kennedy, 2006).

In *C. elegans,* one group has reported that the SIRT1 homologue SIR-2.1 is required for increased longevity in response to CR (Wang and Tissenbaum, 2006) whereas several other labs have found that SIR-2.1 is dispensable for this effect (Greer and Brunet, 2009; Hansen et al., 2007; Kaeberlein et al., 2006; Lee et al., 2006; Mair et al., 2009). In *D. melanogaster*, an initial report found that dSIR2 is required for CR-induced longevity (Rogina and Helfand, 2004), a result not replicated by a subsequent study (Burnett et al., 2011). However subsequent work using RNAi-mediated dSIR2 knockdown in specific tissues or the whole organism supported the initial finding (Banerjee et al., 2012; Bauer et al., 2009; Pallos et al., 2008). It is likely that CR and dSIR2 act at least in part through distinct pathways in flies, since gene expression pattern changes associated with dSIR2 overexpression differ from those induced during CR (Hoffmann et al., 2013).

More recent studies in the fly have revealed that lifespan in this species responds to the relative amounts of protein and carbohydrate in the diet, rather than to an overall reduction in calories *per se*. A complete lack of specific amino acids such as arginine, methionine or isoleucine is detrimental to lifespan, while an intermediate amount of dietary methionine results in a significant extension (Tatar et al., 2014). This mirrors findings in rodents, where methionine restriction can also extend lifespan (Miller et al., 2005; Perrone et al., 2013; Richie et al., 1994). Little is known about the potential role of sirtuins in responding to specific dietary components in the context of lifespan.

SIRT1

Several reports support the hypothesis that SIRT1 is a mediator of aspects of the CR response in mammals, in a tissue-specific manner. For example, SIRT1 protein levels increase in white adipose tissue (WAT), skeletal muscle and hypothalamus in response to CR in mice, however SIRT1 protein expression and NAD^+ levels decrease in the liver (Chen et al., 2008; Cohen et al., 2004; Satoh et al., 2010). Similarly, tissue-specific changes in SIRT1 activity occur during CR, likely due to changes in NAD^+ levels (Chen et al., 2008). Transgenic mice overexpressing SIRT1 in WAT, brown adipose tissue (BAT) and the brain show metabolic phenotypes somewhat reminiscent of those that result from a CR diet (Bordone et al., 2007). Although SIRT1 expression is not increased in the liver or skeletal muscle of these transgenics, they are more glucose tolerant, and show reduced blood cholesterol, glucose and insulin levels, and less WAT accumulation. Consistent with these findings, deletion of *Sirt1* in skeletal muscle abrogates increased insulin sensitivity associated with CR; in contrast no apparent

defect in the response to CR is observed when *Sirt1* is deleted specifically in the liver (Chen et al., 2008; Schenk et al., 2011). *Sirt1* deletion in the CNS and peripheral neurons also impairs insulin sensitivity in response to CR (Cohen et al., 2009). Surprisingly however, *Sirt1* deletion in CNS neurons alone enhances insulin sensitivity and glucose tolerance compared to controls (Lu et al., 2013). Findings from global *Sirt1* knockout and brain-specific SIRT1 transgenic mouse models demonstrate that SIRT1 supports maintenance of body temperature and neuronal activity in hypothalamic nuclei during CR (Satoh et al., 2010). SIRT1 also protects against age-related decline in renal function in mice fed a CR diet (Kume et al., 2010). Overall, SIRT1 is required for both increased physical activity and certain metabolic responses observed in response to CR (Boily et al., 2008; Chen et al., 2008; Chen et al., 2005; Imai, 2009; Satoh et al., 2013).

SIRT2

Little is known about the potential role of SIRT2 in response to a CR diet. One study found that SIRT2 expression is induced in the kidney and WAT of mice fed a CR diet. The authors demonstrate that SIRT2 interacts with and deacetylates FOXO3A in cell culture, resulting in the increased expression of several downstream targets such as mitochondrial superoxide dismutase 2 (SOD2) and the pro-apoptotic factor, BIM. Through this mechanism, SIRT2 is able to reduce cellular ROS levels through SOD2 activation, and promote apoptosis via BIM activity, when oxidative damage is too extensive to repair (Wang et al., 2007). The interpretation that SIRT2 responds to CR and oxidative stress via the FOXO signaling cascade requires testing in *Sirt2* knockout animals, to determine if SIRT2 regulates physiologic aspects of the CR response.

SIRT3

SIRT3 expression increases in liver, skeletal muscle, and adipose tissue during CR, suggesting that SIRT3 may play a role in regulating mitochondrial functions under these conditions (Hallows et al., 2011; Hirschey et al., 2010; Nakagawa et al., 2009; Palacios et al., 2009; Schwer et al., 2009; Shi et al., 2005; Someya et al., 2010). Although overall hepatic mitochondrial protein acetylation increases during CR (Schwer et al., 2009) deacetylation of specific mitochondrial target proteins occurs in this setting (Hebert et al., 2013), resulting from increased SIRT3 expression. As noted previously, SIRT3 plays a major role in suppressing ROS levels. Indeed, SIRT3 is required for reducing cellular ROS levels during CR (Qiu et al., 2010; Someya et al., 2010). As a consequence of this activity, SIRT3 is required for the protection against age-associated hearing loss conferred by CR, via preservation of cochlear cells against age-associated attrition (Someya et al., 2010). CR decreases hepatic acetyl-CoA, serum insulin and triglyceride levels in a SIRT3-dependent manner (Hebert et al., 2013; Someya et al., 2010). SIRT3 deacetylates and activates the urea cycle enzyme ornithine transcarbamoylase (OTC) in murine liver mitochondria in response to CR (Hallows et al., 2011). OTC deficiency results in an accumulation of orotic acid due to urea cycle dysfunction. *Sirt3*-null mice fed either a normal or CR diet exhibit increased OTC acetylation and higher levels of urinary orotic acid compared to wild-type mice fed a CR diet. Also, mass spectrometry analysis of blood from fasted *Sirt3*-null mice revealed a decrease in the urea cycle metabolite, citrulline, which is a direct product of OTC activity. Clearly SIRT3 is necessary for multiple metabolic responses to CR. Given

SIRT3's function as a tumor suppressor, it will be of interest to determine whether SIRT3 is required for improved cancer suppression induced by CR, or indeed if SIRT3 is required for longevity induced by this intervention.

SIRT4

SIRT4 protein levels decline in liver (Haigis et al., 2006; Schwer et al., 2009) but not pancreatic β cells during CR (Haigis et al., 2006). SIRT4 suppresses β cell insulin secretion in response to glucose or amino acids (Ahuja et al., 2007; Haigis et al., 2006). During CR, reduced β cell SIRT4 activity – occurring through mechanisms that are as yet unclear – may permit increased coupling of insulin secretion to amino acid metabolism (Haigis et al., 2006). This effect makes physiologic sense, in that amino acids are used as a metabolic fuel to a greater degree during CR than under normal feeding conditions.

SIRT5

Little is currently known regarding roles for SIRT5 during CR. Overall levels of lysine succinylation, a SIRT5 target modification, increase in liver during fasting (Park et al., 2013); the impact of chronic CR on succinylation, malonylation, or glutarylation has not been reported. Hepatic SIRT5 protein levels are unchanged during CR (Schwer et al., 2009), though nothing is known regarding SIRT5 biochemical activity in this context. SIRT5 has been shown to promote ketogenesis under fasting conditions (Rardin et al., 2013), suggesting that SIRT5 could potentially play a role in use of this alternative fuel during CR. Alternatively, SIRT5 suppresses mitochondrial respiration through specific

mitochondrial complexes (Park et al., 2013), suggesting that a decrease in SIRT5 function during CR might contribute to increased mitochondrial metabolism in response to this intervention. Characterization of *Sirt5* knockout mice under CR conditions will be required to elucidate the roles, if any, for SIRT5 during CR.

SIRT6

A role for SIRT6 in response to CR has not yet been assessed, though increased SIRT6 expression (Kim et al., 2010b) and protein stability (Kanfi et al., 2008) in response to this intervention have been described in several tissues in rodents. Fasting regimens induce metabolic reprogramming by initially upregulating gluconeogenesis to maintain blood glucose levels. Several reports indicate that SIRT6 is a negative regulator of hepatic gluconeogenesis, inhibits expression of genes involved in glycolysis (Dominy et al., 2012; Kim et al., 2010b; Xiong et al., 2013) and negatively affects lipogenesis by repressing the SREBPs, transcription factors important for lipogenesis and cholesterol biogenesis (Elhanati et al., 2013; Tao et al., 2013). Increased SIRT6 expression in response to nutrient deprivation in cell culture models was found to be SIRT1-dependent (Kim et al., 2010b), and expression of *Sirt1* mRNA itself increases in response to CR in rat brain, WAT, kidney and liver (Cohen et al., 2004). Given that both of these sirtuins interact with several factors and pathways relevant to the CR response (reviewed in (Guarente, 2013)), it is tempting to speculate that metabolic reprogramming during CR involves a complex relationship between SIRT1 and SIRT6. However, currently no evidence directly links SIRT6 activity to the induction of lifespan or healthspan benefits of a CR diet.

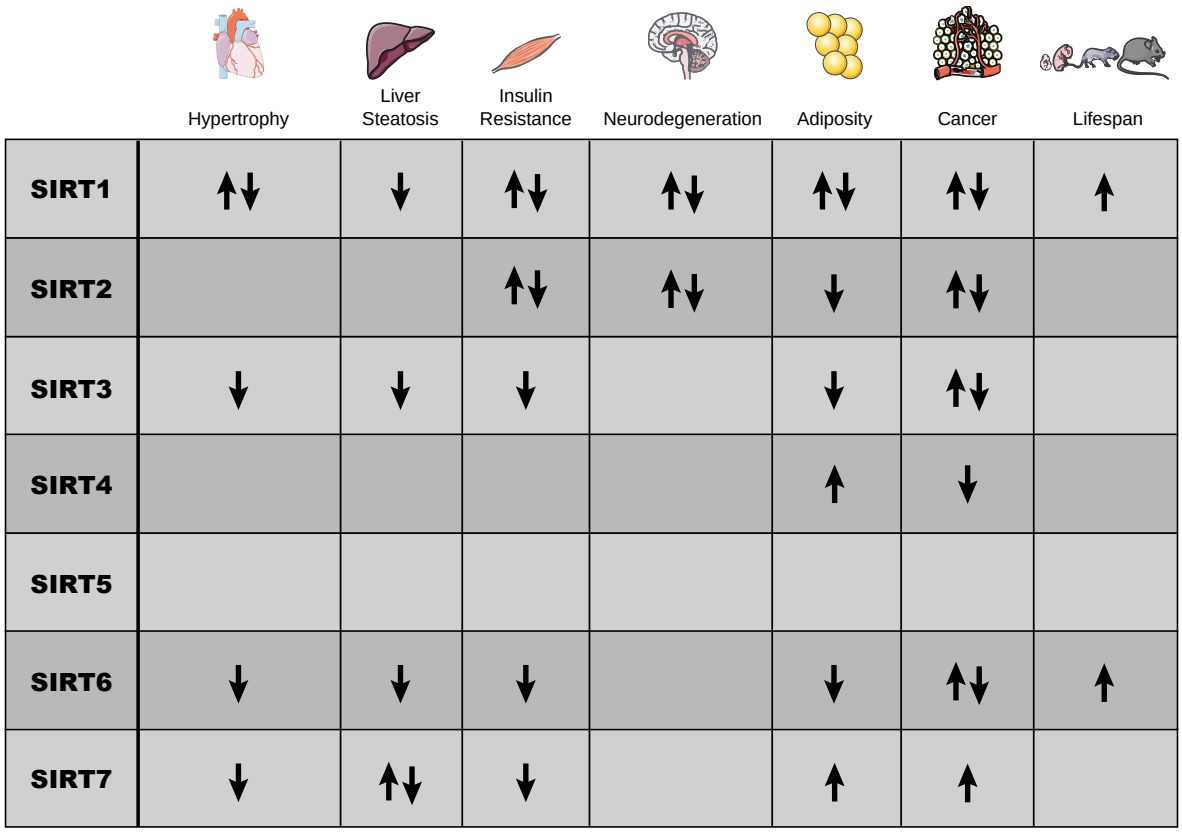

Figure 1.5 Summary of sirtuin involvement in inhibiting age-related pathology. Outline of sirtuin effects on the indicated age-associated diseases. Where indicated, both tumor suppressor and oncogenic properties have been reported, and are context-specific. Brain-specific SIRT1 or whole-body SIRT6 overexpression extends lifespan in mice.

Roles for Sirtuins in Diverse Disease States

Substantial evidence now exists demonstrating that activation of sirtuin activity in different contexts can confer health benefits in mammals, and in some cases can extend lifespan, as discussed previously. While the evidence directly linking sirtuins to increased longevity in mammals has emerged only recently, a large body of work exists demonstrating that sirtuins ameliorate numerous age-associated pathological

conditions. In this section, we discuss recent findings relevant to sirtuin functions as promoters of mammalian healthspan, with a focus on several age-associated diseases (Figure 1.5).

Cancer

A large body of research has elucidated complex, and often seemingly conflicting roles for sirtuins in cancer. The following section highlights recent evidence, largely from cell culture and mouse models, that demonstrate sirtuins modulate tumorigenesis in a cell- and context-specific manner.

SIRT1

SIRT1 acts as both a tumor suppressor and oncoprotein via interaction with and modification of dozens of distinct substrates relevant to cancer proliferation and survival, including the c-MYC oncoprotein and the tumor suppressor p53 (Yuan et al., 2013). Elevated SIRT1 expression has been detected in many human malignancies, including breast, prostate, lung, colon, liver, pancreatic, lymphoma, leukemia and some ovarian and cervical cancers (Yuan et al., 2013).

Conversely, tumor suppressor functions of SIRT1 have been observed in mouse models, wherein SIRT1 promotes the maintenance of genome stability (Yuan et al., 2009), and inhibition of cell growth via survivin (an inhibitor of apoptosis), β-catenin, and other pathways (Lim et al., 2010; Srisuttee et al., 2012). Global SIRT1 overexpression

at moderate levels reduces the incidence of spontaneous carcinomas and sarcomas (Herranz et al., 2010). Similarly, increased expression of SIRT1 in the $APC^{+/min}$ mouse model of intestinal polyposis decreases tumorigenesis (Firestein et al., 2008). Paradoxically, however, global or enterocyte-specific deletion of *Sirt1* reduces the size and number of intestinal polyps formed in this model (Boily et al., 2009; Leko et al., 2013). *Sirt1* deletion results in increased apoptosis in polyps arising in $APC^{+/min}$ mice, implying that SIRT1 can play a pro-survival role during tumor progression (Leko et al., 2013).

SIRT1 directly binds to and deacetylates hypoxia-inducible factor 1 alpha (HIF-1α), a transcription factor that regulates gene expression in response to reduced oxygen tension or increased ROS levels, to mediate metabolic reprogramming in cancer cells or other rapidly proliferating cell types (Lim et al., 2010). Whether SIRT1-dependent deacetylation promotes HIF-1α activity or attenuates its ability to promote expression of its target genes is a matter of debate. One study demonstrated that *SIRT1* knockdown *in vivo* impairs transcriptional output of HIF-1α target genes in hepatocellular carcinoma cells (Laemmle et al., 2012). Others have shown that SIRT1-dependent deacetylation of HIF-1α inhibits transcriptional co-activator binding to HIF-1α target gene promoters, thereby negatively regulating tumor growth and angiogenesis in tumor xenograft models (Lim et al., 2010). SIRT1 also interacts with the oncoprotein c-MYC, though the functional outcome of this interaction is controversial (Mao et al., 2011a; Menssen et al., 2012; Yuan et al., 2009). Overexpression of c-MYC and SIRT1 is present in several cancer types, and is often associated with higher tumor grade (Yuan et al., 2013).

Although SIRT1 expression is stimulated by c-MYC, deacetylated c-MYC is more susceptible to degradation, and therefore SIRT1 indirectly inhibits c-MYC function (Mao et al., 2011a; Yuan et al., 2009).

However, others have found that deacetylation stabilizes c-MYC, and enhances SIRT1 activity by promoting NAD^+ synthesis, establishing a positive feedback loop that may reinforce cellular malignant transformation (Menssen et al., 2012). Thus, while SIRT1 expression may inhibit oncogenesis in some contexts (*e.g.* primary cells), increased SIRT1 expression may confer a growth advantage in cells that have already undergone oncogenic alterations. Future research focusing on the relationship between SIRT1 and its substrates, in particular HIF-1α and c-MYC, in various tissue- and cell-type specific contexts may further delineate the multiple means by which SIRT1 affects neoplasia.

SIRT2

SIRT2 regulates chromatin assembly and promotes chromosomal stability during mitosis, thereby functioning as a tumor suppressor (Inoue et al., 2007; Inoue et al., 2009; Vaquero et al., 2006). SIRT2 deacetylates α-tubulin, controls the early metaphase checkpoint, and affects cell cycle progression by mediating monomethylation of H4K20 through its interaction with the histone methyltransferase PR-Set7 (Dryden et al., 2003; North et al., 2003; North and Verdin, 2007; Pandithage et al., 2008; Serrano et al., 2013).

Evidence from *Sirt2* knockout mice supports a tumor suppressor role for SIRT2 *in vivo*. *Sirt2*-null male mice develop liver and intestinal cancer, while females develop mammary tumors, associated with centrosome amplification, mitotic catastrophe and eventual cellular transformation (Kim et al., 2011b). Accordingly, SIRT2 expression is reduced in human breast and hepatocellular carcinoma samples compared to healthy human tissue when analyzed by tissue microarray. Two independent studies have also demonstrated a tumor suppressor role for SIRT2 in mouse skin (Ming et al., 2014; Serrano et al., 2013).

However, like SIRT1, SIRT2 also has seemingly contradictory roles in cancer. Several studies demonstrate that *SIRT2* knockdown actually induces apoptosis in glioma and HeLa cervical carcinoma cell lines, and SIRT2 expression is increased in neuroblastoma and pancreatic cancer cells (Yuan et al., 2013). Tenovins, a class of small molecules that increase p53 acetylation and activation in tumor cells (McCarthy et al., 2012), can inhibit SIRT1 and SIRT2 activity, induce apoptosis in transformed cell lines, and impede tumor growth *in vivo* (Lain et al., 2008; McCarthy et al., 2010). Given that SIRT1 and SIRT2 have been shown to deacetylate p53 to inhibit its transcriptional activity and promote its ubiquitin-mediated degradation (Langley et al., 2002; Luo et al., 2004; Luo et al., 2001; van Leeuwen et al., 2013; Vaziri et al., 2001), an effect lost upon tenovin treatment (van Leeuwen et al., 2013), tenovins may be therapeutically useful in treating cancers with reduced p53 activity due to elevated SIRT1 and/or SIRT2 expression.

SIRT3

SIRT3 has also been implicated as both a tumor suppressor and oncogene in various contexts. The *SIRT3* gene is deleted in up to 20% of all human cancers, and in 40% of breast and ovarian cancers specifically (Finley et al., 2011). Consistent with this finding, *SIRT3* mRNA expression is reduced in diverse human cancers, including testicular, prostate, and hepatocellular tumors, compared to non-malignant tissue (Kim et al., 2010a). An increased incidence of mammary cancer occurs in mice lacking SIRT3, and SIRT3 protein levels are lower in human breast tumors when compared to healthy breast tissue (Finley et al., 2011; Kim et al., 2010a). By immunohistochemistry, SIRT3 protein expression is greatly reduced in a large fraction of human breast cancers, and low SIRT3 expression is associated with poor prognosis and decreased patient survival (Desouki et al., 2014).

Mechanistically, one major function of SIRT3 in the context of tumor suppression is to suppress ROS-mediated damage. Elevated ROS levels promote tumorigenesis by inducing DNA mutations and genomic instability, and activating pathways regulating metabolism, cell survival, and proliferation (Liou and Storz, 2010). SIRT3 deacetylates and activates mitochondrial SOD2 and isocitrate dehydrogenase 2 (IDH2); deacetylation of IDH2 in turn allows regeneration of the antioxidant glutathione (Qiu et al., 2010; Someya et al., 2010; Tao et al., 2010). *Sirt3* deletion increases ROS and stabilizes HIF-1α, which results in pro-tumorigenic metabolic reprogramming (Bell et al., 2011; Finley et al., 2011; Kim et al., 2010a). In addition, deletion of *Sirt3* in mouse embryonic fibroblasts increases intracellular superoxide levels and aneuploidy in

response to genotoxic stressors, suggesting that SIRT3 guards against chromosomal instability and tumorigenesis by maintaining genomic integrity (Kim et al., 2010a). Overall, suppression of ROS levels is likely a principal means by which SIRT3 inhibits tumorigenesis.

Recently, SIRT3 has also been shown to activate mitochondrial respiration via the pyruvate dehydrogenase complex (PDC) (Fan et al., 2014; Jing et al., 2013). Cancer cell metabolic reprogramming frequently involves reversible inactivation of PDC (*e.g.* (Kaplon et al., 2013)); therefore the activity of SIRT3 towards PDC represents a distinct mechanism by which SIRT3 suppresses neoplasia.

However, data also exist supporting an oncogenic role for SIRT3. Li-Fraumeni Syndrome (LFS) is characterized by a predisposition to a wide spectrum of cancers, and frequently results from mutations in the *TP53* gene. In a study of a family with LFS and no apparent *TP53* mutation, a genomic duplication of the entire genomic region containing the *SIRT3* locus was identified, leading to increased *SIRT3* mRNA expression (Aury-Landas et al., 2013). The authors directly evaluated the potential contribution of SIRT3 to tumorigenesis in these patients, and demonstrated that SIRT3 overexpression in a glioma cell line inhibits apoptosis, deregulates cell cycle progression and results in CpG island hypermethylation, features typically associated with cancer (Hanahan and Weinberg, 2011). Furthermore, SIRT3 has been reported to inhibit p53-induced growth arrest in human bladder cancer cells (Li et al., 2010). Elevated SIRT3 expression has been detected in node-positive breast cancer (Ashraf et

al., 2006) and oral squamous cell cancer (OSCC). In OSCC, *SIRT3* knockdown inhibits proliferation and sensitizes cells to radiation and chemotherapeutic treatments *in vitro* (Alhazzazi et al., 2011). A conflicting report claims that SIRT3 enzymatic activity is reduced in OSCCs, and that upregulation of SIRT3 expression inhibits proliferation of OSCC cell lines (Chen et al., 2013). Thus, as with SIRT1 and SIRT2, the oncogenic and tumor suppressor activities of SIRT3 are likely highly context specific.

SIRT4

SIRT4 functions as a tumor suppressor by suppressing glutamine metabolism and promoting genomic stability through distinct mechanisms (Csibi et al., 2013; Jeong et al., 2014; Jeong et al., 2013). SIRT4 inhibits cells from metabolizing glutamine to replenish tricarboxylic acid (TCA) cycle intermediates (anaplerosis). Jeong *et al.* showed that SIRT4 represses glutamine anaplerosis in response to DNA damage, and that consequently *Sirt4* knockout MEFs do not reduce their glutamine uptake after UV exposure (Jeong et al., 2013). In response to DNA damage, SIRT4 levels increase, and repress mitochondrial glutamine metabolism. Since glutamine is critical for G1 to S cell cycle progression (Colombo et al., 2011), SIRT4 indirectly regulates the cell cycle, allowing for proper DNA repair and maintenance of genomic stability. *In vivo*, SIRT4 deficiency results in growth of larger tumors in a nude mice allograft model. Correspondingly, two independently derived strains of *Sirt4*-null mice show an increased incidence of spontaneous lung tumors (Jeong et al., 2013). SIRT4 deletion hastens lymphomagenesis and death in a mouse model of Burkitt lymphoma (Jeong et al., 2014), whereas SIRT4 overexpression reduces glutamine consumption and

glutamine-dependent growth in MYC-driven human Burkitt lymphoma cells, and sensitizes these cells to glucose depletion.

An independent study found that the mechanistic target of rapamycin complex 1 (mTORC1) pathway regulates glutamine anaplerosis by promoting the activity of glutamate dehydrogenase (GDH), a SIRT4 target (Csibi et al., 2013; Haigis et al., 2006). SIRT4 ADP-ribosylates and inactivates GDH to inhibit glutamine metabolism. SIRT4 overexpression in MEFs lacking the negative regulator of mTORC1, TSC2, shows attenuated transformation, proliferation and tumor development in a xenograft assay (Csibi et al., 2013). Overall, SIRT4 inhibits glutamine metabolism, thereby promoting genome stability and repressing tumorigenesis. Increasing SIRT4 activity may have therapeutic benefit specifically in MYC-driven cancers.

SIRT5

Like SIRT3 and SIRT4, SIRT5 localizes primarily to the mitochondrial matrix. However, a recent study identified a substantial fraction of active SIRT5 present outside the mitochondrion in both mouse liver and human cells (Park et al., 2013). As previously noted, SIRT5 possesses minimal lysine deacetylase function, while showing strong activity towards non-canonical PTMs: succinyl, malonyl, and glutaryl moieties (Du et al., 2011; Park et al., 2013; Peng et al., 2011; Rardin et al., 2013; Tan et al., 2014). Two recent large-scale mass spectrometry analyses of mouse liver have identified thousands of SIRT5 desuccinylation sites on hundreds of protein targets (Park et al., 2013; Rardin et al., 2013), many of which are distinct from acetylation sites. Among

sites whose succinylation could be quantified, succinylation increased on >90% of these in the context of SIRT5 deficiency (Park et al., 2013). These studies have revealed that SIRT5 is a major regulator of cellular succinylation, analogous to the major role SIRT3 plays in regulating mitochondrial acetylation.

Somewhat surprisingly, analysis of *Sirt5*-null mice undertaken to date has generally revealed a lack of striking phenotypes (Lombard et al., 2007), though very mild resistance to HFD has been noted (Yu et al., 2013). SIRT5 has been reported to deacetylate (Nakagawa et al., 2009; Ogura et al., 2010), desuccinylate (Du et al., 2011), and deglutarylate (Tan et al., 2014) carbamoyl phosphate synthetase 1 (CPS1), thereby activating this enzyme to detoxify ammonia via the urea cycle for subsequent renal excretion. Consequently, *Sirt5* knockout mice display elevated blood ammonia after a prolonged fast (Nakagawa et al., 2009). SIRT5 represses PDC and succinate dehydrogenase activities; consequently, SIRT5-deficient cells and mitochondria show elevated respiration (Park et al., 2013). SIRT5 promotes HMGCS2 activity and ketone body formation; *Sirt5*-null mice show a modest reduction in ketone levels during fasting (Rardin et al., 2013). An increase in medium- and long-chain acylcarnitines was reported in liver and skeletal muscle of *Sirt5*-null mice, suggesting that SIRT5 deficiency confers a defect in fatty acid oxidation. Other reported SIRT5 targets include SOD1, a key cellular antioxidant enzyme. Mutating the SIRT5 target site in SOD1 inhibits lung tumor cell growth, potentially implicating SIRT5 as a mediator of cancer proliferation via SOD1 activation and cellular ROS protection (Lin et al., 2013).

In light of these targets, perhaps a major physiologic function of SIRT5 might be to suppress the use of glucose (via repression of PDC); while promoting the use of alternative fuel sources, such as amino acids (and hence, detoxification of their metabolic by-products via CPS1 activation), and ketone bodies (via HMGCS2).

One defining feature of cancer cells is the ability to perform aerobic glycolysis to generate ATP, commonly known as the Warburg effect. In the 1920's, Otto Warburg observed that highly proliferative tumor cells consumed glucose to generate large amounts of lactate instead of oxidizing it to produce ATP via oxidative phosphorylation (Warburg, 1956). He then proposed that this was the result reduced oxidative phosphorylation. It has been subsequently demonstrated that many tumor cell lines do not have defective oxidative phosphorylation capacity (Moreno-Sanchez et al., 2007). Two enzymes that play key roles in the TCA cycle, whose intermediates contribute to biosynthetic pathways that produce nucleotide precursors, amino acids and lipids, among others, are PDC and SDH. As discussed above, SIRT5 regulates the activities of these enzymes, thereby impacting many aspects of cellular metabolism. In future studies, it will be of great interest to test SIRT5's roles in response other metabolic stressors, and, analogous to published work on SIRT3, assess potential SIRT5 roles in cancer cell metabolic reprogramming.

Cardiovascular Dysfunction

Cardiovascular disease (CVD), including coronary heart disease and peripheral arterial disease, account for roughly one-third of all deaths in the United States, (Go et al., 2014) and the risk of developing clinically evident CVD increases dramatically in older individuals (Lakatta and Levy, 2003). With advancing age, endothelial cells are increasingly unable to efficiently proliferate to heal vasculature injury or ischemia (Brandes et al., 2005; Ungvari et al., 2010). Aging is associated with atherosclerotic disease and vascular stiffening, predisposing older individuals to hypertension and ischemic injury.

SIRT1

Several studies demonstrate that SIRT1 is essential for vasorelaxation (Mattagajasingh et al., 2007), vasoprotection (Csiszar et al., 2008), endothelial ischemic recovery, and cholesterol metabolism (Potente and Dimmeler, 2008). *SIRT1* knockdown *ex vivo* and *Sirt1* genetic deletion specifically in the endothelial lineage *in vivo* inhibits endothelial cell migration and angiogenesis (Potente et al., 2007). *In vivo* studies in mouse and zebrafish models have identified SIRT1 as a key mediator of endothelial function and vascular growth. In zebrafish, SIRT1 is required for endothelial sprout formation and vessel migration. However, endothelial cell-specific *Sirt1* knockout mice are developmentally unremarkable, though they are unable to revascularize tissue in response to ischemia-induced injury (Guarani et al., 2011)

The pro-angiogenic and vascularization functions of SIRT1 can be rationalized mechanistically through SIRT1's interaction with the FOXO family transcription factors

and the NOTCH signaling pathway (Oellerich and Potente, 2012). FOXO transcription factors, particularly FOXO1, are potent negative regulators of angiogenesis (Paik, 2006; Paik et al., 2007; Potente et al., 2005). SIRT1 deacetylates FOXO1 in endothelial cells, reducing its transcriptional activity and anti-angiogenic function (Potente et al., 2007). NOTCH signaling orchestrates postnatal vascular morphogenesis in a dose-dependent manner. In endothelial stalk cells, NOTCH signaling is inversely correlated with vessel sprouting behavior (Phng and Gerhardt, 2009). SIRT1 deacetylates and destabilizes the NOTCH1 intracellular domain (NICD), promoting its proteasomal degradation and inhibiting NOTCH effector responses (Guarani et al., 2011). Consequently, endothelial cells lacking SIRT1 activity have increased NOTCH signaling, impaired vessel growth and defective sprout elongation. *In vivo*, SIRT1 ablation in zebrafish and mice reduces vascular branching and density due to enhanced NOTCH signaling. Therefore, activation of SIRT1 in endothelial cells may be a useful means to protect endothelial tissue from age-related functional decline, particularly after injury.

Circulating blood flow in the mammalian cardiovascular system induces mechanical stress on the vascular endothelial cells lining the vessel walls. Atheroprotective flow results from undisturbed, steady pulsatile flow in straight sections of the artery, and promotes downregulation of pro-inflammatory pathways (Chien, 2008). When undirected or branched flow patterns occur, for example, at bends in the arterial tree, pro-inflammatory and proliferative pathways are activated. Pulsatile shear (PS) stress thus promotes endothelial homeostasis and benefits vascular physiology via antioxidative and anti-inflammatory effects on vascular endothelial cells. Endothelial

homeostasis in response to PS stress is enhanced by SIRT1. PS stress induces expression of anti-inflammatory and antioxidant genes such as *Sod1* and *Sod2*, an effect that is lost upon knockdown of CaMKKβ (Ca^{2+}/calmodulin-dependent protein kinase kinase). CaMKKβ is an AMPK kinase that phosphorylates and stabilizes SIRT1, and together these two proteins suppress oxidative stress and inflammation. In a sensitized genetic background and in response to an atherogenic diet, increased atherosclerotic lesions are observed in mice lacking either CaMKKβ or SIRT1, indicating that these proteins could conceivably represent clinically relevant targets for intervention to treat age-associated CVD (Wen et al., 2013).

Pathological cardiac hypertrophy (CH) is a response to chronic hypertension or other sources of cardiac injury. Cardiomyocyte metabolism shifts from fatty acid oxidation to glycolysis during CH, likely due to repression of fatty acid oxidation and oxidative phosphorylation genes (Kolwicz and Tian, 2011). SIRT1 interacts with and activates PPARα to inhibit this metabolic switch and the development of hypertrophy via inactivation of NF-κB. Treating mice with the sirtuin activator, resveratrol, attenuates markers of induced CH in wild-type, but not PPARα-null mice (Planavila et al., 2011). Thus, SIRT1 is able to orchestrate metabolic reprogramming and inflammatory responses to protect against development of CH. However, overexpression of both PPARα and SIRT1 in mice impairs mitochondrial function and promotes heart failure during CH, by downregulating genes involved in mitochondrial respiration, oxidative stress and cardiac contractility (Oka et al., 2011). The impact of SIRT1 on CH is highly dose-dependent. As noted previously, SIRT1 transgenic mice are protected from CH

and age-dependent loss of cardiac function when SIRT1 overexpression is relatively modest (up to 7.5-fold higher than basal), but higher levels of SIRT1 overexpression produce deleterious effects on myocardium (Alcendor et al., 2007).

However, another study arrived at conflicting results, and found that *Sirt1*-null mice showed resistance to the development of exercise- or agonist-induced CH (Sundaresan et al., 2011). In this regard, in response to growth factor stimulation, SIRT1 deacetylates and activates AKT and 3-phosphoinositide dependent protein kinase-1 (PDK1), a kinase that activates AKT. AKT is a serine-threonine kinase that is a central player in a network of diverse cellular processes, such as cell proliferation, apoptosis, glucose metabolism, and angiogenesis (Manning and Cantley, 2007). In myocardium, the end result of persistent hyperactive IGF-AKT signaling is hypertrophy and eventual heart failure (Condorelli et al., 2002; Shiojima et al., 2002). SIRT1-deficient hearts are proportionally smaller than those of wild-type mice, and show hyperacetylated hypoactive AKT (Sundaresan et al., 2011). In transgenic CD1 mice, a 4-fold overexpression of SIRT1 specifically in the heart increases AKT activation and results in AKT-dependent hypertrophy, indicating that SIRT1 and AKT activation can induce CH in this strain.

Other sirtuins

Both SIRT3 and SIRT6 negatively regulate CH in part by inhibiting the IGF-AKT signaling cascade. Overexpressing SIRT3 in cultured cardiomyocytes and transgenic mouse lines, or supplementing mice with exogenous NAD^+ precursors, represses the

hallmarks of agonist-induced CH (Pillai et al., 2010; Sundaresan et al., 2009). SIRT3 protects against CH by inducing expression of the antioxidant proteins SOD2 and catalase. The SIRT3-mediated reduction in ROS levels inhibits AKT signaling and downstream gene expression associated with induction of CH (Sundaresan et al., 2009).

In failing human and hypertrophic mouse hearts, SIRT6 protein expression is reduced compared to controls. *Sirt6* gene deletion, specifically in the mouse heart or globally, results in CH, whereas cardiac-specific SIRT6 overexpression protects mice from induction of CH. Mechanistically, SIRT6 negatively regulates CH by co-repressing c-Jun-dependent transcription at the chromatin level, thereby inhibiting downstream IGF-AKT signaling. Importantly, *in vivo* inhibition of IGF signaling in whole-body and cardiac-specific *Sirt6* knockout mice inhibits the hypertrophic response (Sundaresan et al., 2012).

SIRT7 also plays a role in protecting against the development of CH. Mice harboring a *Sirt7* germline deletion develop extensive fibrosis and succumb to CH (Vakhrusheva et al., 2008). The authors propose that SIRT7 deacetylates p53 in the myocardium to suppress p53-driven apoptosis; loss of SIRT7 leads to diminished stress responses and hypertrophy. It is currently unknown whether increased SIRT7 activity might play a cardioprotective role.

SIRT3, SIRT6, SIRT7 and potentially moderate amounts of SIRT1 protect against CH in cell culture and mouse models, through overlapping and distinct mechanisms. It will be of great interest to assess the therapeutic potential of sirtuin activation in patients with CH.

Sirtuin Activating Compounds

High-throughput screens have been conducted to identify small molecule sirtuin-activating compounds (STACs). These studies initially identified resveratrol (RSV) and other polyphenols as SIRT1 activators (Howitz et al., 2003); subsequent studies have identified a large series of artificial, higher potency STACs. Concerns have been raised as to whether these polyphenols actually directly activate SIRT1 (Baur and Sinclair, 2006; Kaeberlein et al., 2005; Pacholec et al., 2010; Park et al., 2012). STACs have been reported to interact with a specific region on the SIRT1 protein (Hubbard et al., 2013). In this regard, a specific amino acid in SIRT1 required for STAC-mediated activation has recently been identified. Cells bearing a SIRT1 mutant at this site do not show the increased mitochondrial copy number and ATP content normally induced by STAC treatment (Hubbard et al., 2013). RSV has been reported to extend longevity in yeast, worms, flies, and short-lived fish (Baur, 2010b); in mammals, RSV supplementation rescues the shortened lifespan of mice on a HFD (Baur et al., 2006). RSV supplementation shifts the gene expression pattern observed in mice on a HFD towards a profile associated with a standard diet. This shift occurs in parallel with improved overall health, insulin sensitivity, increased mitochondrial content and

maintenance of motor function (Barger et al., 2008a; Barger et al., 2008b; Pearson et al., 2008). However, RSV treatment does not extend longevity in mice fed a standard diet (Miller et al., 2011; Pearson et al., 2008).

Despite substantial recent progress (reviewed in (Hubbard and Sinclair, 2014), many key questions remain in this area. For example, which RSV effects occur through SIRT1, and which are due to effects on other targets? Whether RSV and other STACs actually activate mammalian SIRT1 or its paralogs *in vivo*, and if so whether they function via direct mechanisms, or through upstream mediators such as AMPK, has been hotly debated (Baur and Sinclair, 2006; Kaeberlein et al., 2005; Pacholec et al., 2010). In mice, RSV treatment stimulates mitochondrial function, activates AMPK and increases NAD^+ levels. These RSV-induced phenotypes are SIRT1-dependent, though at a higher dose RSV does not require functional SIRT1 to activate AMPK (Price et al., 2012). In response to moderate RSV doses, SIRT1 activates AMPK in the skeletal muscle, which results in an increase in NAD^+ levels through an unknown mechanism to generate a positive feedback loop to maintain mitochondrial function in energetically active tissues. This study places SIRT1 upstream of AMPK activation and proposes a model of sustained sirtuin activation via RSV treatment that results in a net accumulation of NAD^+.

Despite the apparent beneficial effects of RSV and other STACs in multiple systems, in human patients with non-alcoholic fatty liver disease, RSV treatment appeared to exert toxic effects on hepatocytes, and did not ameliorate liver steatosis or insulin resistance

(Chachay et al., 2014). However this study was limited, in that only male participants were included and no assessment of RSV metabolites was reported.

One difficulty with the use of RSV *in vivo* is that it has significant off-target effects (Baur, 2010a). To elucidate the effects of SIRT1 activation more specifically, structurally unrelated synthetic STACs have been evaluated, though off-target effects, if any, of these molecules have not yet been determined. One STAC, SRT1720, extends mean mouse lifespan in response to a HFD by 18% (Minor et al., 2011) and by 8.8% in mice fed a standard diet (Mitchell et al., 2014). Lifelong SRT2104 supplementation, beginning at 6 months of age, extends mean lifespan of male C57BL/6J mice fed a standard diet by 9.7% and increases the maximal lifespan by 4.9% (Mercken et al., 2014b). Although no difference in body weight, caloric intake or physical activity was observed, SRT2104-supplemented mice exhibit a lower percentage of fat mass, decreased fasting blood glucose and insulin levels, and increased skeletal muscle endurance. Microarray analysis revealed that SRT2104 likely has anti-inflammatory properties in skeletal muscle tissue, evidenced by a decrease in expression of NF-κB target genes. SRT2104 protects against experimentally induced muscle atrophy in wild-type mice, and muscle-specific *Sirt1* knockdown *in vivo* accelerates muscle loss. Also, SIRT1-dependent stimulation of osteogenic differentiation by SRT2104 treatment was reported using myoblast cell cultures, suggesting SRT2104 activates SIRT1 to protect against age-related muscle loss and osteoporosis.

Non-allosteric methods to activate sirtuins have also received intense scrutiny as an alternative to STACs. Pharmacologically increasing cellular NAD^+ levels by supplementation with NAD^+ precursors such as NR and NMN, or inducing expression of NAMPT to convert NAM to NAD^+ more efficiently, have recently provided alternative means of promoting sirtuin function (Canto et al., 2012; Yoshino et al., 2011) (Figure 1.6). For example, in a mouse model of T2D, NMN supplementation mitigates negative metabolic effects – insulin insensitivity, glucose intolerance and inflammation – of age-related or diet-induced diabetes, potentially due to the activation of SIRT1 and other sirtuins, and their downstream target pathways (Yoshino et al., 2011). Also, mice lacking the NAD^+-consuming enzyme CD38 have increased cellular NAD^+ and SIRT1 activity in several metabolically active tissues (Barbosa et al., 2007). These mice are highly resistant to weight gain in response to a HFD relative to controls. One caveat in interpreting any findings involving NAD^+ modulation is that increased NAD^+ levels may activate not only sirtuins, but also additional NAD^+-dependent enzymes, such as PARP1. In the context of CD38-deficient mice, protection against weight gain was lost when animals were treated with a sirtuin inhibitor, implicating sirtuin activation in this effect. Phenotypes resulting from increased NAD^+ levels must be rigorously elucidated in model organisms before use of these non-allosteric approaches can be attempted in humans.

Conclusion

Sirtuin proteins comprise a group of nutrient- and stress-responsive factors that regulate diverse cellular processes to promote healthspan, and in the case of two sirtuins, SIRT1 and SIRT6, lifespan extension when overexpressed in otherwise wild-type mice. While increased dosage of the prototypical sirtuin, *SIR2*, was reported to extend replicative lifespan of yeast over a decade ago, the first hints that sirtuins might increase mammalian longevity have emerged only recently. Greater attention will now focus on tissue-and cell-type specific roles for sirtuins, as well as their regulation under varied dietary conditions. Such work, using sophisticated mouse models with tissue- and temporal-specific sirtuin overexpression or ablation, is already well underway.

One obvious question arising from even a casual review of the sirtuin literature is why so many discrepant results have been reported. Generally speaking, strain differences (both in invertebrates and in mice), and differences in experimental protocols may account for many of these differences. However, the specific biology of sirtuin proteins offers another potential explanation for these discrepancies. Sirtuins require NAD^+ for activity, levels of which are regulated by cellular nutrient status, organismal diet, stress conditions, and even organismal age. Thus, sirtuin activity is likely to be highly sensitive to laboratory environmental conditions, potentially leading to different experimental results from different labs. In all likelihood, sirtuins did not evolve to promote longevity *per se*, but rather to maintain metabolic homeostasis in the face of varied nutrient intake

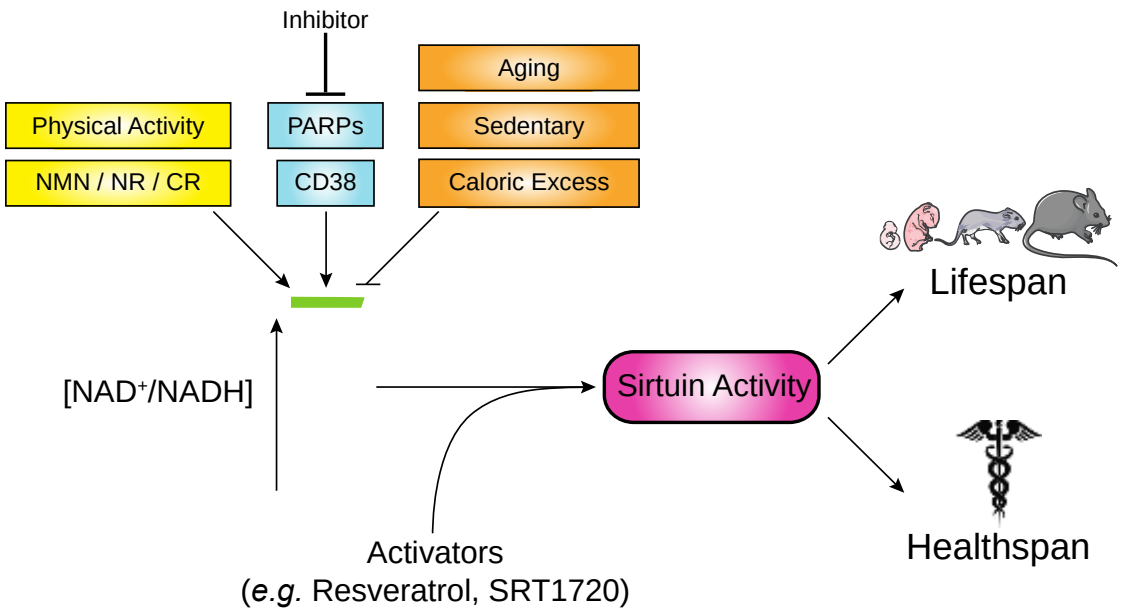

Figure 1.6 Means of sirtuin activation. Allosteric sirtuin activation with small molecules, with the goal of promoting healthspan and longevity, has been an area of intense investigation. An increase in the cellular NAD^+/NADH ratio will increase sirtuin activity. NMN, nicotinamide riboside (NR) supplementation, calorie restriction (CR) or physical activity increases cellular NAD^+ levels. Inhibition of NAD^+- consuming enzymes, poly[ADP-ribose] polymerases (PARPs) or CD38, also enlarges the cellular NAD^+ pool. Reduced NAD^+ levels induced by advanced age, caloric excess, or a sedentary lifestyle would impair activity of sirtuins and other NAD^+-dependent cellular processes.

and other environmental stressors, a task that requires co-regulation of numerous substrates in several pathways.

A consequence of sirtuin NAD^+-dependence is that a chronic decline in NAD^+ levels would be predicted to impair sirtuin activity, resulting in metabolic decline, progressive loss of homeostatic maintenance, and ultimately facilitate the onset of disease states resembling those described in sirtuin loss-of-function models. This may be relevant during organismal aging. Notably, an age-related decrease in NAD^+ levels have been reported in *C. elegans* (Mouchiroud et al., 2013), in several tissues of mice and rats

(Braidy et al., 2011; Braidy et al., 2014; Mouchiroud et al., 2013; North et al., 2014; Ramsey et al., 2008), and in the skin of elderly humans (Massudi et al., 2012). In this context, supplementation with NAD^+ would be predicted to mitigate some age-associated phenotypes, and could promote longevity by maintaining sirtuin-mediated homeostatic control in older organisms. Restoration of cellular NAD^+ levels via supplementation with NAD^+ precursors NR or NMN has been reported in heart and testes from old mice (North et al., 2014), and can protect against diet-induced obesity (Canto et al., 2012), restore the decline in mitochondrial function in aged mice (Gomes et al., 2013), rescue the age-related depletion of the neural stem/progenitor cell pool (Stein and Imai, 2014), and extend lifespan of *C. elegans* (Hashimoto et al., 2010; Mouchiroud et al., 2013; Schmeisser et al., 2013). It will be of great interest to test sirtuin function and longevity in mouse strains with chronically elevated NAD^+ levels; however, the desirability and safety of sustained sirtuin hyperactivity are still somewhat unclear.

Much attention has been given to effects of sirtuin overexpression; in this regard, it is clear from work both in invertebrates (Whitaker et al., 2013) and mice (Alcendor et al., 2007) that the effects of sirtuin overexpression are exquisitely sensitive to expression levels, as might be predicted with pleiotropic regulators that modify a host of downstream proteins. Tissue-specific effects of sirtuins are also highly relevant in this regard. For example, in the BRASTO mouse lines high levels of SIRT1 overexpression in other hypothalamic nuclei were associated with loss of the beneficial effects of DMH-

and LH-specific overexpression. This may imply that SIRT1 exerts opposing, region-specific pro- and anti-longevity effects in the hypothalamus (Satoh et al., 2013).

A great deal of interest exists in the potential for manipulating sirtuin activities as a treatment for various pathologic conditions, including cancer, neurodegeneration, metabolic dysfunction, and others. One means of achieving this is through modulating levels of NAD^+, the critical co-factor for sirtuin activity (Figure 1.6). For example, NAD^+ concentrations and SIRT1 activity increase in skeletal muscle in response to CR, fasting and exercise, whereas a decrease in the NAD^+/NADH ratio is observed in mice challenged with excess caloric intake (Canto et al., 2010; Chen et al., 2008; Kim et al., 2011a). Altered NAD^+ would theoretically affect activities of all sirtuins, though this has yet to be thoroughly tested. However, mitochondrial NAD^+ levels can be regulated independently of those in other compartments (Yang et al., 2007) implying that it might be possible to target mitochondrial versus non-mitochondrial sirtuins differentially.

In response to DNA damage, activated PARPs deplete intracellular NAD^+ through the transfer of ADP-ribose from NAD^+ to its substrates. Activation of SIRT1 upon genetic deletion or pharmacologic inhibition of PARP in skeletal muscle or brown adipose tissue in mice results in higher energy expenditure, increased mitochondrial content and protection from metabolic dysfunction (Bai et al., 2011a; Bai et al., 2011b). By contrast, nuclear PARP1 deficiency does not enhance SIRT2 or SIRT3 activity, implying that therapies directed at enhancing NAD^+ levels might have unexpected sirtuin-specific effects. This may indicate that mammalian sirtuins differ with respect to their affinities

for NAD^+ *in vivo*. Similarly, CD38 is a cell surface receptor on lymphocytes that catalyzes the synthesis and hydrolysis of cyclic ADP-ribose using NAD^+ as the precursor. In cells lacking CD38, NAD^+ levels rise and SIRT1 activity increases, conferring protection against diet-induced obesity and glucose tolerance in response to high fat intake (Barbosa et al., 2007). In light of all of these findings, a new avenue of sirtuin activation via modulation of cellular NAD^+ levels has emerged (Figure 1.6). It will be critical to assess the safety and efficacy of these interventions, and whether they are able to specifically activate nuclear sirtuins, or act more broadly.

Although the known repertoire of sirtuin functions continues to expand, little research to date has focused on functional interactions between the seven sirtuins, in the context of redundancy or antagonism. Several key cellular proteins (*e.g.* c-MYC, p53, HIF-1α, CPS1, GDH, and many others) are targets of multiple sirtuins. In some cases, sirtuins act in opposition to one another (*e.g.* SIRT3 and SIRT5 on SDH, SIRT3 and SIRT4 on GDH). How this functional opposition is achieved *in vivo* -- and its physiological significance -- when all sirtuins are NAD^+-responsive remains somewhat mysterious. Other means of sirtuin regulation may be relevant in this regard, occurring through protein-protein interactions, regulation of sirtuin expression levels, post-translational modifications, levels of metabolites such as free fatty acids, and other mechanisms. Future studies will explore these issues, for example via analysis of compound sirtuin mutant mouse models.

Furthermore, sirtuins do not act in isolation to promote vertebrate healthspan and lifespan. mTOR signaling and IIS regulate lifespan in evolutionarily distant organisms (Lopez-Otin et al., 2013). These pathways overlap with sirtuin function in multiple contexts. For example, SIRT1 regulates insulin secretion and insulin signaling at numerous levels, and several reports point to roles for SIRT6 in suppressing IIS and mTORC1 signaling (Hong et al., 2014; Kanfi et al., 2012; Sundaresan et al., 2012; Xiao et al., 2010). To further complicate matters, some sirtuins have redundant functions that may need to be targeted simultaneously in order to elicit biological effects. Both SIRT1 and SIRT2 regulate mTORC1 signaling, for instance, at the level of S6 kinase (Hong et al., 2014).

In the past 15 years, a large body of research has illuminated complex relationships between mammalian sirtuins, healthspan, and even longevity. It is clear that these proteins can exert beneficial effects in the context of important diseases of aging, and may therefore represent therapeutic targets in this context. However, a mechanistic understanding of these effects is still incomplete; no doubt this work will provide fruitful avenues for the next 15 years of sirtuin research.

In this thesis, I explore the roles for sirtuins in maintaining mammalian lifespan and healthspan, specifically SIRT1 and SIRT5. In chapter 2, I focus on SIRT1 and its role in maintaining pericentromeric heterochromatin, a structure essential for proper chromosomal function and segregation. I use a naturally aged mouse model to implicate SIRT1 as a cause of age-associated epigenetic decline, and suggest a means

of preventing such a dysfunction by SIRT1 overexpression. In chapter 3, I describe the mitochondrially localized SIRT5 as a pro-survival factor for human melanoma. As indicated above, SIRT5 has received little attention, in contrast to SIRT1, in terms of its role in modulating oncogenesis. Data in this chapter will serve as an important scaffold for future research regarding SIRT5 as a therapeutic target in melanoma. Finally, in chapter 4, I give an overview, discuss potential future directions and summarize my findings.

Acknowledgements

I thank Dr. John Denu and members of the Lombard lab for helpful discussions. Some graphics in the figures were obtained and modified from Servier Medical Art from Servier (http://www.servier.com/Powerpoint-image-bank). The final published version of this chapter appears in the Handbook of the Biology of Aging (Giblin, W., and Lombard, D.B. (2016). Chapter 3 - Sirtuins, Healthspan, and Longevity in Mammals. In Handbook of the Biology of Aging (Eighth Edition) (San Diego: Academic Press), pp. 83-132.). The chapter is reproduced with permission from the publisher: Elsevier License Number 3994350095188.

CHAPTER 2

Age-Associated Epigenetic Dysregulation in Mouse Heart

Abstract

Epigenetic alterations are a conserved feature of biological aging in diverse organisms, and have been designated as a “hallmark of aging”. Chromatin organization – in particular, diminished heterochromatinization of repetitive regions – is progressively lost during cellular and organismal aging. Experimentally, work in *S. cerevisiae* has revealed an age-associated loss of chromatin structure, and elucidated its deleterious impacts on gene expression and genomic stability. The first example of age-associated heterochromatin perturbation in mammals was identified in a seminal study over 25 years ago by Gaubatz and Cutler, JBC, 1990. This work focused on the Major Satellite Repeats (MSRs), pericentromeric repeats in the mouse that help to ensure proper chromosomal segregation and maintenance of euploidy. This study showed that MSR repression is lost during aging specifically in mouse myocardium. The mechanistic basis for this effect has never been elucidated.

In this chapter, we demonstrate that MSR derepression is not associated with decreases in levels of the canonical repressive marks – DNA methylation, H3K9me3, or H3K56me3 – at the MSRs. Instead, levels of the activating marks, H3K9ac and

H4K16ac, targets of the SIRT1 deacetylase, increase during aging in the heart. These findings have led to the hypothesis that loss of SIRT1 activity contributes to derepression of MSR loci in aged myocardium. Consistent with this hypothesis, we have found that *Sirt1* deletion results in increased MSR expression in heart tissue. We also find that the pro-longevity intervention calorie restriction (CR) attenuates MSR derepression in aged mice. We then present data that suggests that SIRT1 activity maintains chromatin structure and transcriptional silencing at the MSRs, in part using aged muscle-specific SIRT1 overexpressors.

Introduction

Epigenetic alterations are a conserved feature of biological aging in diverse organisms, and have been designated as a "hallmark of aging" (Lopez-Otin et al., 2013). Many laboratories have catalogued changes in levels of epigenetic marks on both DNA and histones that occur during aging. Experimental manipulation of epigenetic regulators can produce marked improvements in health- and lifespan. Epigenetic changes may represent attractive targets for restorative therapies aimed at slowing or even reversing aspects of the aging process, since epigenetic damage is at least in principle amenable to repair (Rando and Chang, 2012).

Maintenance of heterochromatin – tightly packaged chromatin with low levels of transcriptional activity – represents an important aspect of overall epigenetic fidelity. Heterochromatin has been postulated to represent a major target of age-associated

epigenetic deterioration (Imai and Kitano, 1998; Villeponteau, 1997). The first example of age-associated heterochromatin perturbation in vivo was identified in a seminal study 25 years ago (Gaubatz and Cutler, 1990). This work focused on the Major Satellite Repeats (MSRs), pericentromeric repeats in the mouse that play roles in ensuring proper chromosomal segregation and maintenance of chromosomal number. This study showed that MSR repression is lost during aging specifically in mouse myocardium (Gaubatz and Cutler, 1990). The mechanistic basis for this effect has never been elucidated, despite current intensive research interest in links between epigenetics and aging.

More recently, it has been reported that expression of several classes of repetitive elements, *i.e.* MSRs and long and short interspersed nuclear elements (LINEs and SINEs), rises in aged mouse liver and skeletal muscle, an increase that is attenuated by calorie restriction (De Cecco et al., 2013b). Histone H3K9 trimethylation mediated by the Su(var)3-9 methyltransferases homologs 1 and 2 (Suv39H1/2) plays a major role in MSR silencing (Lehnertz et al., 2003b). In Suv39H1/2 knockout mouse embryonic fibroblasts, loss of MSR transcriptional silencing occurs, along with increased chromosomal missegregation and aneuploidy (Lehnertz et al., 2003b; Peters et al., 2001).

The work presented in this chapter provides mechanistic insight into this long-standing observation in aging biology. Using northern blot analysis, we have found that age-associated MSR depression is mostly restricted to myocardium. Surprisingly, this

phenomenon is not associated with decreases in levels of the canonical repressive marks: DNA methylation or histone H3 lysine 9 trimethylation (H3K9me3). Instead, levels of the activating marks, acetylation of histone H3 lysine 9 (H3K9ac) and H4 lysine 16 (H4K16ac), increase during aging in the heart. This suggests that loss of activity of the NAD^+-dependent deacetylase SIRT1 may contribute to age-associated MSR derepression. We have assayed heart tissue from mouse strains individually deficient in several nuclear sirtuins, and find that SIRT1-deficient mice, but not the other strains, show premature MSR derepression, phenocopying the effects of aging.

Moreover, we have found that the pro-longevity intervention calorie restriction attenuates MSR derepression in aged mice. CR has been shown to increase levels of the sirtuin co-substrate, NAD^+, in some contexts. We then test the hypothesis that increased NAD^+ levels achieved by genetic and pharmacological means will augment SIRT1 activity and suppression of MSR expression in aged mice

Roles for epigenetic changes in age-associated cellular dysfunction represent a major current focus of biogerontology research. These studies have provided new mechanistic insight into the first example of age-associated heterochromatin perturbation identified, loss of MSR repression in myocardium. It has recently been shown that enhanced ploidy maintenance in myocardium is associated with improved cardiac performance in older animals (Baker et al., 2012). Advancing age is a major risk factor for many forms of cardiovascular disease, the single greatest cause of overall worldwide mortality (Barquera et al., 2015). This work provides insight into potential

means of enhancing myocardial heterochromatin maintenance and cardiac function in older individuals.

Results

Major Satellite Repeat Expression Increases in the Aged Myocardium

Major Satellite Repeats (MSRs) are transcriptionally inert, heterochromatinized regions flanking the centromeric minor satellite repeats present in every mouse chromosome (Figure 2.1 A.). This is a major type of repetitive element, as it is comprised of 234bp monomers, accounting for ~10% of the mouse genome (Garagna et al., 2002; Pardue and Gall, 1970; Prashad and Cutler, 1976; Vissel and Choo, 1989; Waring and Britten, 1966). Using RNA extracted from aged mouse tissue, Gaubatz and Cutler, in 1990, reported a progressive loss of silencing of the MSR, beginning at around 1 year of age and persisting to 32 months of age (Figure 2.1 B.) (Gaubatz and Cutler, 1990). Interestingly, this report demonstrated that expression of MSR RNA is undetectable at any age tested in the brain and liver of these aged mice. Using a similar approach, we sought to expand upon this finding to begin to delineate the mechanistic basis of MSR silencing failure. As the MSR monomers are repeated upwards of 10,000 times, transcription initiation within these regions would then generate variable length transcripts (Figure 2.2 A.). Genetic deletion of the SUV39H1 and H2 homologs in mouse embryonic fibroblasts (MEFs) results in an increase in MSR expression (Lehnertz et al., 2003b; Peters et al., 2001). Using RNA extracts from these cell lines

A.

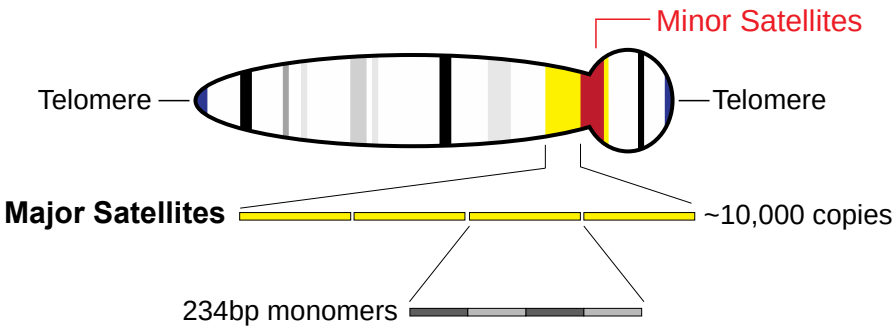

B.

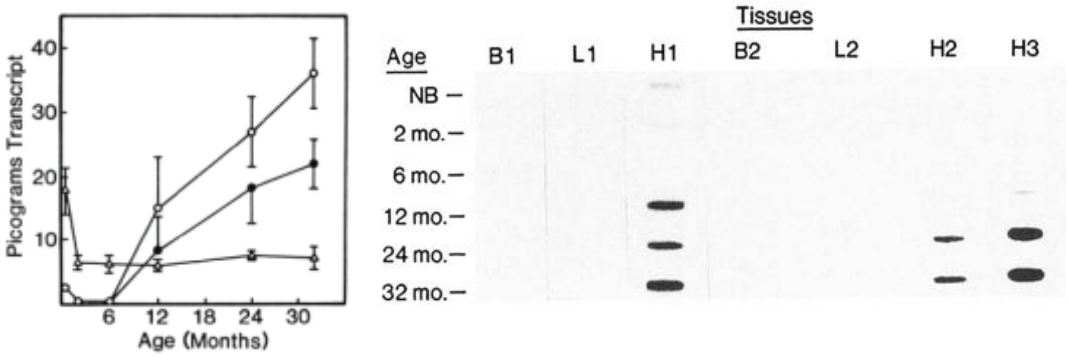

adapted from Gaubatz and Cutler, JBC 1990
(reproduced in accordance with JBC Copyright Permission Policy)

Figure 2.1 MSR silencing is lost during aging in cardiac tissue. **A**. Schematic of repetitive elements in the mouse genome. Minor satellites compose the centromeric region (red), while pericentromeric constitutive heterochromatin consisting of the major satellites are in yellow. Interspersed repetitive elements and telomeric sequences are illustrated in gray. **B**. Slot blotting of aged mouse tissues follow by hybridization of a radioactive MSR probe as reported by Gaubatz and Cutler, 1990, suggest that loss of pericentromeric heterochromatin specifically in heart tissue occurs with age. B, brain; L, liver; H, heart. (right panel). Quantification of MSR transcript at each age is graphed in the left panel.

as a positive control, we assessed the induction of MSR expression in C57BL/6 male mouse heart tissue. We dissected mice of three different age groups: Young (2-3-month-old), Middle Aged (12-14-month-old), and Old (22-24-month-old), and subjected DNA-free RNAs to northern blotting using a radiolabeled probe complementary to the MSR sequence. As expected and previously reported, SUV39H double-knockout (DKO) MEFs and old mouse heart samples have

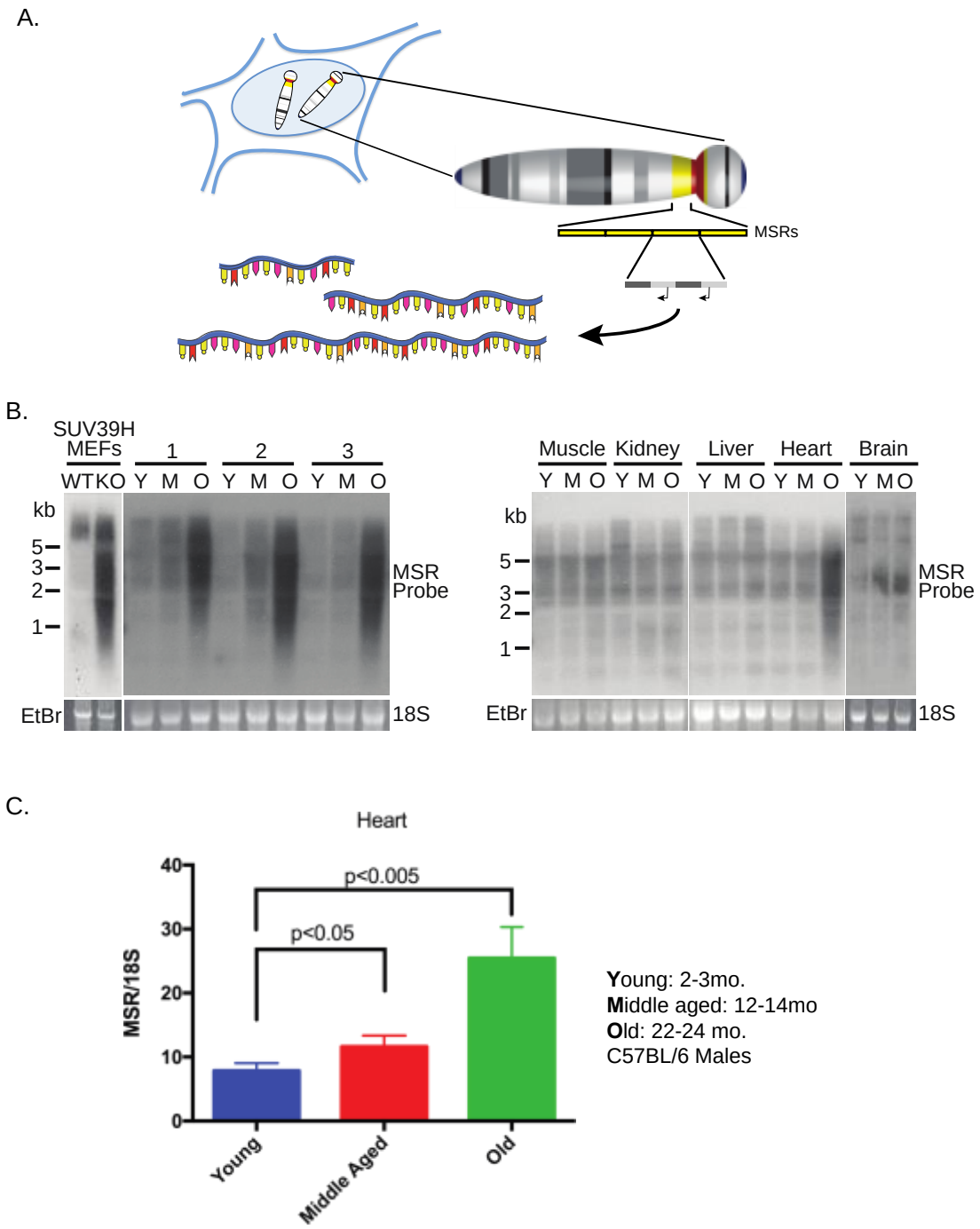

Figure 2.2 MSR expression is increased specifically in the aged myocardium. **A**. Northern blotting of MSR expression generates RNAs of heterogeneous length. **B.** DNA-depleted RNA extracted from young (Y), middle aged (M), or old (O) mouse heart (left panel) and other tissues (right panel) was northern blotted with a radiolabeled riboprobe hybridizing to the sense strand of the MSR transcript. Upper panel, northern blot; lower panel, ethidium bromide stained gel of 18S rRNA. MSR, major satellite repeat; EtBr, ethidium bromide. RNA extracted from various tissues is indicated. Positive controls wild-type (WT) or SUV39H1/2 double-null (SUV39H KO) immortalized MEFs are indicated. **C.** Quantification of MSR expression (**B**.), normalized to 18S rRNA.

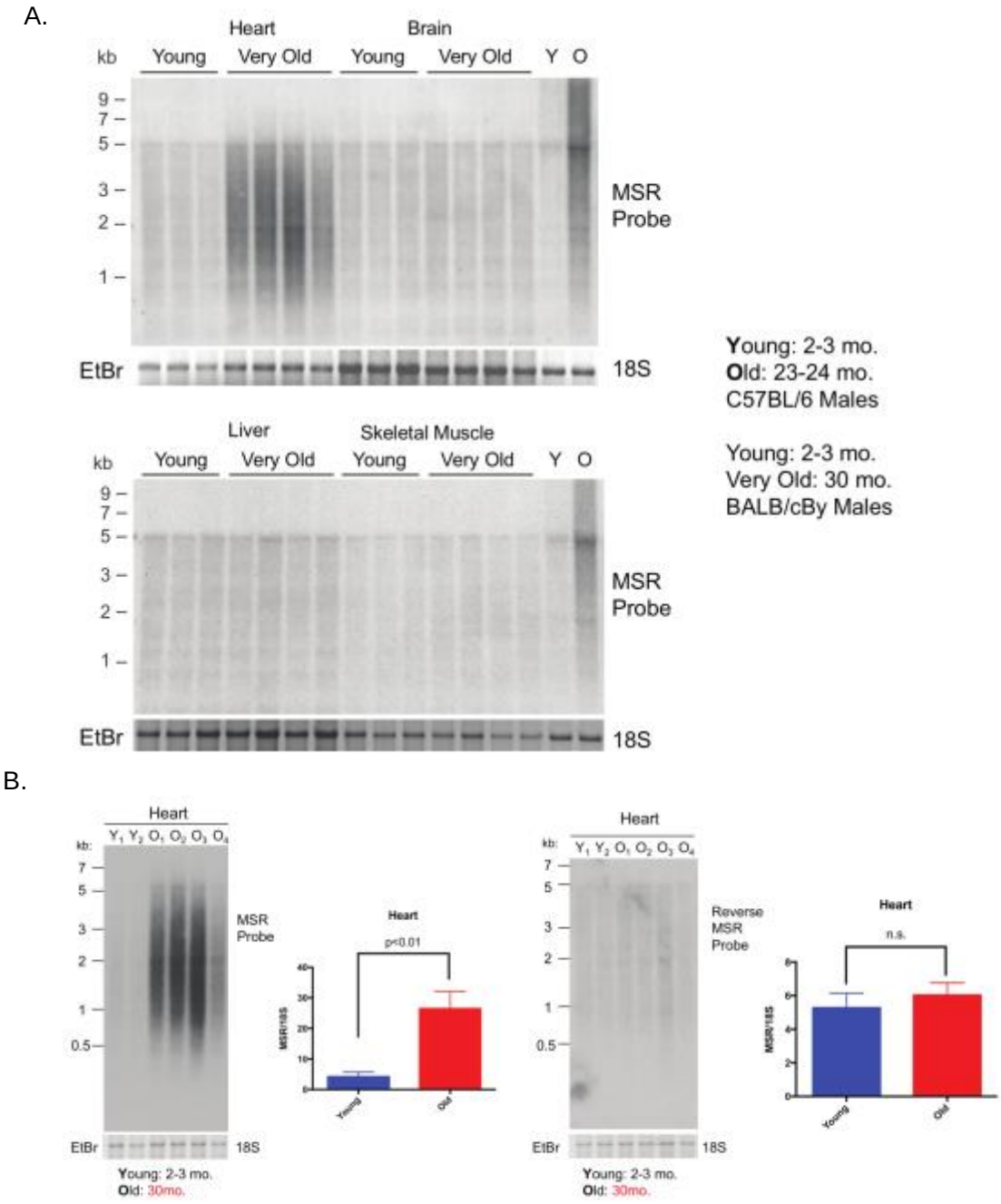

Figure 2.3 MSR expression is restricted to the heart in 30-month-old mice. **A**. Northern blot analysis of MSR expression in various tissues, as indicated, in very old (30-month-old) mice compared to young (2-3-month-old) BALB/cBy mice. Positive controls: Y, young and, O, old C57BL/6 mice as indicated. **B**. Quantification of MSR expression normalized to 18S rRNA in young versus very old mice using a riboprobe complementary to the sense MSR strand (left panel) and using a riboprobe complementary to the anti-sense ("reverse") MSR strand (right panel). Upper panel, northern blot; lower panel, EtBr stained gel of 18S rRNA. MSR, major satellite repeat.

an increased concentration of MSR transcript (Figure 2.2 B.). Also noted is the expected “smear,” representing MSR transcripts of variable size, typically ranging from 0.5 to greater than 5kb in length. To further investigate this phenotype, RNAs extracted from skeletal muscle, liver, kidney and the brain were subjected to MSR northern blotting (Figure 2.2 B.). The most robust age-associated MSR expression, when normalized to the 18S ribosomal RNA (rRNA), was detected in the mouse heart, again as predicted (Figure 2.2 C.). Although, an increase in MSR expression in other tissues, such as brain, liver and skeletal muscle has been reported (De Cecco et al., 2013a; Oberdoerffer et al., 2008), these studies rely on qRTPCR-based methods, which have proved unreliable in our hands. Hence, these data focused our attention on the use of northern blotting and the heart as a model for age-associated epigenetic decline. Although at 22-24 months of age, the mouse heart presents with the most striking increase in MSR expression among tissues tested, we asked if one reason for the discrepancy between these results and those published is one of biological age. That is: Do different tissues age at different rates in terms of MSR derepression? If so, then one might expect an increase in MSR expression at latter stages of life in other tissues. To test this hypothesis, we procured 30-month-old BALB/c mice from the NIA and subjected their tissues to MSR northern blotting. The percent survival of this strain of mice at the 30-month-old timepoint is 25%, compared to the 75% survival rate of 24-month-old animal (https://www.nia.nih.gov), indicating the advanced geriatric state of these animals. A significant ($p<0.01$) increase in MSR expression, as observed in the C57BL/6 strain, was detected specifically in the heart, and not in the brain, liver or skeletal muscle (Figure 2.3 A.). Furthermore, the magnitude of MSR expression (a 4-6

fold increase), as normalized to the 18S rRNA, is consistent with that observed in C57BL/6 male mice (Figure 2.2 C., compare young versus old). The use of qRTPCR to determine MSR expression levels would detect MSR RNA emanating from either DNA strand in the genome. To confirm that an increase of MSR RNA originates from only one strand, northern blotting of the same young and old heart RNA samples was done using a radiolabeled probe complementary to the reverse MSR strand (Figure 2.3 B., "reverse MSR probe"). No change in "reverse" MSR transcript abundance was apparent in aged samples. Thus, taken together, these data demonstrate that MSR transcription produces variable length transcripts emanating from one strand of the DNA, and is robustly induced specifically in the myocardium of at least two different strains of aged mice.

Age-Associated MSR Expression is Mechanistically Distinct from SUV39H Loss

Given that MSR expression increases in SUV39H DKO cell and specifically in aged heart tissue (Figure 2.4 A.), we reasoned that post-translational modifications (PTMs) of histones in the aged heart tissue would parallel those detected in a SUV39H DKO context. Via western blotting analysis of PTMs of histones associated with heterochromatin in aged heart tissue, this phenomenon is not associated with decreases in levels of the canonical repressive marks: histone H3 lysine 9 trimethylation (H3K9me3) and H3 lysine 56 trimethylation (H3K9me56), as described in SUV39H DKO

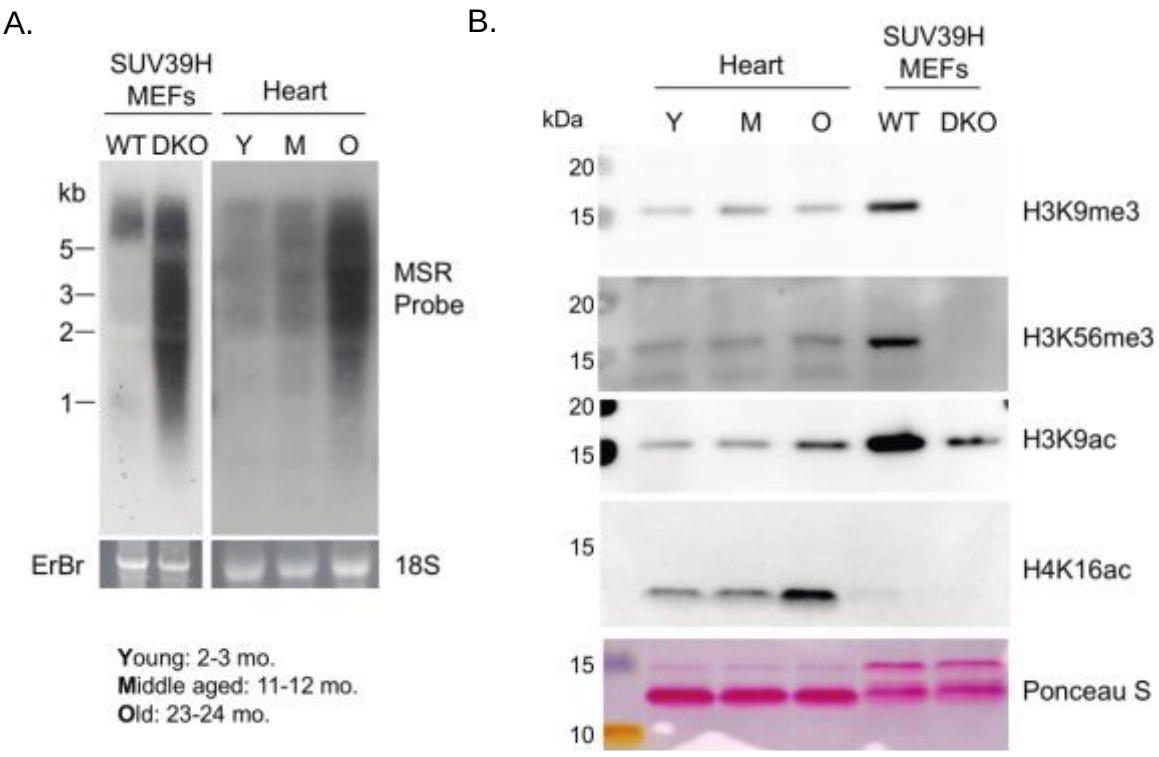

Figure 2.4 Loss of SUV39H-mediated MSR silencing is molecularly distinct from age-associated MSR derepression. A. Northern blotting for MSR expression in wild-type (WT) and SUV39H1/2 double knockout (DKO) MEFs (left panel) and aged heart tissue, as indicated (right panel) reveals increased MSR expression in SUV39H DKO MEF and aged heart samples. **B.** Immunoblotting analysis of samples indicated in (**A.**) for histone PTMs associated with heterochromatin. Membranes were probed for the indicated antibodies. H3K9me3, Histone H3 lysine 9 trimethylation; H3K56me3, Histone H3 lysine 56 trimethylation; H3K9ac, Histone H3 lysine 9 acetylation; H4K16ac, Histone H4 lysine 16 acetylation. Ponceau S indicates equivalent amounts of histones in the loaded whole-cell lysates.

samples. Instead, levels of the activating marks, acetylation of histone H3 lysine 9 (H3K9ac) and H4 lysine 16 (H4K16ac), which are targets of the NAD^+-dependent SIRT1 deacetylase, increase during aging in the heart (Figure 2.4 B.).

A reduction of DNA methylation within the MSR regions of SUV39H DKO MEFs has been reported (Lehnertz et al., 2003b), which prompted the hypothesis that DNA

methylation at MSR loci is lost in aged myocardium. Using methyl-sensitive restriction DNA endonucleases, followed by Southern blotting with a radiolabeled MSR DNA probe, we have found that MSR DNA is not hypomethylated in aged tissue (Figure 2.5 B.). DNA demethylation is thought to be mediated by the TET dioxygenases that convert 5-methylcytosine to cytosine via several intermediates, such as 5-hydroxymethylcytosine (Huang and Rao, 2014). It has been proposed that 5-hmC is a stable mark that has a role in modulating gene expression (Guibert and Weber, 2013). We therefore tested the hypothesis that these intermediates are enriched in DNA extracted from aged heart tissue (Figure 2.5 A.). Dot blotting of 2-fold serial dilutions of genomic DNA extracted from young, middle-aged and old mouse hearts, followed by incubation with antibodies specific to 5-hydroxymethylcytosine (5-hmC), reveals a significant ($p<0.05$) increase in 5-hmC levels in aged tissue. Loss of the chromatin-bound sirtuin, SIRT6, in mouse embryonic stem cells results in an increase in 5-hmC (Etchegaray et al., 2015), and was used as a positive control. Thus, via PTM and DNA methylation analysis, MSR derepression in age mouse heart does not parallel previously reported perturbations that occur upon SUV39H inhibition. These findings led to the hypothesis that loss of SIRT1 activity contributes to derepression of MSR loci observed in the aged myocardium.

SIRT1 Loss Accelerates Age-Associated MSR Derepression

It has been proposed that accumulation of low-level chronic genotoxic stress induces SIRT1 relocalization from MSRs and other loci to sites of DNA damage, thereby

progressively derepressing MSR expression in the mouse cortex (Oberdoerffer et al., 2008). Since histone targets of SIRT1 accumulate at the bulk level in the mouse upon aging (Figure 2.4 B.), we reasoned that loss of SIRT1, specifically in the muscle, would predispose this tissue to MSR derepression and result in increased MSR expression. To test this hypothesis, we analyzed by MSR northern blotting, MSR expression in SIRT1-deficient heart tissue. A recent report has also implicated SIRT2 in facilitating MSR silencing, by H4K16ac deacetylation and recruitment of the PR-Set7 methyltransferase (Serrano et al., 2013). In light of these findings, we included germline knockout samples of several of the sirtuins known to localize to the nucleus: SIRT2, SIRT6, and SIRT7 (Figure 2.6 B.). Loss of SIRT1, but not the other nuclear sirtuins resulted in robust MSR expression in the mouse heart; however, a slight increase in MSR signal is noted in one of the SIRT7 knockout samples. To further investigate this finding, we tested expression by immunoblot of these sirtuins in aged mice, and found that SIRT2, SIRT6 and SIRT7 protein levels do not change with age when normalized to GAPDH in the mouse heart (Figure 2.6 A.). These data imply that SIRT1 is a key mediator in MSR silencing, which prompted the question: Do SIRT1 protein levels or activity decrease with age? To begin to answer this question we tested, again by immunoblot, the steady state levels of SIRT1 in young versus aged heart tissue, and found that total SIRT1 protein remains constant with age (Figure 2.7, bottom panel). Crucially, SUV39H protein levels also remain constant with age, highlighting the distinct nature of age-associated MSR derepression from SUV39H deficiency (Figure 2.7, top panel).

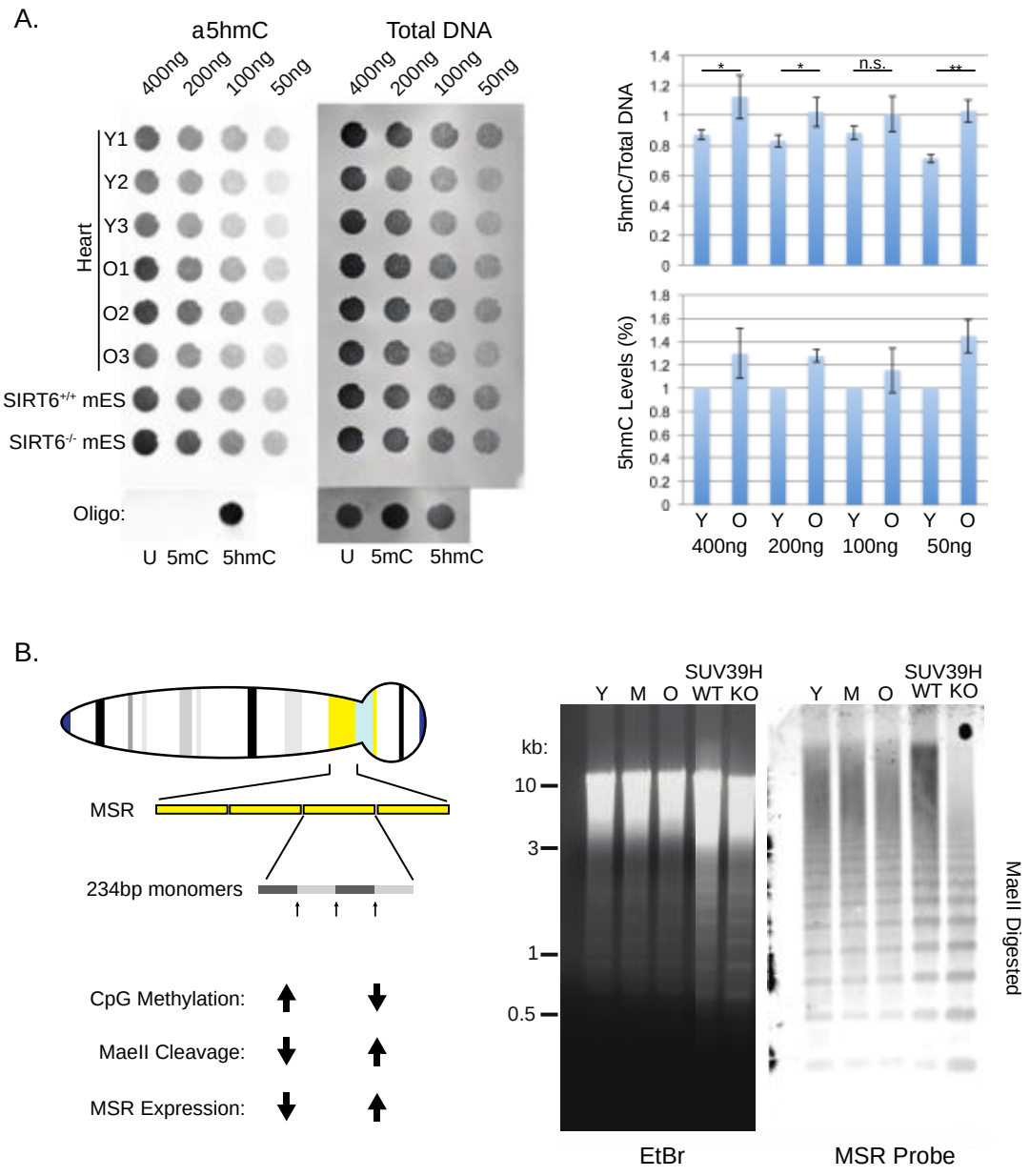

Figure 2.5 5-Hydroxymethylcytosine is increased in aged heart tissue. A. Two-fold serial dilutions of genomic DNA extracted from young (Y) or old (O) mouse heart were probed with anti-5hmC and subjected to chemiluminescent immunoblotting. Equal DNA loading was confirmed using the SYBR Gold fluorescent nucleic acid stain. Antibody specificity was determined using unmodified (U), 5-methylcytosine (5mC), and 5-hydroxymethylcytosine (5hmC) oligonucleotides as indicated (left panel). The ratio of 5hmC to total DNA is plotted in the top graph, while the percent of 5hmC levels in old vs young is plotted in the bottom graph (right panel). Quantification was performed with ImageJ, *p<0.05, **p<0.01. **B**. Genomic DNA extracted from young (Y), middle aged (M), old (O) mouse heart, and WT and SUV39H-deficient MEF cell lines was digested with the methyl-sensitive restriction enzyme, MaeII. Equal amounts of DNA were separated on a 1% agarose gel, and transferred to a membrane for Southern blot analysis using a radiolabeled MSR probe, as indicated.

Modulation of MSR Expression Via NAD^+ Enhancement

NAD^+ is a required co-substrate for sirtuin activity (Figure 1.1). Intense research into modulating NAD^+ to promote mammalian lifespan and healthspan has resulted in a growing body of evidence suggesting that NAD^+ levels decline in mammalian tissues during aging (Imai and Guarente, 2014), including the heart (North et al., 2014). This reduction in NAD^+ predisposes organisms to phenotypes associated with sirtuin loss-of-function. In this regard, aged hearts show biochemical evidence of impaired SIRT1 and SIRT3 function (Hafner et al., 2010; Porter et al., 2014). Administration of the NAD^+ precursors nicotinamide riboside (NR) or nicotinamide mononucleotide (NMN) reconstitutes cellular NAD^+ levels and protects against diet-induced obesity and reduced mitochondrial function in aged mice (Canto et al., 2012; Gomes et al., 2013).

The ability to modulate sirtuin function via NAD^+ fluctuation allows us to test the ability of increased NAD^+ to activate SIRT1, thereby mitigating the effects of age on MSR derepression. To test this model, we first used the well-established pro-longevity intervention, calorie restriction (CR). CR without malnutrition is a robust and reliable method to extend lifespan in all species tested (Guarente, 2013; Vaquero and Reinberg, 2009). CR has been reported to increase cellular NAD^+ levels and maintain genomic stability through the maintenance of chromatin, potentially though the activity of SIRT1 and other sirtuins (Figure 2.8). Upon MSR northern blotting analysis of mice fed a calorie-restricted diet (60% of the *ad libitum* cohort), MSR expression, though variable, is strikingly decreased at both 12-14 months of age (M) and at 22-24 months of age (O)

(Figure 2.8, right panel). While the cellular NAD^+ concentration is unknown in these mice, these data are consistent with the hypothesis that increased SIRT1 activity upon CR promotes MSR silencing.

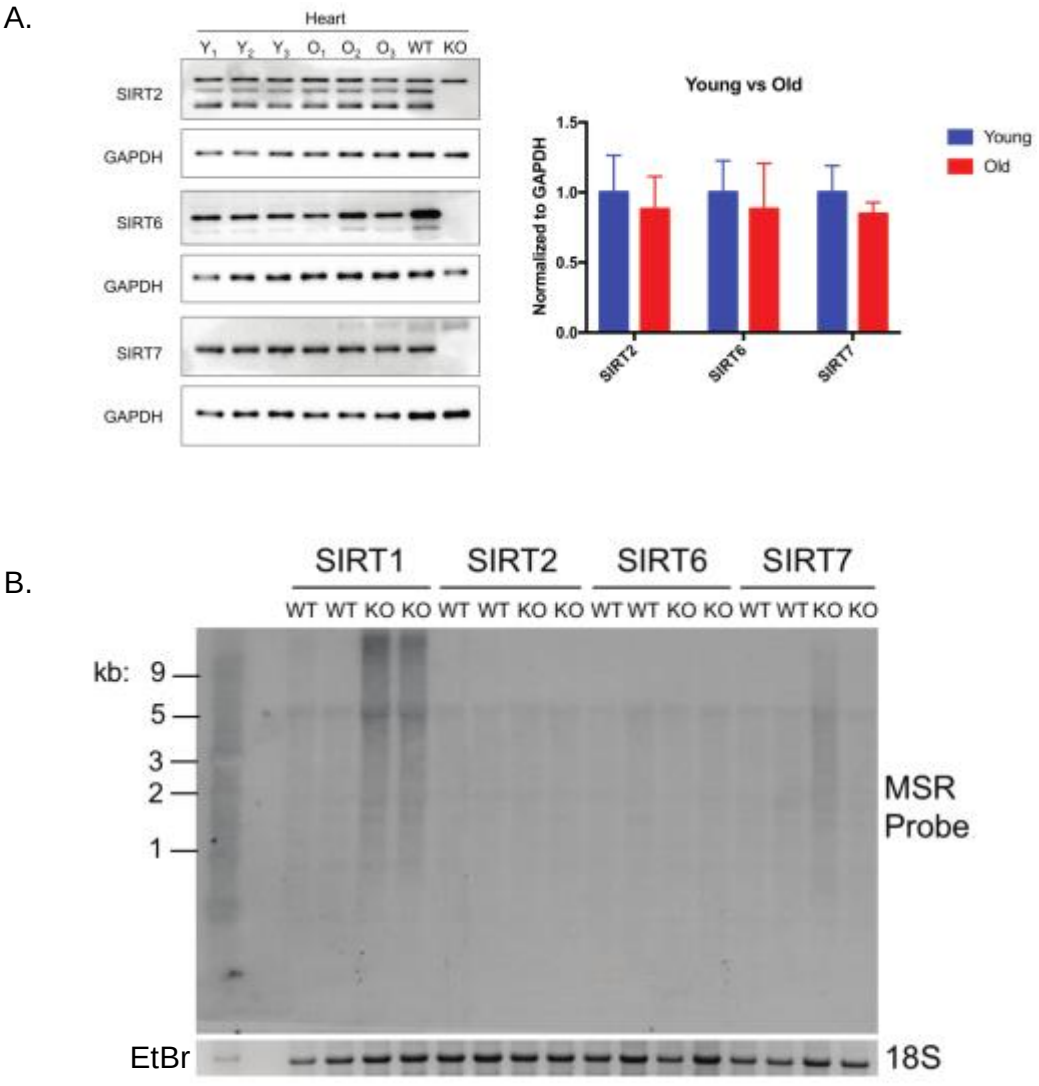

Figure 2.6 Loss of SIRT1, but not other nuclear sirtuins, promotes MSR expression. **A**. Nuclear sirtuin expression in young (Y) and old (O) mouse heart is analyzed by immunoblotting using antibodies against mouse SIRT2, SIRT6, SIRT7 and GAPDH as indicated. Positive controls: WT and germline KO heart lysate of the indicated sirtuin (left panel). Quantification of sirtuin expression in aged heart, normalized to GAPDH reveals a non-significant change in protein levels (right panel). **B**. MSR northern blotting of total RNA extracted from hearts of SIRT1, SIRT2, SIRT6 or SIRT7 WT and KO pairs highlights that loss of SIRT1 promotes MSR expression.

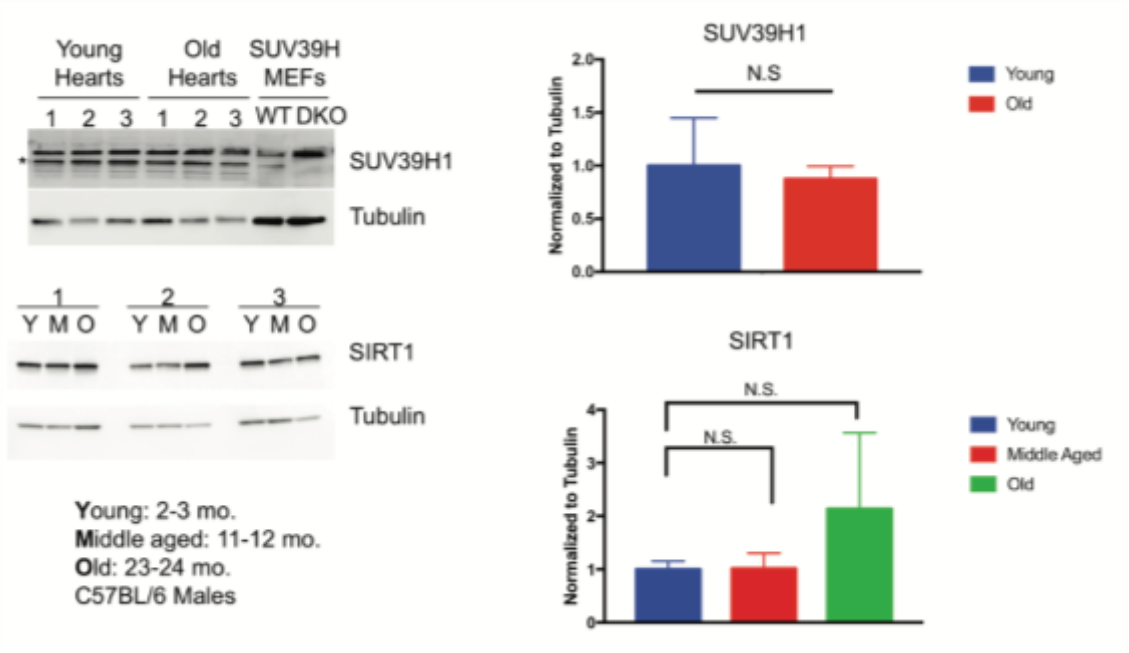

Figure 2.7 SIRT1 and SUV39H1 protein levels remain constant with age. Upper panel: Immunoblot analysis of Young and Old heart protein lysates, as indicated, for SUV39H1 protein levels (*lower band). Positive controls: SUV39H WT and DKO MEF lysates. Lower panel: Immunoblot analysis of (Y)oung, (M)iddle-aged, and (O)ld heart protein lysates, as indicated, for SIRT1 protein levels. Tubulin is used as the loading control. Quantification of SIRT1 and SUV39H1 expression in aged heart, normalized to tubulin reveals a non-significant (N.S.) change in protein levels (right panel).

To further investigate the role of increased NAD^+ in modulating age-associated MSR expression, we used a previously described mouse model of NAMPT overexpression (Frederick et al., 2015). NAMPT catalyzes the rate-limiting step in converting the sirtuin-inhibitor NAM to the sirtuin activator NAD^+ (Figure 1.1, Figure 2.10 B.). Increased NAMPT expression in the heart is associated with a ~20% increase in NAD^+ levels (Frederick et al., 2015). Therefore, we reasoned that in aged mice, overexpression of NAMPT would activate SIRT1 via NAD^+ enhancement, and therefore, reduce MSR expression. MSR northern blot analysis of *Nampt* transgenic and control 17-month-old mice revealed a non-significant change in MSR transcript levels in the hearts of these

mice. This result prompted us to ask if a ~20% increase in NAD^+ would result in SIRT1 activation, as evidenced by a reduction of its target histone PTMs by immunoblot. Immunoblot analysis shows variable, but equivalent amounts of H3K9ac and H4K16ac in *Nampt* transgenic and control 17-month-old mice (Figure 2.9 B.), indicating that in this mouse model NAD^+ levels are not sufficient to activate SIRT1-dependent MSR silencing.

In a second model of NAD^+ enhancement, mice, which have been supplemented with the NAD^+ precursor, NMN, to increase systemic NAD^+ levels, were analyzed by MSR northern blotting. Mice that received 300mg/kg/day of NMN in the drinking water, beginning at 5 months of age until euthanized at 17 months of age, displayed easily detectable MSR expression in their heart tissue (Figure 3.10 A.). Mock-treated mice showed a non-significant change in MSR transcript levels. A second route of NMN administration has been described to increase NAD^+ levels by ~40-60% in the heart and other tissues (North et al., 2014). In short, young (2-3-month-old) and old (22-24-month-old) mice were injected intraperitoneally at a dose of 500mg/kg once a day for 7 consecutive days with PBS (vehicle) or NMN (Sigma) resuspended in PBS, prior to the dark cycle. Upon dissection, hearts and livers were immediately processed for RNA for MSR expression analysis and NAD^+ measurement by mass spectrometry. Northern blot analysis reveals the expected increase in MSR expression in age mice (Figure 2.10 B., Young:PBS versus Old:PBS). Once again, NAD^+ supplementation failed rescue MSR expression in aged mice (Figure 2.10 B., Old:PBS versus Old:NMN). Mass spectrometry analysis demonstrates an increase the NAD^+ concentration upon NMN

supplementation in the liver, but not the heart (Figure 2.10 C.). Considering these data, we cannot yet conclude that a change in NAD^+ levels in the heart will mitigate the age-associated MSR phenotype, and requires further experimentation, specifically confirming increased SIRT1 activity upon genetic or pharmaceutical enhancement of NAD^+ in aged mouse heart.

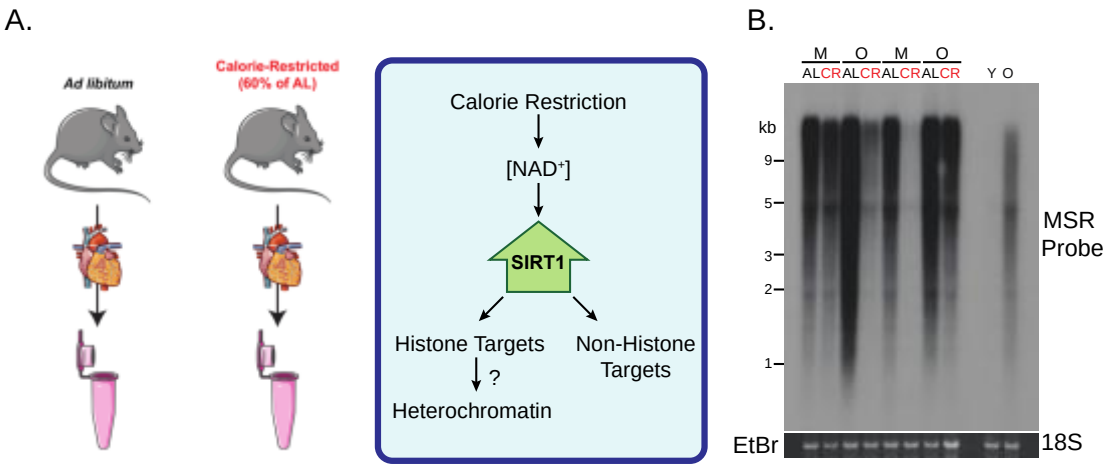

Figure 2.8 Calorie restriction suppresses MSR expression in aged heart. **A**. Calorie restriction increases cellular NAD^+, activating SIRT1 deacetylase activity. **B.** MSR northern blot of RNA extracted from two sets, as indicated, of middle-aged (M) and old (O) male B6D2F1 mice fed ad libitum (AL) or a calorie-restricted diet (CR, 60% of AL diet) for 20 days (right panel). Loading control, EtBr stain of the 18S rRNA. Positive controls, young (Y) and old (O) mouse heart samples are indicated.

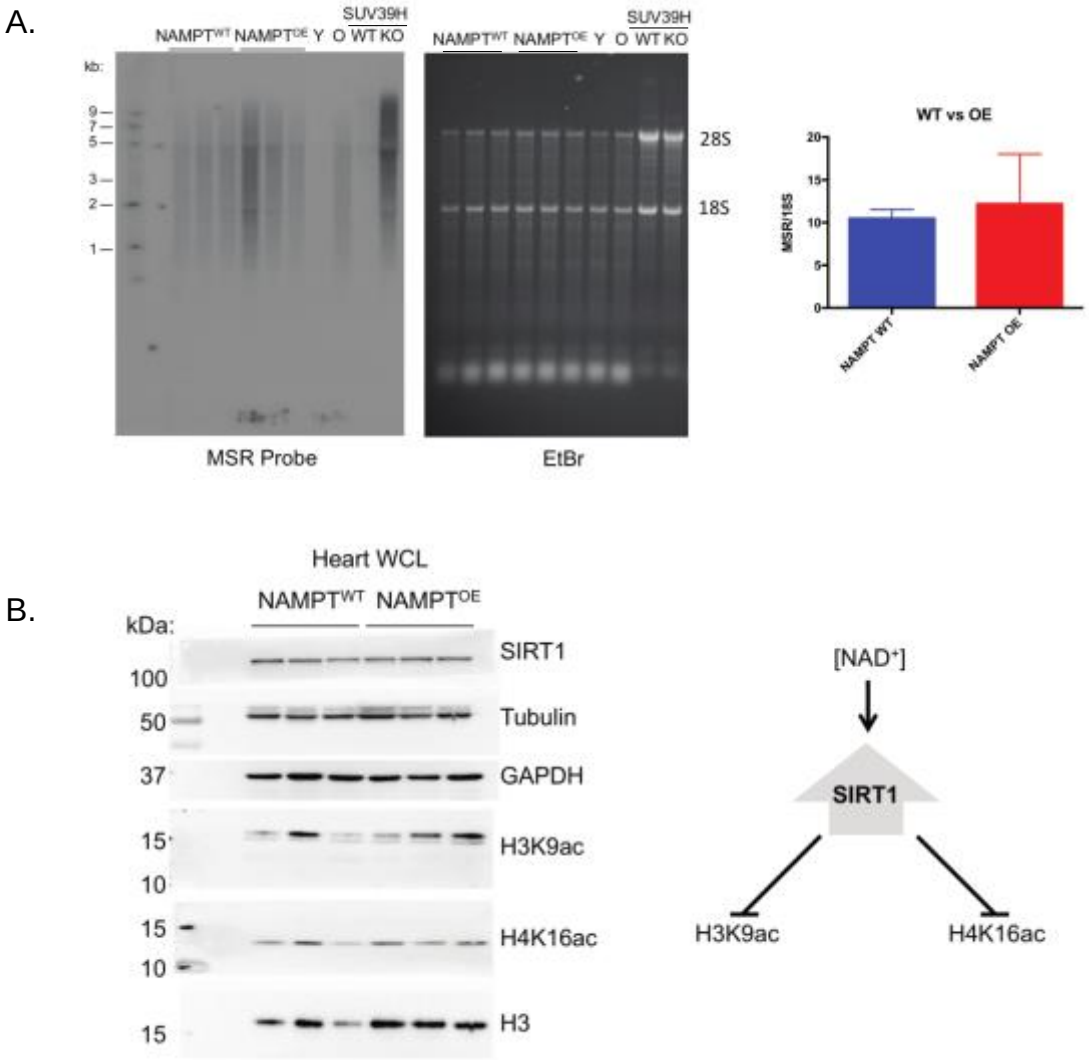

Figure 2.9 NAMPT overexpression does not alleviate MSR derepression. **A**. Right Panel: Twenty-four-month-old NAMPT WT or OE mice were analyzed for MSR expression in mouse heart tissue. Young (Y) and old mice (O), and SUV39H1/2 WT and KO RNAs serve as positive controls, as indicated. Left Panel: EtBr stained agarose gel demonstrate equal RNA loading. 18S and 28S rRNAs are indicated. **B**. Left Panel: western blot analysis of whole-cell lysates (WCL) extracted from NAMPT WT and OE mouse heart tissue. Membranes were probed for the indicated antibodies. H3K9ac, Histone H3 lysine 9 acetylation; H4K16ac, Histone H4 lysine 16 acetylation; H3, Histone 3. Right Panel: a model of NAD^+-mediated deacetylation of SIRT1 histone targets.

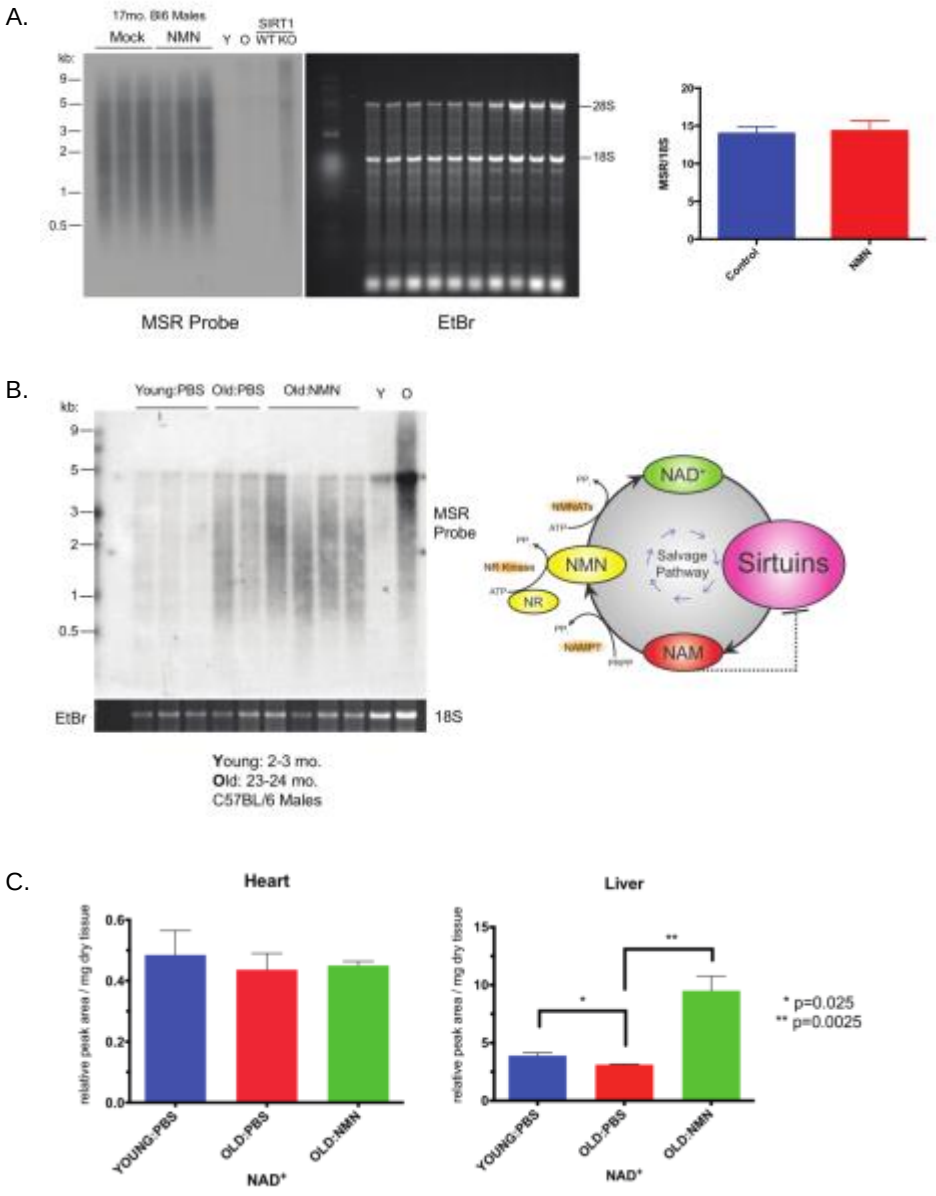

Figure 2.10 NMN supplementation does not silence MSR expression. **A**. MSR northern blotting of RNAs extracted from hearts from 17-month-old C57BL/6 mice supplemented with NMN or vehicle (Mock) at a dose of 300mg/kg/day in the drinking water. Positive control: young (Y), old (O), SIRT1 WT and KO heart samples, as indicated. EtBr-stained agarose gel is used to demonstrate equal loading (left panel). Quantification of MSR expression, normalized to 18S rRNA reveals a non-significant change in MSR transcript upon NMN-supplementation. (right panel). **B.** MSR northern blotting of RNAs extracted from hearts from young (Y) and old (O) C57BL/6 mice supplemented with NMN or vehicle (PBS) at a dose of 500mg/kg/day for 7 days via IP injection. Positive controls: young (Y) and old (O) mouse heart samples. Loading control, EtBr stain of the 18S rRNA. NMN catalyzes the rate-limiting step in the conversion of NAM to the sirtuin co-substrate, NAD^+ (right panel schematic). **C.** NAD^+ measurements by mass spectrometry of heart and liver samples dissected from mice used in (**B**.) were quantified and graphed.

SIRT1 Overexpression Partially Rescues Age-Associated MSR Derepression

If indeed SIRT1 is required to rescue defects in age-associated MSR silencing, then simply increasing the amount of SIRT1 protein would be expected to prevent induction of MSR expression observed upon aging. To test this model, we used a previously described mouse model of muscle-specific SIRT1 overexpression (White et al., 2014). MSR analysis of *Sirt1* transgenic mice at the age of 20 months revealed a significant ($p<0.02$) attenuation of MSR expression when compared to wild-type controls of the same age (Figure 2.11 B.). These mice experience robust lifelong SIRT1 expression (Figure 2.11 B. bottom panel).

For comparison, muscle-specific genetic *Sirt1* knockout mice at the age of 12-14 months exhibit an approximately 20-fold ($p<0.001$) increase in MSR expression compared to their wild-type counterparts, emphasizing the importance for SIRT1 in silencing MSR elements (Figure 2.11 A.). Interestingly, SIRT1 appears dispensable for preventing MSR expression at 2-3 months of age (Figure 2.11 A.). The SIRT1 knockout model, produces a catalytically-dead SIRT1 protein, which is detectable by immunoblot (Cheng et al., 2003) (Figure 2.11 A., bottom panel). While we cannot mechanistically define the effect of increased NAD^+ on SIRT1 activity and MSR expression, these data are consistent with the hypothesis that upregulation of SIRT1 activity in the aged mouse heart mitigates the effects of age on MSR silencing.

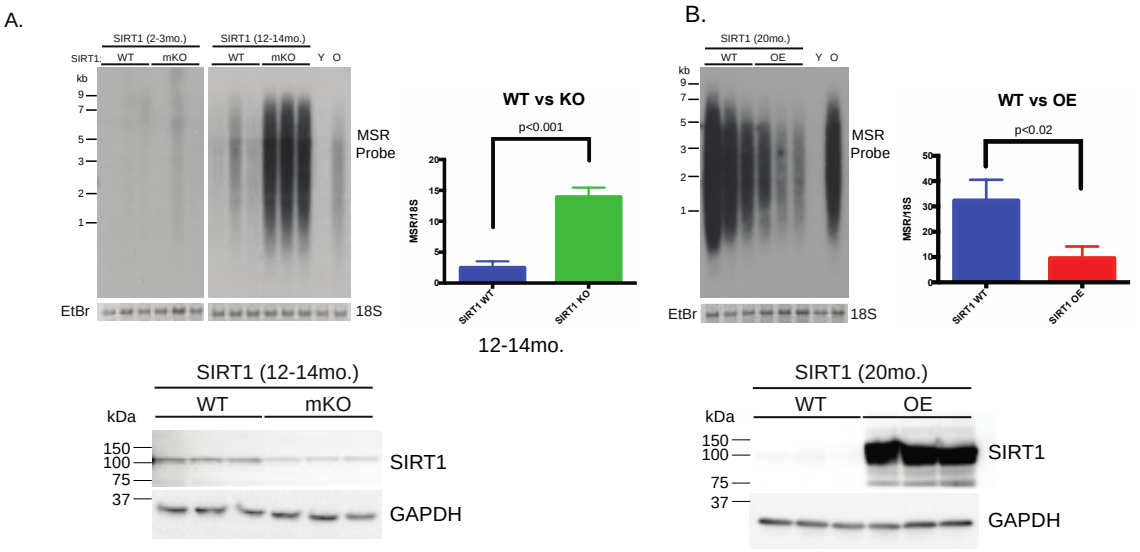

Figure 2.11 SIRT1 overexpression partially rescues MSR derepression in aged heart A. RNA extracted from wild-type (WT) or muscle-specific SIRT1 knockout (mKO) mice at 12-14 months of age were subjected to northern blotting using an MSR probe. Loading control, 18S rRNA EtBr stain. Left Panel: Quantification of MSR expression in WT vs mKO, normalized to 18S rRNA. **B.** RNA extracted from wild-type (WT) or muscle-specific SIRT1 transgenic overexpressor (OE) mice at 20 months of age were subjected to northern blotting using an MSR probe. Loading control, 18S rRNA EtBr stain. Left Panel: Quantification of MSR expression in WT vs OE, normalized to 18S rRNA. Loading control, 18S rRNA EtBr stain. Representative western blotting of each genotype for SIRT1 is depicted below.

Alterations in Global Histone PTMs in Age Mouse Heart

While this work seeks to address the role of SIRT1 in modulating histone PTMs implicated in the activation of MSR transcription, we decided take an unbiased approach to investigate global histone PTM changes in aged mouse heart using previously described high-regulation mass spectrometry of purified histone preparations (Lin and Garcia, 2012). Histones extracted from three young and three old C57BL/6 mice were analyzed by this method. Significant ($p<0.05$) changes in histone peptide

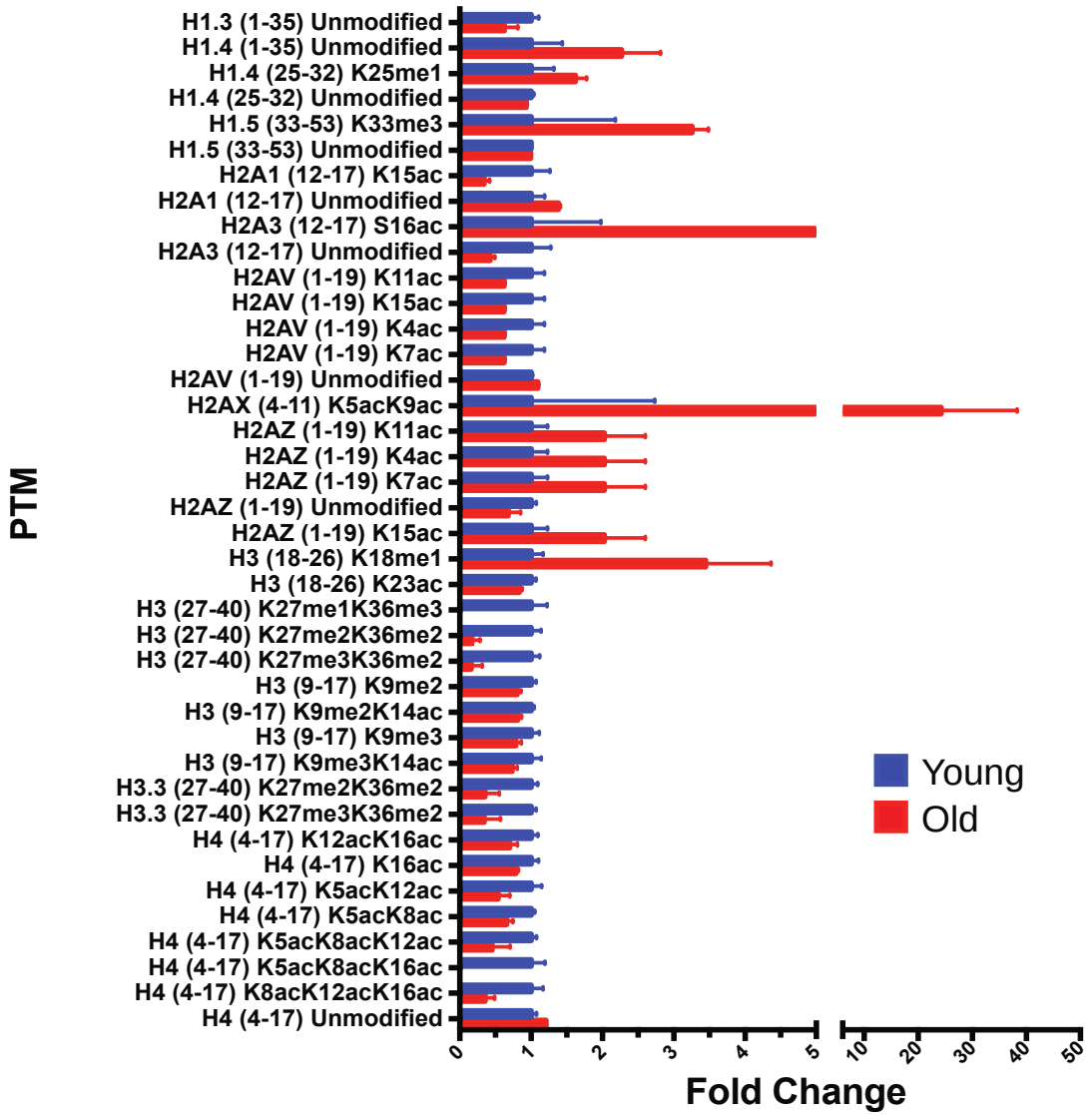

Figure 2.12 Analysis of global histone PTMs in aged mouse myocardium. Acid-extracted histones were purified from nuclei prepared from heart homogenates extracted, as described in Lin, S. & Garcia, B. A. Methods Enzymol (2012) (Lin and Garcia, 2012), from three young and three old mice. Relative quantification of histone variants and PTMs were calculated using high-resolution mass spectrometry in collaboration with the Garcia lab. Graphed are significant ($p \leq 0.05$) fold changes in histone PTMs of old mice compared to young. Numbers in parentheses indicate the polypeptide of the corresponding histone analyzed.

modifications are graphed relative to young (Figure 2.12). Surprisingly, SIRT1 targets, H3K9ac and H4K16ac, were not significantly enriched in aged mouse samples, as previously detected by immunoblot. In addition to H3K9ac and H4K16ac, SIRT1 also stabilizes facultative heterochromatin by facilitating recruitment of linker histone H1 (Vaquero et al., 2004). Interestingly, among to most highly altered modifications in this dataset are associated with H2A.X, H3K27 or H3K36 methylation, and several H1 variants. Furthermore, exogenous expression of MSR in cultured cells induces genomic instability evidenced, in part, by an increase in γH2A.X foci, a marker of DNA damage that can result from aberrant mitotic segregation (Janssen et al., 2011; Zhu et al., 2011b). Also, H3K36me3 has been reported to be associated with longevity and transcriptional fidelity in *S. cerevisiae* and *C. elegans* (Sen et al., 2015). Thus, there are clearly epigenetic alterations that occur with age, though which changes are the result of SIRT1 activity loss and how are MSR loci, and heterochromatin in general, are impacted are still open questions.

Discussion

The Heterochromatin Island Hypothesis postulates that chromatin organization – in particular, diminished heterochromatinization of repetitive regions – is progressively lost during cellular and organismal aging (Imai and Kitano, 1998). Experimentally, work in the budding yeast *S. cerevisiae* has demonstrated an age-associated loss of chromatin structure, in particular at repetitive DNA sequences, and elucidated its deleterious impacts on gene expression and genomic stability (Saka et al., 2013; Sinclair and

Guarente, 1997). In mice, MSRs comprise the pericentromeric DNA. MSRs are 234bp repeats present on all mouse chromosomes except the Y, together accounting for ~10% of the mouse genome (Garagna et al., 2002; Pardue and Gall, 1970; Prashad and Cutler, 1976; Vissel and Choo, 1989; Waring and Britten, 1966). MSR DNA is heterochromatinized by transcription factors, histone methyltransferases and deacetylases, chromatin remodeling complexes, and associated factors (Bulut-Karslioglu et al., 2012; David et al., 2003; Lehnertz et al., 2003a; Peters et al., 2001; Postepska-Igielska et al., 2013).

More recently, it has been reported that expression of several classes of repetitive elements, *i.e.* Major Satellite Repeats (MSRs) and long and short interspersed nuclear elements (LINEs and SINEs), rises in aged mouse liver and skeletal muscle, an increase that is attenuated by calorie restriction (CR) (De Cecco et al., 2013b). Histone H3K9 trimethylation mediated by the Su(var)3-9 methyltransferases homologs 1 and 2 (SUV39H1/2) plays a major role in MSR silencing (Lehnertz et al., 2003b). In SUV39H1/2 knockout mouse embryonic fibroblasts (MEFs), loss of MSR transcriptional silencing occurs, along with increased chromosomal missegregation and aneuploidy (Lehnertz et al., 2003b; Peters et al., 2001). Previous reports place SIRT1 at MSR loci in mouse embryonic stem cells, and indicate that upon genotoxic stress, SIRT1 relocalizes from the sites of MSR heterochromatin to the sites of DNA damage in order to facilitate repair (Oberdoerffer et al., 2008). A concomitant increase in MSR RNA was also detected, suggesting a role for SIRT1 in maintaining MSR silencing. This report also demonstrates, via ChIP analysis, that the SIRT1 target Histone H1 lysine 26

acetylation is increased at MSR loci. Although SIRT1 is known to regulate SUV39H1, MSR derepression in an aging context lacks the features of SUV39H1 deficiency. Indeed, SUV39H1 protein expression is unchanged in the mouse myocardium upon aging, and histone PTMs associated with loss of SUV39H1 activity are unaltered. Although it is possible that though the bulk levels of these histone PTMs are unaltered with age, a redistribution of SUV93H1-mediated repressive marks away from MSRs may occur, resulting in an increase in MSR expression. While the steady state levels of SIRT1 remain unchanged in aged heart tissue, it is also possible that SIRT1 is redistributed upon aging. If SIRT1 abundance or activity is unaltered with age, but its localization is altered, modulating its activity via NAD^+ supplementation may fail to rescue the age-associated MSR phenotypes observed, consistent with data presented in the chapter (Figure 2.9 A. and Figure 2.10 A.). If NAD^+ levels are maintained with age in the heart to support sirtuin activity, then overexpression of SIRT1 would be predicted to allow for more molecules to reside at the MSR loci to preserve its structure, again in agreement with data presented in the chapter (Figure 2.11 B.). Surprisingly, SIRT1 loss in young mice has no effect on MSR expression, indicating SIRT1 may belong to a silencing complex that becomes progressively unstable with age.

Perturbed MSR heterochromatinization is associated with chromosomal missegregation, aneuploidy, and an elevated cancer incidence (David et al., 2006; Peters et al., 2001; Vaquero et al., 2007; Wang et al., 2008). Enforced satellite sequence expression can on its own induce aneuploidy (Zhu et al., 2011a). The very first example of attenuated heterochromatin maintenance with age in mammals in vivo

involved the MSRs (Gaubatz and Cutler, 1990). Via northern hybridization, Gaubatz and Cutler showed that MSR RNA expression was undetectable in hearts of young mice, but progressively increased in this tissue in mice one year of age and older. They observed no age-associated MSR induction in brain, liver, or kidney.

During aging, progressive aneuploidization occurs in several mouse tissues, including heart, skeletal muscle, kidney and lung (Baker et al., 2013). Overexpression of BubR1, a mitotic checkpoint protein, improves ploidy maintenance during aging, and is protective against age-related cardiac dysfunction (Baker et al., 2013). Whether an age-related increase in MSR expression contributes to age-associated genomic instability is unclear. Also, the ability to delay age-associated genomic instability, for example though overexpression or upregulation of SIRT1 activity, which results in attenuated MSR expression, has yet to be determined. Consistent with this idea, ectopic expression of human or mouse satellite DNA induces genomic instability in cultured cells, marked by mitotic catastrophe and an increase in γH2A.X foci, a marker of DNA damage that can result from aberrant mitotic segregation (Janssen et al., 2011; Zhu et al., 2011b). Several studies suggest that pro-longevity interventions like CR may potentiate lifespan extension in part by preserving chromatin structure and function in higher eukaryotes (Guarente, 2000; Heydari et al., 2007; Vaquero and Reinberg, 2009). Although, the possibility that increased NAD^+ as a result of CR allows for increased SIRT1 activity, a second possibility is that CR results in less DNA damage (Heydari et al., 2007), which in turn preserves SIRT1 concentrations at MSR loci, facilitating MSR silencing. It is still unknown whether the effect CR has on MSR expression is SIRT1

dependent, and what effect SIRT1 loss would have on genomic stability and CR-mediated lifespan extension is an open question.

Work presented in this chapter addresses an age-related epigenetic defect that was first described 25 years ago; the molecular basis for age-associated MSR depression in myocardium. Though this was the first example of age-associated heterochromatin dysfunction in vivo described in mammals, the mechanistic basis of this phenomenon has never been determined. Our studies suggest impaired SIRT1 function at MSR loci, perhaps due to diminished NAD^+ levels or relocalization, as playing a role in this effect. We further propose that impaired MSR heterochromatinization plays a causal role in age-associated myocardial aneuploidy (Baker et al., 2012). These studies will provide new insight into a longstanding question in epigenetics and aging, and into mechanisms of cardiac genome stability. Cardiovascular disease (CVD) represents the single greatest cause of worldwide mortality (Barquera et al., 2015), and advancing age is a dominant risk factor for CVD (Bell et al., 2015). Therapies to attenuate age-associated heterochromatin changes in the heart may provide novel therapeutic avenues to promote cardiac health in the elderly.

Materials and Methods

Cell Culture

SUV39H1/2 double-knockout and wild-type mouse embryonic fibroblasts (Lehnertz et al., 2003b) were cultured in DMEM (Gibco) containing 4.5g/L glucose, 110mg/L sodium pyruvate, 4mM L-glutamine, 1% non-essential amino acids, 10units/mL penicillin, 10µg/mL streptomycin and 20% heat-inactivated FBS, and were grown in a humidified chamber at 37°C containing 5% CO_2.

Mice

All aged mice, including calorie-restricted and those fed *ad libitum* (AL), were procured from the NIA Aging Rodent Colony (https://ros.nia.nih.gov). Unless otherwise indicated, all experiments were done with tissues harvested from young (2-3-month-old), middle-aged (12-14-month-old) and old (22-24-month-old) C57BL/6 male mice. Middle-aged and old male B6D2F1 mice fed AL or a calorie-restricted diet (CR, 60% of AL diet) for 20 days. All mice were housed at the Biomedical Science Research Building (UM). Experiments were approved by and performed in accordance with the regulations of the University Committee on Use and Care of Animals.

NMN treatment

Nicotinamide mononucleotide (NMN) treatment was done as previously described (North et al., 2014). Briefly, young (2-3-month-old) and old (22-24-month-old) mice were injected intraperitoneally at a dose of 500mg/kg once a day for 7 consecutive days with PBS (vehicle) or NMN (Sigma) resuspended in PBS, prior to the dark cycle. A

second set of heart tissues dissected from NMN-supplemented mice were a gift of Dr. Shin-ichiro Imai (Washington University, St. Louis). These mice were NMN-supplemented at as dose of 300mg/kg/day in the drinking water, beginning at 5 months of age until euthanized at 17 months of age. NAD^+ measurements were done by mass spectrometry analysis in collaboration with Dr. Charles Evans (UM).

Northern Blotting for MSRs

Total RNA was extracted using TRIzol reagent (Invitrogen), according to the manufacturer's instructions. Precipitated RNA was resuspended in 500µl of RNAse-free H_2O and incubated at 56ºC for 10 minutes and returned to room temperature. To remove contaminating genomic DNA, RNA was incubated with 100 units of RNAse-free DNAse I (Roche) at 37ºC for 3 hours in the presence of 40 units of RNAse inhibitor (Roche). RNA was precipitated with two rounds of phenol (pH 5.2):chloroform extraction, followed by a final extraction chloroform. RNA was then ethanol precipitated in the presence of 0.3 M sodium acetate pH 5.2 overnight at -20ºC, spun down and washed twice with 500µl of 70% ethanol. RNA was resuspended in RNAse-free H_2O. RNA integrity was confirmed by gel electrophoresis.

An equal volume of NorthernMax-Gly Sample Loading Dye (Ambion) was added to 5 µg of total RNA and incubated for 1 hour at 56ºC. Samples were resolved on a 1% Bis-Tris-PIPES-EDTA agarose gel at 5 V/cm (as measured between electrodes). Resolved RNA was transferred overnight onto a pre-wet Zeta Probe membrane (Bio Rad) by

upward capillary action using 10X SSC as the solvent. Once transferred, the membrane was briefly rinsed in 2X SSC and UV crosslinked in a Stratalinker (Stratagene). The membrane was prehybridized for 1 hour at 68ºC in ULTRAhyb Hybridization Buffer (Ambion). During prehybridization, 1 µg of the MSR dsDNA template (cloned from pγsat plasmid; Addgene) containing the T7 promoter was used to generate a radiolabelled riboprobe using the T7 MAXIscript Kit (Ambion) and isotopically labeled UTP, [α-32P] (Perkin Elmer), according to manufacturer's instructions. The labeled probe was purified in a MicroSpin G-25 column (GE Healthcare). The prehybridized membrane was incubated with the probe overnight at 68ºC and washed for 30 minutes at 68ºC twice in 2X SSC, twice in 2X SSC, 0.1% SDS and twice in 0.1X SSC, 0.1%SDS. The membrane was imaged by autoradiography. Quantification was performed by ImageJ software analysis.

Immunobloting

Whole-cell protein extracts were prepared from cell pellets or flash-frozen mouse tissues that were pulverized in Laemmli sample buffer (62.5mM Tris pH 6.8, 2% SDS, 10% glycerol), supplemented with 710mM β-mercaptoethanol. Lysates were sonicated for 30 seconds using a Branson Sonifier set to output "2." Lysates were then clarified by centrifugation at 15 000rcf for 30 minutes at 4ºC. Protein concentrations were determined using the DC Protein Assay (Bio Rad). Equivalent amounts (10-25µg) of total protein were fractionated by SDS-PAGE on a 10% or 12% polyacrylamide gel, electrophoretically transferred to PVDF, and probed with antibodies diluted in 5% nonfat

milk in 1XTBS-0.1% Tween-20 as indicated in Table 2.1. Probed membranes were imaged on an ImageQuant LAS 4000 Scanner (GE Healthcare) after application of Immobilon Western HRP Substrate (Millipore).

Antibody	Company	Clone/Cat#	Dilution	~kDa
SIRT1	Cell Signaling	D1D7	1:2K	110
SIRT2	Cell Signaling	D4O5O	1:2K	39, 43
SIRT6	Cell Signaling	D8D12	1:2K	36, 42
SIRT7	Cell Signaling	D3K5A	1:2K	45
GAPDH	Santa Cruz	6C5	1:5-10K	37
α-Tubulin	Santa Cruz	B-5-1-2	1:5-10K	55
Histone H3	Abcam	ab1791	1:25K	17
H3K9ac	Abcam	ab4441	1:5K	17
H3K9me3	Abcam	ab8898	1:5K	17
H3K56me3	--	--	1:1K	17
H4K16ac	Cell Signaling	E2B8W	1:1K	11
5-hmC	Epigentek	A-1018	1:1K	N/A

Table 2.1 Antibodies used in this chapter

Dot Blotting for Methylated DNA

Genomic DNA samples were prepared with twofold (400ng to 50ng) serial dilutions in TE buffer and then denatured in 0.4 M NaOH/10 mM EDTA at 95ºC for 10 min and placed on ice. Denatured DNA samples were spotted on a Zeta Probe membrane prewet in H_2O for 5 minutes then in 10XSSC in an assembled Dot Blot apparatus (BioRad). The membrane was briefly rinsed with 2XSSC buffer and ultraviolet-crosslinked in a Stratalinker using the autocrosslink setting, twice. Then the membrane was blocked with 5% non-fat milk for 1 hour and incubated with anti-5hmC (Epigentek)

in 5% BSA/0.1% Tween-20 overnight for HRP-conjugated secondary antibodies and enhanced chemiluminescence detection. The membrane was subsequently stained with SYBR gold (Invitrogen) total DNA stain to confirm corresponding amounts of DNA for each sample. Quantification was performed by ImageJ software analysis.

Histone Extraction for Post-Translational Modification Mass Spectrometry Analysis

Histones were prepared as described (Lin and Garcia, 2012). Briefly, flash-frozen heart tissues were pulverized in liquid nitrogen. NIB-250 (15mM Tris-HCL pH 7.5, 60mM KCl, 15mM NaCl, 5mM $MgCl_2$, 1mM $CaCl_2$, 250mM sucrose, 0.3% NP-40, 1mM DTT, protease and deacetylates inhibitors) was added to a final ratio of 10:1 (10mL of buffer to 1mL equivalent of tissue). The mixture was dounce homogenized and incubated on ice for 5 minutes. Nuclei were washed 10:1 NIB-250 (without NP-40 detergent), and centrifuged at 4ºC for 5 minutes at 600rcf.

To the isolated nuclei, 0.4N H_2SO_4 to a 5:1 final ratio (v/v) was added while vortexing, then incubated on ice for 1 hour and centrifuged at 4ºC for 5 minutes at 3400rcf. The supernatant was transferred to a new 15ml conical tube. To the remaining pellet, 0.4N H_2SO_4 to a 5:1 final ratio (v/v) was added while vortexing, then incubated on ice for 1 hour and centrifuged at 4ºC for 5 minutes at 3400rcf. Supernatants were combined. To the supernatant, trichloroacetic acid was added to a final concentration of 20% and allowed to precipitate overnight at 4ºC. Histones were pelleted at 4ºC for 5 minutes at

3400rcf. The pellet was washed in acetone/0.1% HCl, and then washed twice with 100% acetone. The final pellet was air dried and resuspended in 50µl H_2O.

Acknowledgments

I thank members of the Lombard lab for thoughtful discussions of these data. Dr. Györgyi Csankovszki (UM) provided the H3K56me3 antibody (Jack et al., 2013). Dr. Charles Evans (UM) did mass spectrometry analysis for NAD^+ levels in aged mouse tissue. I thank Dr. Simon Schenk (UCSD) for SIRT1 wild-type, knockout and overexpressing mice. I thank Dr. Joseph Baur (UPenn) for providing the NAMPT overexpressing mice, and Dr. Shin-ichiro Imai (Washington University, St. Louis) for the NMN-treated mouse tissue. I thank Dr. Danica Chen (Berkeley) for providing SIRT7 wild-type and knockout mouse heart samples. I thank Dr. Thomas Jenuwein (Max Planck Institute, Germany) for the SUV39H1/2 double-knockout and wild-type immortalized MEFs. I thank Michelle Azar (UM) for help with immunoblotting analysis and RNA preparation. High-resolution mass spectrometry of histone PTMs (Figure 2.11) was done in collaboration with Dr. Benjamin Garcia (UPenn).

CHAPTER 3

SIRT5 is a Pro-Survival Factor in Human Melanoma

Abstract

Melanoma is the most lethal skin cancer, with an estimated 73,870 new melanoma cases and 9,940 melanoma-related deaths occurring in the US in 2015. There is an urgent need for development of novel strategies to treat metastatic melanoma, which causes great morbidity and mortality, despite the advent of immune- and kinase-directed therapies. Unfortunately, even with the best current therapies, the majority of patients with disseminated melanoma will still eventually succumb to this disease. In melanoma and other cancer types, metabolism is reconfigured to meet the anabolic demands of uncontrolled cellular proliferation. Reversal of this metabolic reprogramming can induce senescence and cell death in melanoma.

We have found that SIRT5 is critical in melanoma cell survival. SIRT5 removes succinyl, malonyl, and glutaryl modifications from lysines on diverse protein targets, primarily in the mitochondrial matrix, thereby regulating multiple metabolic pathways. In 10/10 human melanoma cell lines tested, SIRT5 knockdown resulted in rapid loss of proliferative potential and cell death. Likewise, we have found that SIRT5 loss impeded

melanoma xenograft formation in mice, and SIRT5 knockdown results in increased apoptotic cell death, which can be partially rescued by overexpressing anti-apoptotic BCL2. Lastly, via metabolomics, SIRT5 regulates glucose and glutamine metabolism in melanoma.

Introduction

Sirtuin NAD^+-dependent protein deacylases regulate metabolism and other diverse aspects of cell biology (see Chapter 1). Of the three mitochondrial sirtuins, SIRT5, an inefficient deacetylase, is the only one with demonstrated desuccinyl, demalonyl, and deglutaryl activity (Du et al., 2011; Park et al., 2013; Peng et al., 2011b; Rardin et al., 2013; Tan et al., 2014a). Until recently, the major known function of SIRT5 was to regulate the hepatic urea cycle, via activation of carbamoyl phosphate synthase I (CPS1), the rate-limiting enzyme in this process (Nakagawa et al., 2009; Nakamura et al., 2012; Ogura et al., 2010). By activating CPS1, SIRT5 inhibits cellular ammonia generation and autophagy (Polletta et al., 2015).

Most sirtuins are now linked to neoplasia, either as tumor suppressors and/or oncogenes (see Chapter 1). Tumor cell metabolism has emerged as a common target for sirtuin-mediated regulation (Zwaans and Lombard, 2014). For example, SIRT3 functions as a tumor suppressor via promotion of mitochondrial respiration and suppression of ROS levels. In SIRT3-deficient cells, increased ROS activate HIF1, promoting Warburg metabolism and genomic instability, and also lead to defects in

intracellular iron metabolism (Bell et al., 2011; Finley et al., 2011; Jeong et al., 2014; Kim et al., 2010). SIRT3 also activates PDC and promotes oxidative metabolism to suppress tumorigenesis (Fan et al., 2014). SIRT4 acts as a tumor suppressor by suppressing glutamine metabolism, particularly under conditions of genotoxic stress (Csibi et al., 2013; Haigis et al., 2006; Jeong et al., 2013). Among the seven mammalian sirtuins, SIRT5 is the only one not yet definitely implicated in malignancy. A recent report showed that SIRT5 promotes chemoresistance in non-small cell lung carcinoma via enhancement of NRF2 activity, though the mechanistic details of this interaction remain unclear (Lu et al., 2014). Another report indicated that SIRT5 desuccinylates SOD1 to activate its function, suppressing ROS and promoting growth of lung cancer cells (Lin et al., 2013). Previous efforts from our lab have identified 2565 succinylation sites on 779 proteins, most of which (~90%) were SIRT5 targets. This revealed potential impacts of succinylation on enzymes involved in mitochondrial metabolism: amino acid degradation, TCA cycle, and fatty acid metabolism. We have described SIRT5-dependent regulation of two substrates, PDC and Succinate Dehydrogenase (SDH). SIRT5 inhibited biochemical activities of both complexes, and suppressed overall mitochondrial respiration (Park et al., 2013).

Melanoma is the most lethal skin cancer, with an estimated 73,870 new melanoma cases and 9,940 melanoma-related deaths occurring in the US in 2015 (Siegel et al., 2015). There is an urgent need for development of novel strategies to treat clinically advanced melanoma, which still causes great morbidity and mortality, despite the advent of immune- and kinase-directed therapies. In melanoma and other cancer

types, metabolism is reconfigured to meet the anabolic demands of uncontrolled cellular proliferation (Theodosakis et al., 2014). Reversal of this metabolic reprogramming can induce senescence and cell death in melanoma (Kaplon et al., 2013); however, no therapies have taken advantage of this vulnerability.

The data presented in this chapter reveal a major requirement for SIRT5 in melanoma cell survival, through suppression of apoptosis and potentially through the regulation of metabolism. We have found that in 10/10 human melanoma cell lines we have tested, with varied genetic drivers, SIRT5 knockdown resulted in rapid loss of proliferative potential and cell death. Likewise, we have found that SIRT5 loss greatly impeded melanoma xenograft formation in mice. Overexpression of anti-apoptotic BCL2 thwarts the cell death phenotype induced upon SIRT5 depletion. Via metabolomics and respirometry, we have found that SIRT5 regulates glucose and glutamine metabolism in melanoma to promote metabolic reprogramming.

Results

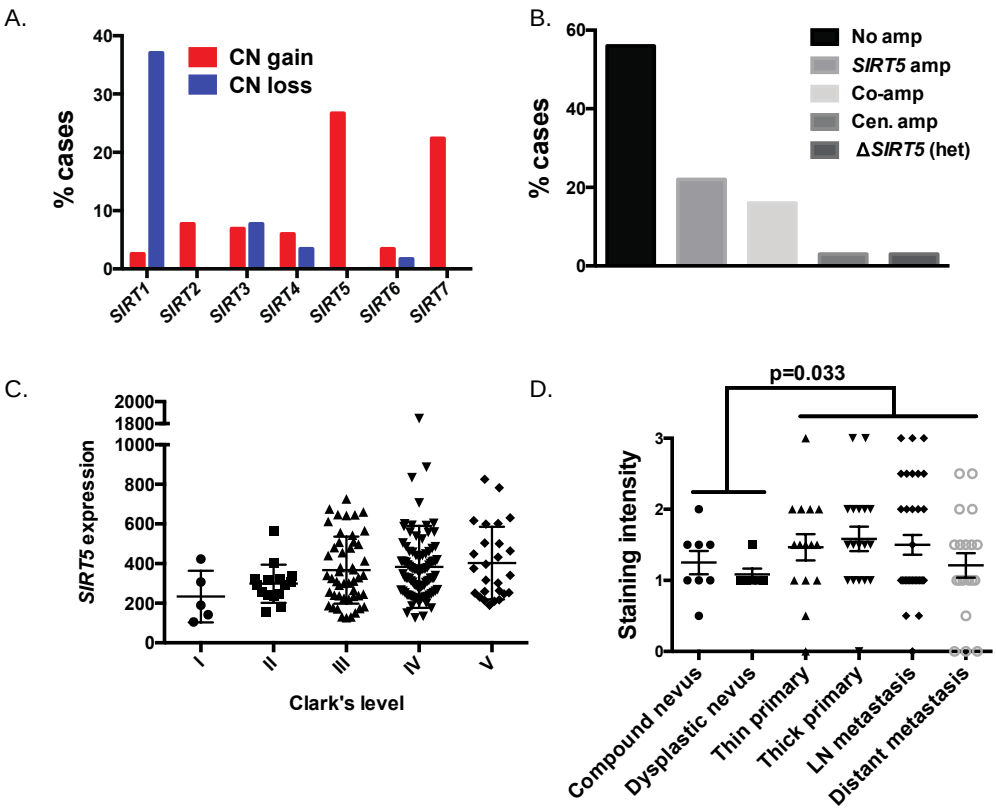

Figure 3.1 *SIRT5* is amplified in human melanoma. **A**. Sirtuin gene copy number (CN) in human melanoma samples, as assayed by high density SNP array (n=139). **B**. *SIRT5* (6p23) and centromere (Cen) 6p amplification (amp) or co-amplification (Co-amp) in melanoma (n=32). **C**. *SIRT5* mRNA expression levels correlate with Clark's depth of the melanoma lesion (p=0.0044, linear regression; p=0.037, ANOVA). **D**. SIRT5 protein levels are increased in melanoma relative to benign melanocytic lesions (p=0.0333, Chi-squared; n=14 nevi, n=87 melanoma).

Bioinformatic analysis reveals striking *SIRT5* amplification in human melanoma

Human melanoma is often typified by genetic alterations in either *NRAS* (chr 1) or *BRAF* (chr 7) (Hodis et al., 2012). Yet, amplification human chromosome 6p is often

A.

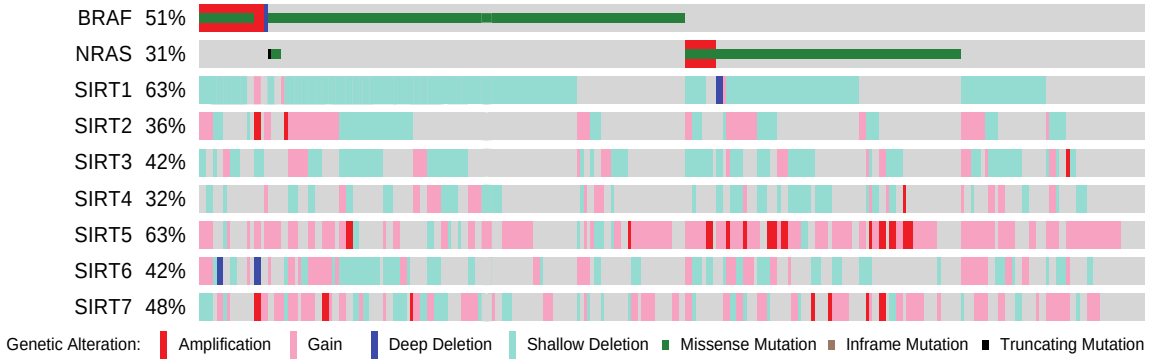

B.

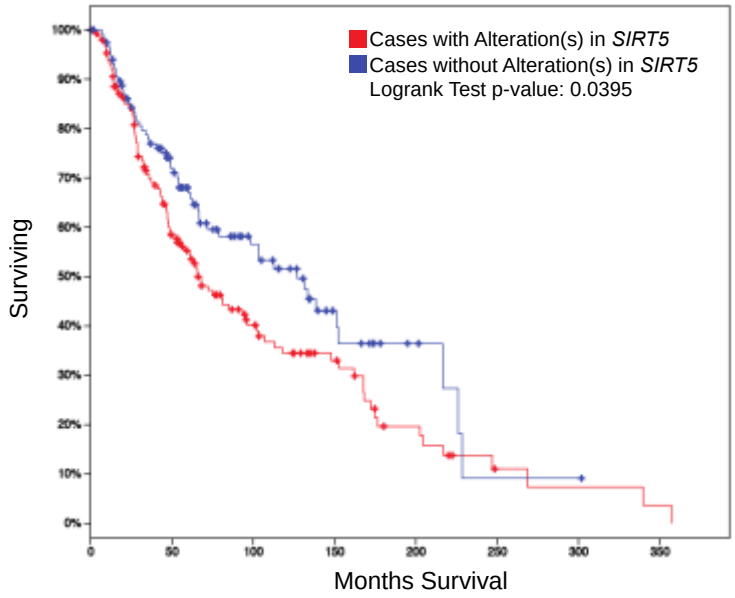

Figure 3.2 Reduced survival when *SIRT5* is amplified in human melanoma. A. *SIRT5* shows amplification and/or increased expression in melanoma. BRAF and NRAS alterations are shown for comparison (n=278; data from TCGA, Provisional, analyzed on cBioPortal). Negative cases have been omitted for clarity. **B.** Kaplan–Meier analysis of survival in melanoma patients with alterations in *SIRT5*.

correlated with cancer progression, including melanoma (Santos et al., 2007). Given that SNP array analysis reveals that *SIRT5* copy number gain is associated with human clinical melanomas (Figure 3.1 A. and B.), we asked if *SIRT5* RNA expression is increased in human melanoma samples. We found that compared to benign nevi,

SIRT5 expression is increased in more aggressive melanocytic lesions, reported as Clark's depth. (Figure 3.1 C. and D.). Mining the TCGA database, *SIRT5* copy number gain is shown to be present in many melanoma cases – strikingly, more frequent than alterations in other sirtuins and mutations in the canonical *NRAS* and *BRAF* melanocytic genetic drivers (Figure 3.2 A.). Consistent with the hypothesis that SIRT5 expression correlates with melanoma growth and survival, Kaplan-Meier analysis indicates that melanoma patients with a *SIRT5* amplification have lower mortality rates than patients without a *SIRT5* alteration (p=0.0395; Figure 3.2 B.). These data indicate that SIRT5 promotes melanoma growth and survival. To test the role for SIRT5 in promoting melanoma survival, we used a panel of cell lines harboring the well-described mutations in either *NRAS* or *BRAF* (Figure 3.3, Table 3.1). As shown in Figure 3.3, SIRT5 protein is present in varying abundance in both *NRAS* and *BRAF* mutant cell lines. Taken together, these data suggest that SIRT5 serves as a potential pro-survival factor for human melanoma.

Loss of SIRT5 inhibits NRAS^{Q61R} and BRAF^{V600E} driven melanoma cell growth

Since SIRT5 is readily detected by immunoblot in all cell lines tested (Figure 3.3, Table 3.1), and given that melanoma with a *SIRT5* amplification results in a lower patient survival rate, we tested the hypothesis that SIRT5 is required for melanoma cellular proliferation and survival. To do this we generated cells lines lacking SIRT5 using a lentiviral shRNA system, targeting *SIRT5* in one of two regions of the mRNA (KD1 or KD2). Compared to cells harboring a non-targeting (NT, or non-silencing control)

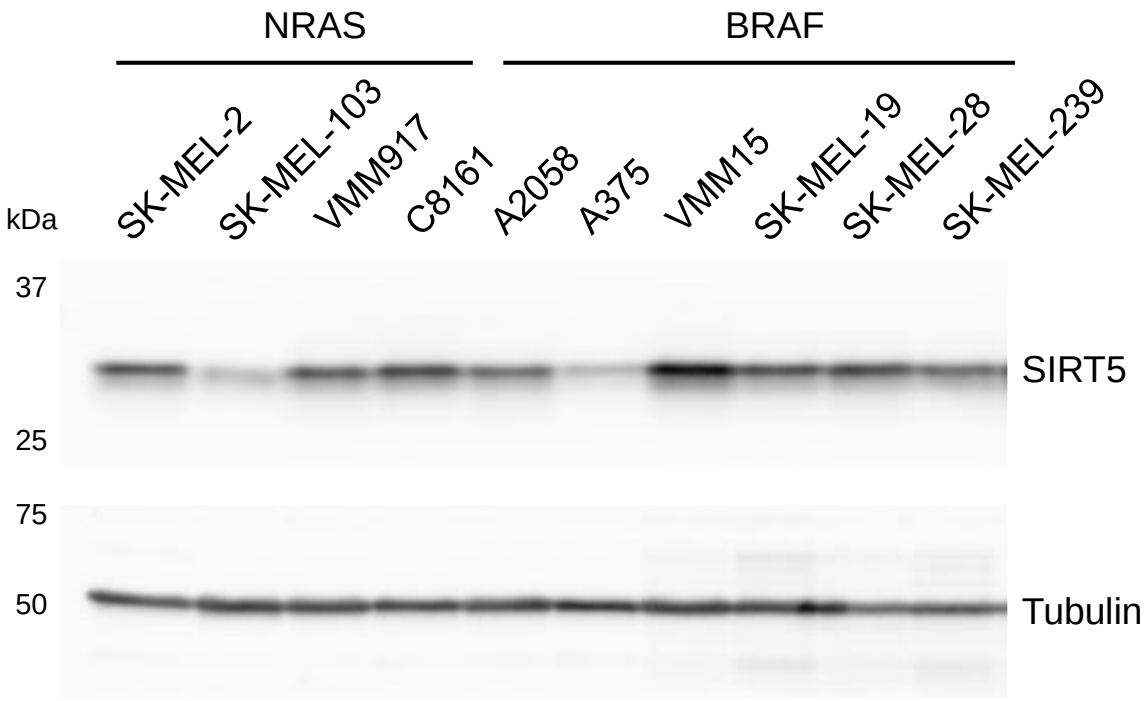

Figure 3.3 SIRT5 is expressed in melanoma cell lines. SIRT5 protein is readily detectable in whole cell extracts by immunoblot in various NRAS Q61R mutant or BRAF V600E mutant melanoma cell lines. Tubulin serves as the total protein loading control.

shRNA, we observe that both SIRT5 shRNA lentiviruses inhibited melanoma survival as measured by a WST-1 tetrazolium salt cleavage system (Figure 3.4 A, B). We find that 7 days post-infection, KD1 and KD2 significantly reduce cell numbers as measured by ABS_{450nm} in 10/10 cell lines, and this phenotype is independent of the genetic mutations typically found in melanomas, $NRAS^{Q61R}$ or $BRAF^{V600E}$ (Figure 3.2A, 3.4 B). Thus, regardless or genetic driver, targeting *SIRT5* with an shRNA reduces cellular proliferation and/or survival in all melanoma cells tested in a cell culture system. As a qualitative measure of melanoma cell growth, we imaged two $NRAS^{Q61R}$ mutant (SK-MEL-103 and VMM917) and two $BRAF^{V600E}$ mutant (A2058 and VMM15) cell lines 96

hours post-infection (48 hours post-puromycin selection). Brightfield micrographs of representative fields reveal fewer cells in both SIRT5 knockdown samples (Figure 3.5, KD1 and KD2 compared to NT, control). Thus, consistent with the results from the colorimetric WST-1 assay, targeting SIRT5 with either KD1 or KD2 lentivirus reduces cell number when compared to the non-targeting control.

To confirm that treatment with shRNAs, KD1 and KD2, do indeed result in loss of the SIRT5 protein, we generated whole-cell lysates from A2058 and SK-MEL-103 cells that have been infected with a non-targeting control (C), SIRT5 knockdown 1 (KD1), or SIRT5 knockdown 2 lentivirus. At 72 and 96 hours post-infection, the level of SIRT5 protein is markedly reduced, but not undetectable by immunoblotting (Figure 3.6 A). At both timepoints, complete cell death has not occurred (Figure 3.4, see A2058 and SK-MEL-103 panels, Day 2 and Day 3; Figure 3.5). In order to begin to delineate a SIRT5-mediated inhibition of proliferation from activation of apoptosis we chose these timepoints to ask if A2058 and SK-MEL-103 cells have increased cleaved caspase 3. Caspase 3, a protease that is cleaved to initiate the apoptotic signaling cascade (Elmore, 2007), can be easily detected by the appearance of two smaller molecular weight species on an immunoblot. Figure 3.6 A, second panel, shows the appearance of these caspase 3 cleavage produces in the melanoma samples where SIRT5 is reduced (C vs KD1 and KD1). Therefore, reduced SIRT5 protein in a $BRAF^{V600E}$ mutant cell line, A2058 and an $NRAS^{Q61R}$ mutant cell line, SK-MEL-103 correlates with reduced cell number and increased pro-apoptotic caspase 3 cleavage.

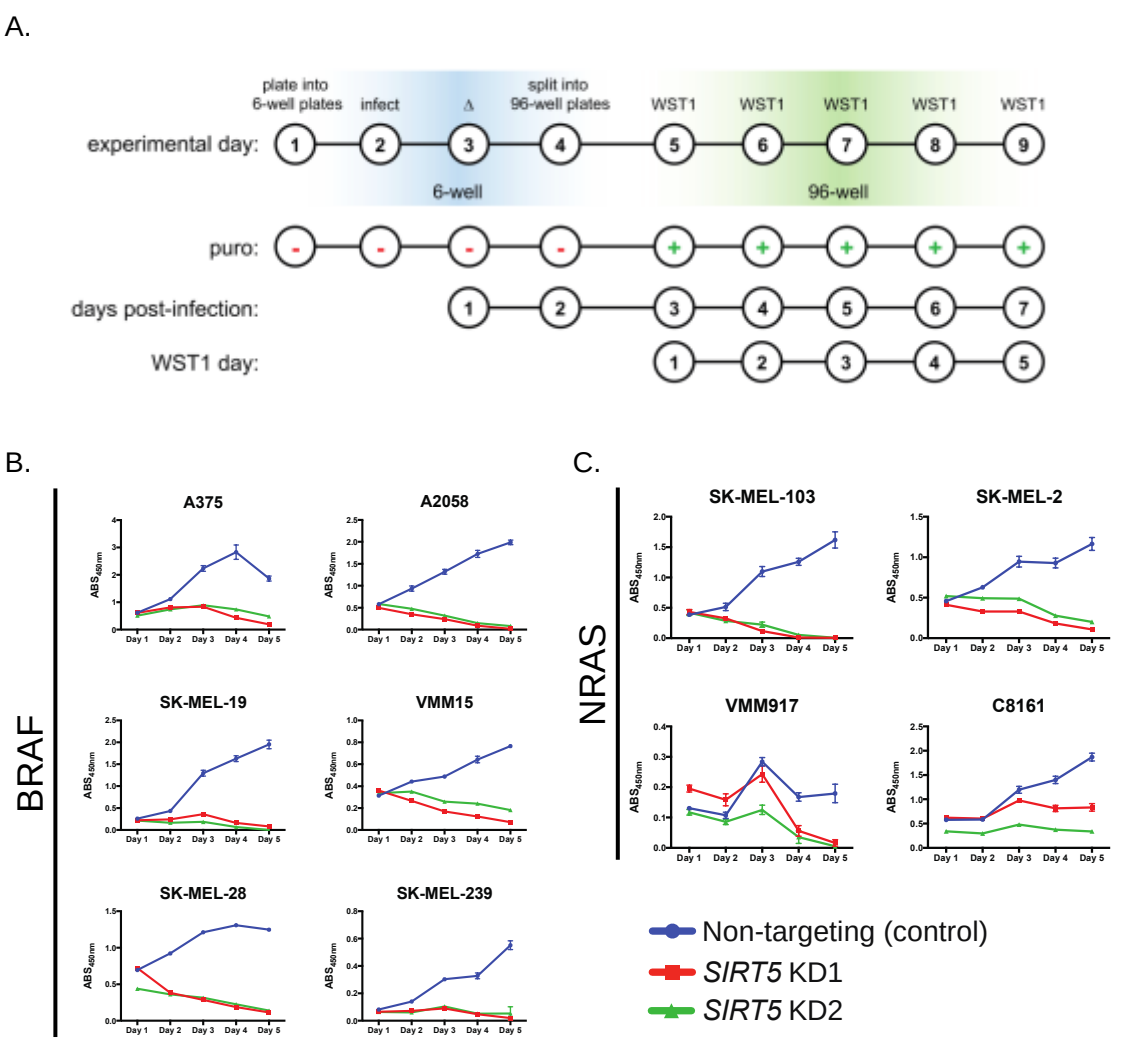

Figure 3.4 SIRT5 knockdown reduces cell survival in various melanoma cell lines. **A**. Schematic of WST-1 viability assay. Equivalent cells are plated on experimental day 1. Cells are then infected with a non-targeting shRNA or one of two *SIRT5* shRNAs (KD1 or KD2). Cells are plated into 5 96-well plates in the presence of puromycin 48 hours post-infection. Each day, WST-1 is added and ABS(450nm) is read two hours later. **B.** Average results (n=6/timepoint) are graphed. Error bars represent standard deviation.

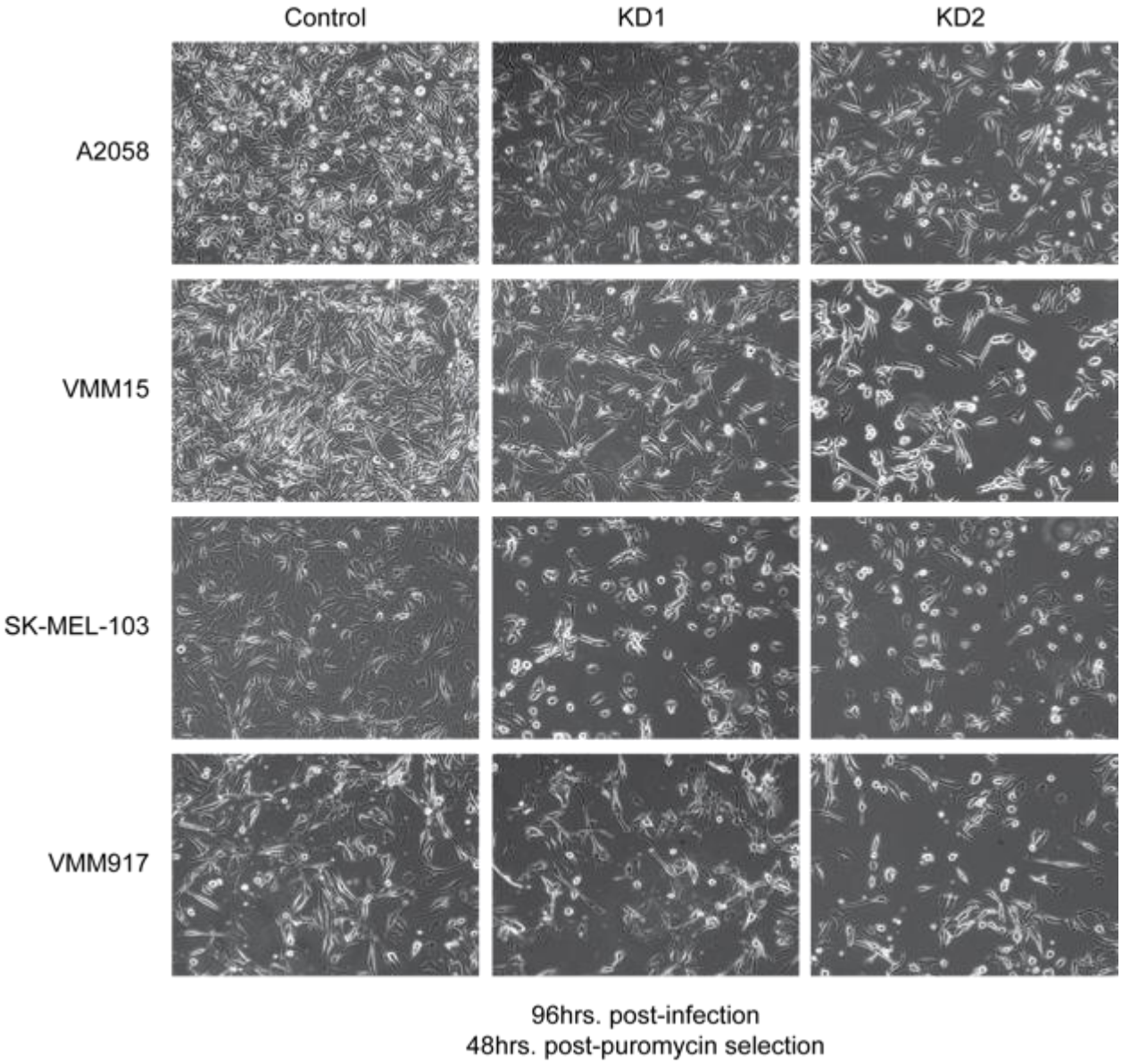

Figure 3.5 SIRT5 knockdown reduces cellular density in cell culture.
Representative qualitative micrographs of decreased cellular density upon SIRT5 knockdown were taken 96 hrs. post-infection with a lentivirus expressing a non-targeting (control) or SIRT5-targeting (KD1 or KD2) shRNA. $BRAF^{V600E}$ mutant cell lines, A2058 and VMM15 and $NRAS^{Q61R}$ mutant cell lines, SK-MEL-103 and VMM917 are depicted above. Equivalent cell numbers were plated 24hrs. prior to lentiviral transduction.

Does loss of SIRT5 protein result in the hallmarks of loss of SIRT5 catalytic activity? A major biochemical function of SIRT5 is to remove succinyl, malonyl, and glutaryl moieties from lysine residues (Du et al., 2011; Nakagawa et al., 2009; Park et al., 2013; Peng et al., 2011a; Rardin et al., 2013; Tan et al., 2014b). Genetic knockout of *Sirt5* in mice results in an accumulation of succinyllysine residues in the heart and other tissues (Park et al., 2013; Sadhukhan et al., 2016; Yu et al., 2013). We analyzed the status of total succinyllysine by immunoblot in melanoma cells after SIRT5 knockdown, using SIRT5 WT and KO mouse heart lysates as a control. As expected, increased succinyllysine is present in the mouse SIRT5 KO samples compared to the WT samples, evidenced by a darker “smear” on the membrane (Figure 3.6 B.).

Surprisingly, probing melanoma lysates with the pan-succinyllysine antibody revealed near equivalent levels of succinyllysine in both knockdowns compared to control (KD1 and KD2 vs NT) at both timepoints (Figure 3.6 B.). Overall, the levels of succinyllysine are lower in human melanoma than in WT mouse heart tissue. Thus, SIRT5 is dispensable in maintaining the level of succinyllysine in whole cell protein extracts in A2058 and SK-MEL-103 cells.

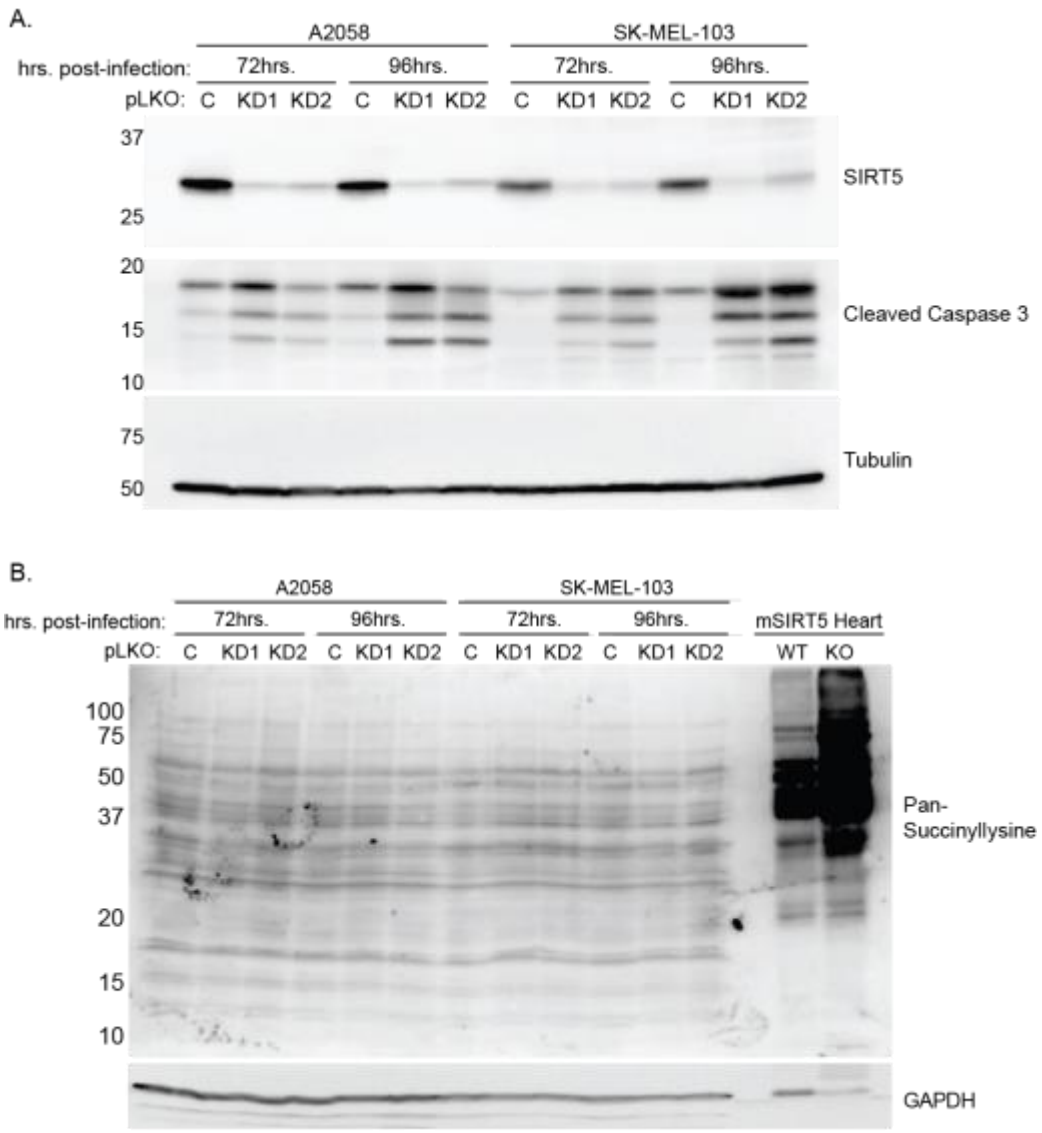

Figure 3.6 SIRT5 knockdown induces caspase 3 cleavage, but maintains cellular succinyllysine levels. A. Immunoblot analysis of SIRT5 protein levels 72 and 96 hrs. post-infection with control (C) or one of two shRNAs targeting *SIRT5* (KD1/KD2) in A2058 and SK-MEL-103 cell lines. Induction of cleaved caspase 3 is observed at both timepoints. Tubulin serves as the total protein loading control. **B.** Pan-succinyllysine analysis of total cellular protein after SIRT5 knockdown via immunoblot was done at 72 and 96 hrs. post-infection as in (A.). Mouse SIRT5 (mSIRT5) wild-type (WT) and knockout (KO) heart lysate serve as a positive control. GAPDH serves as the total protein loading control.

The ex vivo and in vivo effects of SIRT5-depletion on melanoma growth

One hallmark of cancer is sustaining cell growth, or “replicative immortality” (Hanahan and Weinberg, 2011). We, therefore, asked if modulation of SIRT5 could impact the ability of melanoma cells to grow in a colony, mimicking tumor growth in 2 dimensions, under the challenge of limited dilution in cell culture. In order to test the hypothesis that SIRT5-depletion would result in fewer colonies in a clonogenic formation assay, we plated A2058 and SK-MEL-103 cells in 6-well plates. Cells were infected with a lentivirus expressing SIRT5 KD1 or SIRT5 KD2 or an NT control, as done previously. After 12 days of culture, under puromycin selection, colonies were stained with crystal violet and counted (Figure 3.7 A. and B.). As expected, significantly ($p<0.0001$) fewer colonies were observed in both SIRT5 knockdown samples compared the control (approximately 6-fold fewer in SK-MEL-103 and 13-fold fewer in A2058; Figure 3.7 A.). Slightly more colonies were observed in SK-MEL-103 KD2 samples compared to KD1, which correlates with increased level of SIRT5 protein in KD2 vs KD1 (Figure 3.6 A.) that we consistently observe with this lentivirus system. Thus, reduction of SIRT5 reduces the number of colonies in a 2 dimensional clonogenic growth assay.

To further investigate the ability of SIRT5 to support melanoma growth, we took advantage of a xenograft mouse model to test the hypothesis that SIRT5 knockdown will mitigate tumor growth in vivo. The well characterized NOD.Cg-*Prkdc*^{scid}*Hr*^{hr}/NCrHsd

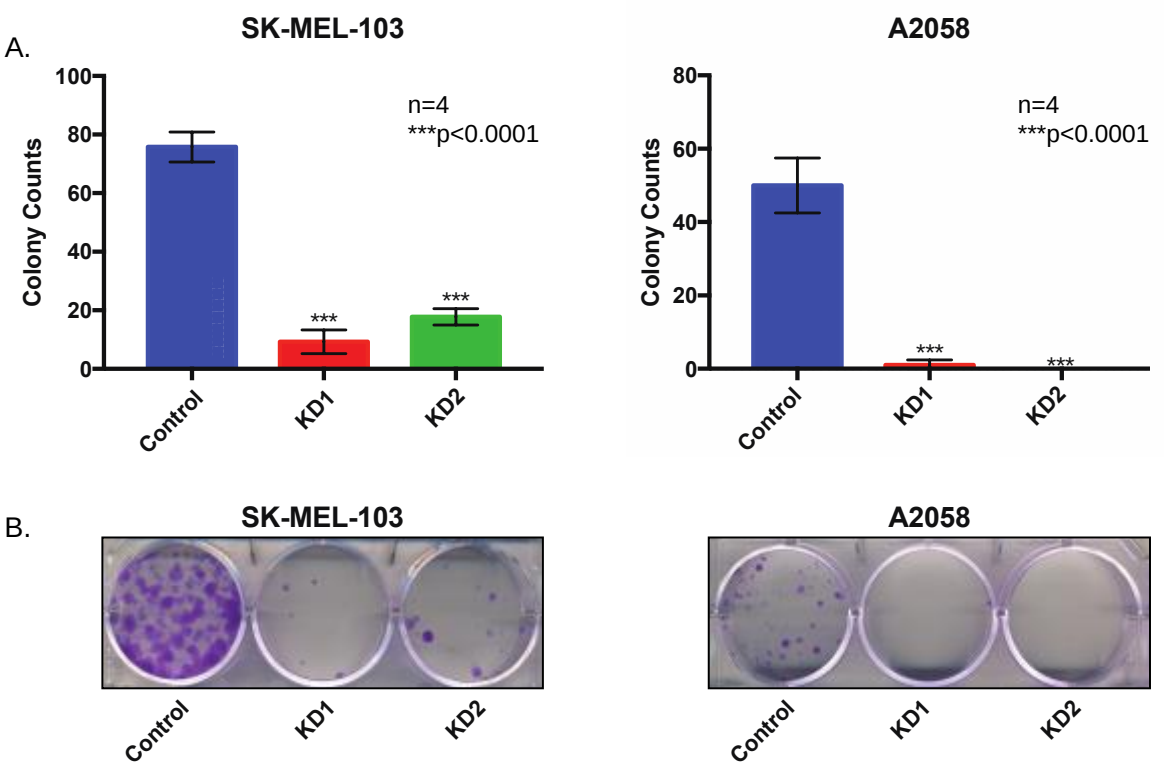

Figure 3.7 SIRT5 knockdown reduces clonogenic colony formation potential in cell culture. A. SIRT5 knockdown results in significantly ($p<0.0001$) fewer crystal violet-positive colonies in A2058 and SK-MEL-103 cells 12 days post-infection. Graphed are averages of n=4 wells per condition. Error bars represent standard deviation. **B.** Representative crystal violet-stained wells depict fewer colonies in both SIRT5 knockdowns (KD1 and KD2) compared to non-targeting (control) in both cell lines.

(NOD/SCID) mouse strain was used to follow melanoma cell-driven tumorigenesis in vivo. A2058 and SK-MEL-103 cells were once again infected with NT (control), SIRT5 KD1, or SIRT5 KD2 and harvested 72 hours post-infection for subcutaneous injection into the flanks of 5 NOD/SCID mice per group (*i.e.* 5 mice received NT and KD1, and 5 mice received NT and KD2; Figure 3.8 A.). One million live cells of each condition, as determined by trypan blue exclusion, were resuspended in Matrigel basement membrane matrix, and injected into female NOD/SCID mice. As expected, flanks that received SIRT5 KD1 or KD2 SK-MEL-103 (Figure 3.8 A.) or A2058 (Figure 3,8 B.)

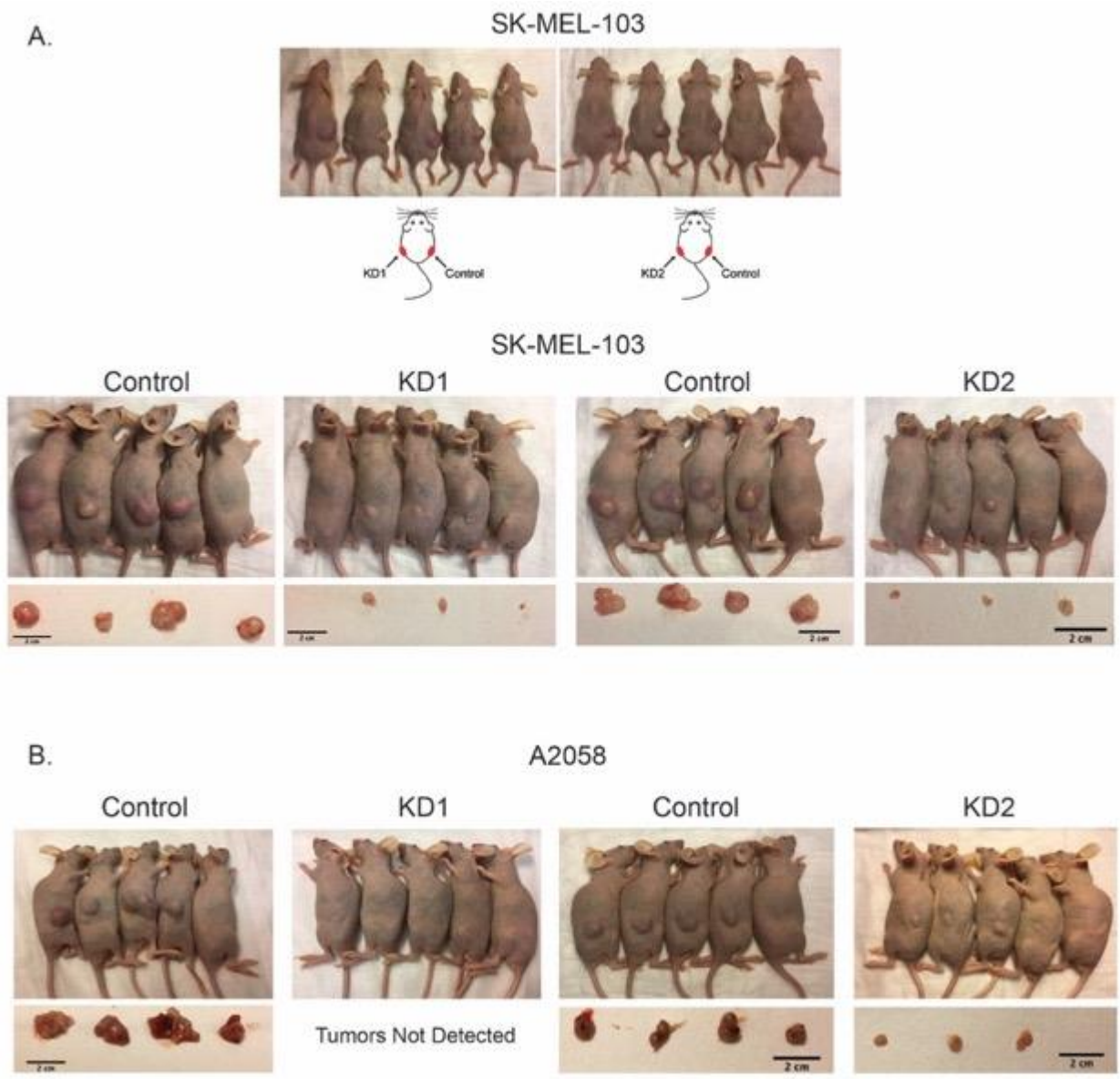

Figure 3.8 SIRT5 knockdown inhibits *in vivo* tumor growth in a xenograft mouse model. Non-targeting (Control) or SIRT5 knockdown (KD1 or KD2) cells were injected into the right or left flanks, respectively, of immunocompromised mice, as indicated. Loss of SIRT5 in SK-MEL-103 (**A**.) or A2058 (**B**.) resulted in attenuated tumor growth. Scale bar below dissected tumors represents 2cm. Mice were sacrificed and tumors were dissected 28 days (for A2058) or 35 days (for SK-MEL-103) after initial injection.

produced smaller tumors compared to the flanks that received cells infected with a non-targeting shRNA control virus. As illustrated in Figure 3.8 A. and B., fewer and smaller tumors resulted in vivo from SIRT5 knockdown in the xenograft model.

Quantitative analysis of in vivo tumor growth was performed by measuring tumor volume, using Vernier calipers, on the days indicated (Figure 3.8 C.). Subcutaneous tumor growth was initially visible approximately 13 days after injecting A2058 cells and approximately 18 days after injection of SK-MEL-103 cells. The non-targeting control cells of both lines quickly formed tumors, while SIRT5 KD1 and KD2 cells exhibited markedly reduced tumor growth. Despite 4/5 tumors engrafting for each group (Figure 3.8 A. and B.), control tumor growth was still significantly ($p<0.05$) higher than both SIRT5 knockdown samples in both cell lines (Figure 3.8 D.). Mice receiving A2058 cells were analyzed at 28 days after injection, which revealed a greater than 10-fold increase in endpoint control tumor size, compared to KD1 and KD2. Similarly, 35 days post-injection, tumors derived from SK-MEL-103 cells exhibited a greater than 20-fold increase in the non-targeting control tumor volume compared to KD1 and KD2 (Figure 3.8 D, lower bar graph). Thus, both qualitative and quantitative analyses demonstrate that SIRT5 reduction in A2058 and SK-MEL103 consistently and reliably inhibit xenograft tumor formation in NOD/SCID mice, recapitulating the phenotype observed in the colony formation assay (Figure 3.7).

Exogenous SIRT5 overexpression does not rescue SIRT5-mediated cell death

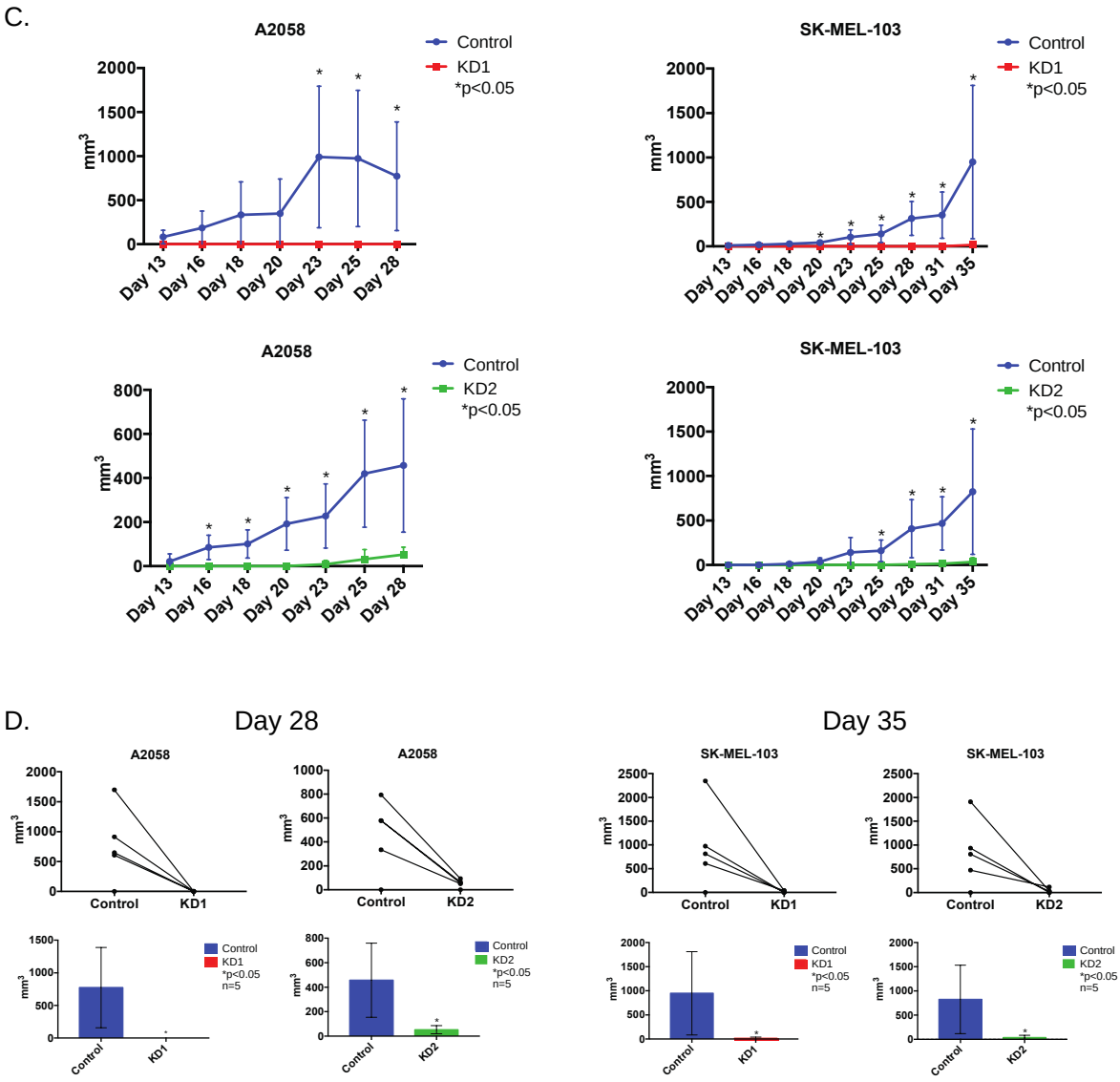

Figure 3.8 SIRT5 knockdown inhibits *in vivo* tumor growth in a xenograft mouse model. C. Quantification of tumor growth was initiated on day 13 after initial injection of cells. Tumor sizes were recorded with Vernier calipers on the days indicated. Each point represents the average measurements of n=5 mice for each condition (Control, KD1, or KD2). Error bars represent standard deviation. **D**. Pairwise representation of endpoint tumor size in each mouse within each group is graphed. Average tumor volume measurements in mm^3 at day 28 for A2058 and day 35 for SK-MEL-103 are represented in the lower panel.

Reduced cell viability in 10/10 human melanoma cell lines and a reduced tumorigenic potential upon SIRT5-depletion prompted us test whether we can rescue the SIRT5 knockdown phenotype by expressing shRNA-resistant *SIRT5* in cells. To do this, we lentivirally generated SK-MEL-103 and A2058 cells lines that stably overexpress SIRT5. There are 4 known transcripts that express 4 unique SIRT5 isoforms. Isoform 1 and isoform 2 are generated from alternative splicing and have been reported to localize to distinct subcellular compartments: Isoform1 to the nucleus, cytoplasm and mitochondria, and Isoform 2 predominately to the mitochondria (Matsushita et al., 2011). We, therefore generated isoform 1 and isoform 2 overexpressing A2058 and SK-MEL-103 cell lines (Iso1 or Iso2). We also mutated amino acid H159 to tyrosine (labeled H159Y, or HY) to generate catalytically inactive SIRT5 protein. This conserved histidine is critical for SIRT5 catalytic activity and mutation to tyrosine ablates SIRT5-mediated catalysis (Nakagawa et al., 2009). SIRT5 isoform 1 contains silent mutations to confer resistance to SIRT5 KD1 shRNA, but not KD2. Successful overexpression of SIRT5 isoform 1 and 2 in SK-MEL-103 was confirmed by immunoblot (Figure 3.9 A.). Isoform 2 is lower in molecular weight as evidenced by a smaller band on the immunoblot (Iso 2 arrow, Figure 3.9 A.). Using isoform 2-overexpressing SK-MEL-103 cells, we tested the ability of SIRT5 shRNA to target *SIRT5*. Figure 3.9 B. illustrates successful knockdown of SIRT5 in the vector-control cell lines (compare “Vector” lanes in control, KD1 and KD2 panels), while KD1 does not reduce the level of shRNA-resistant isoform 2 (Figure 3.9 B, middle panel, KD1). As expected, endogenous isoform 1 is equally reduced in each sample being targeted by SIRT5 KD1 shRNA.

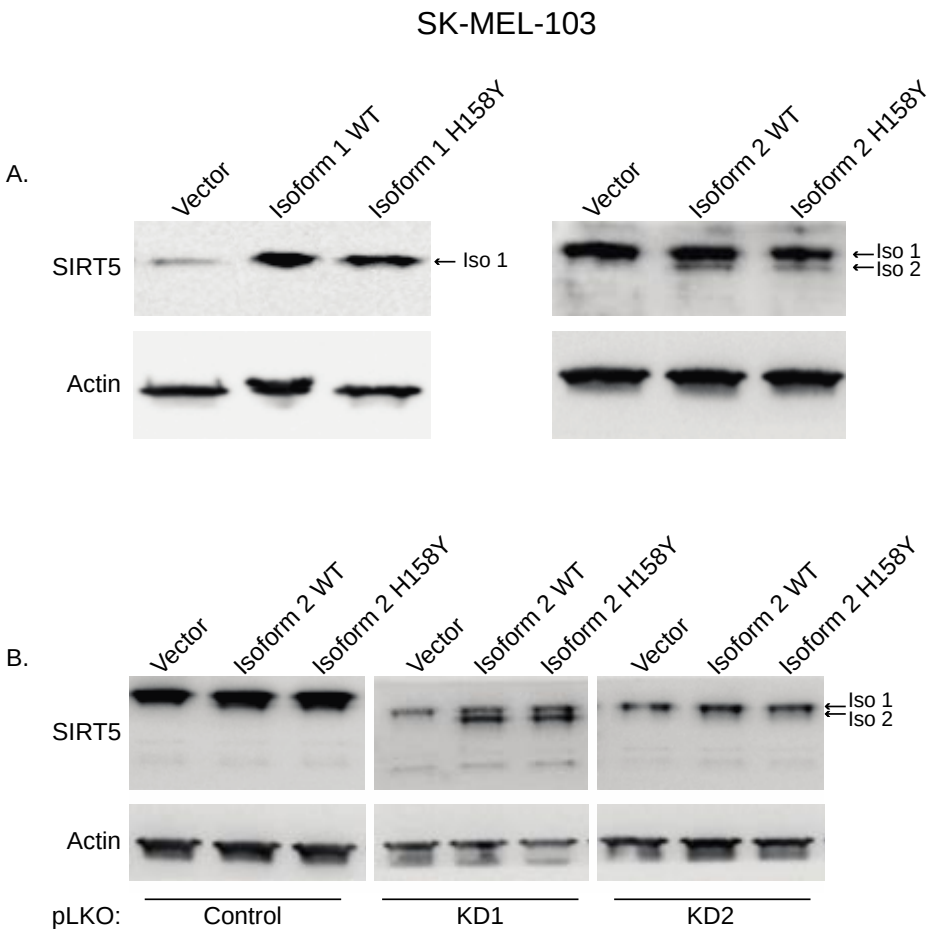

Figure 3.9 Isoform-specific SIRT5 overexpression in SK-MEL-103 cells. **A**. SIRT5 isoform 1 and isoform 2 are overexpressed in SK-MEL-103 cells using a lentiviral-based system (Vector, control virus). Isoform 2 is lower molecular weight than isoform 1, as illustrated by arrows. Histidine at amino acid 158 in the SIRT5 protein was mutated to tyrosine (H158Y) to generate the previously described catalytically-dead SIRT5 enzyme. Exogenously-expressed SIRT5 Isoform 1 and 2 are resistant to shRNA KD1, but sensitive to KD2. **B**. Knockdown of endogenous SIRT5 in SK-MEL-103 reveals equivalent SIRT5 protein levels, expressed from the transduced *SIRT5* cDNA (compare Vector lanes in each panel). KD2-sensistive isoform 2 is reduced upon KD2 infection.

If SIRT5 is required for cell viability, knockdown of endogenous SIRT5, but not lentivirally expressed resistant isoform 1 or 2 is expected to maintain cell growth. To test this, we targeted *SIRT5* using KD1 and KD2 in SIRT5 isoform 1 and 2 overexpressing cells. Surprisingly, neither SIRT5 isoform 1 nor isoform 2 was able to

rescue cell growth in the WST-1 viability timecourse (Figure 3.10). If SIRT5 catalytic activity is required for melanoma proliferation, we reasoned that introduction of the catalytically-dead mutation H158Y would promote cell death upon knockdown of endogenous WT SIRT5. Since both SIRT5 KD1 and KD2 resulted in SK-MEL-103 cell death in all samples (both isoforms, WT and H158Y), it is still unclear whether SIRT5 maintains human melanoma survival via its catalytic functions. Thus, reintroduction of an shRNA resistant SIRT5 does not rescue the lethality observed upon introduction of lentiviral shRNAs.

To confirm previous reports (Matsushita et al., 2011; Park et al., 2013) that SIRT5 resides in nuclear, cytoplasmic and mitochondrial cellular compartments, we tested by immunoblotting the ability of overexpressed SIRT5 isoform 1 and isoform 2 to localize to these cellular structures. Upon subcellular fractionation of A2058 SIRT5 overexpressing cells, an increase in SIRT5 isoform 1 protein abundance was observed in the nucleus, cytoplasm and mitochondria compared the vector-only control. The lower molecular weight isoform 2 was present in the nucleus and mitochondria, as expected (Figure 3.11, top panel). To assess the purity of these subcellular fractions, we immunoblotted for PDH E1α, a mitochondrial marker and Histone H3, a nuclear marker (Figure 3.11, lower panels). While this analysis revealed slight crosscontamination of the fractions, we conclude that SIRT5 isoform 1 and 2 are overexpressed and localize as expected. To further support this finding,

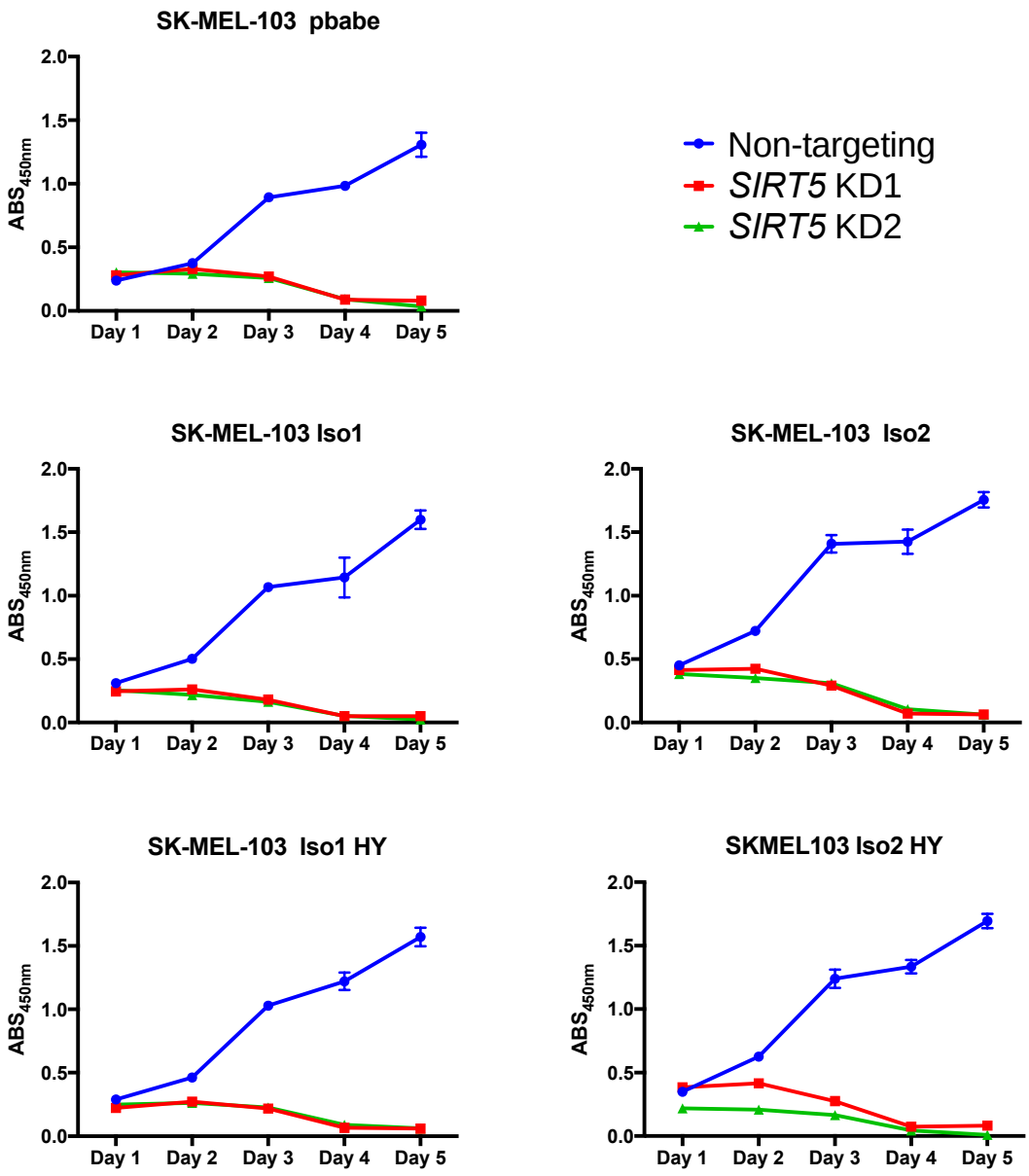

Figure 3.10 Overexpression of shRNA-resistant *SIRT5* results in SK-MEL-103 cell death upon SIRT5 knockdown. WST-1 viability assays (as done in Figure 3.4) demonstrate that reconstitution of SIRT5 protein from a lentivirally-transduced cDNA does not promote cellular growth and viability upon SIRT5 knockdown. pbabe, vector control; Iso1, SIRT5 Isoform 1 WT; Iso2, SIRT5 Isoform 2 WT. HY indicates H158Y mutant SIRT5. Iso1, Iso1 HY, Iso2, and Iso2 HY are resistant to KD1 shRNA, but sensitive to KD2 shRNA.

immunofluorescence staining for SIRT5 reveals a SIRT5 signal (green) in the nucleus and co-localization with the mitochondrial stain, mitotracker (Figure 3.12). Loss of the immunofluorescent SIRT5 signal (green) in cells infected with SIRT5 KD1 and KD2 shRNAs confirms the specificity of the SIRT5 signal in the non-targeting control cells (Figure 3.12, top panel).

Loss of SIRT5 induces apoptosis in melanoma cells

The induction of cleaved caspase 3 (Figure 3.6) upon SIRT5 loss prompted us to gain a better mechanistic understanding into the death phenotype of melanoma cell lines upon SIRT5 knockdown. We, therefore, asked if cell death was the result of apoptosis. In order to test this, we analyzed by flow cytometry cells stained with Annexin V and propidium iodide (PI). Cells undergoing early or late apoptosis will stain positively for Annexin V. Cells that have lost membrane integrity will be positive for PI by flow cytometry, affording the ability to distinguish between apoptotic (Annexin V^+) and necrotic (Annexin V^-/PI^+) cell death. We lentivirally infected A2058 and SK-MEL-103 cell lines with a non-targeting control, SIRT5 KD1, or SIRT5 KD2 shRNA virus. Ninety-six hours after infection a significant (at least $p<0.05$) increase in the number of Annexin V-positive cells was observed in both knockdowns in both A2058 and SK-MEL103 cell lines (Figure 3.13 A. and B.). Summing Q2: Annexin V^+/PI^+ and Q3: Annexin V^+/PI^-, there is a 2-3.5 fold increase in the percentage of Annexin V^+ cells in A2058 and a 5-10 fold increase in the percentage of Annexin V^+ cells in SK-MEL-103 upon SIRT5 knockdown (Figure 3.13 B.). These data indicate that loss of SIRT5 in melanoma cells

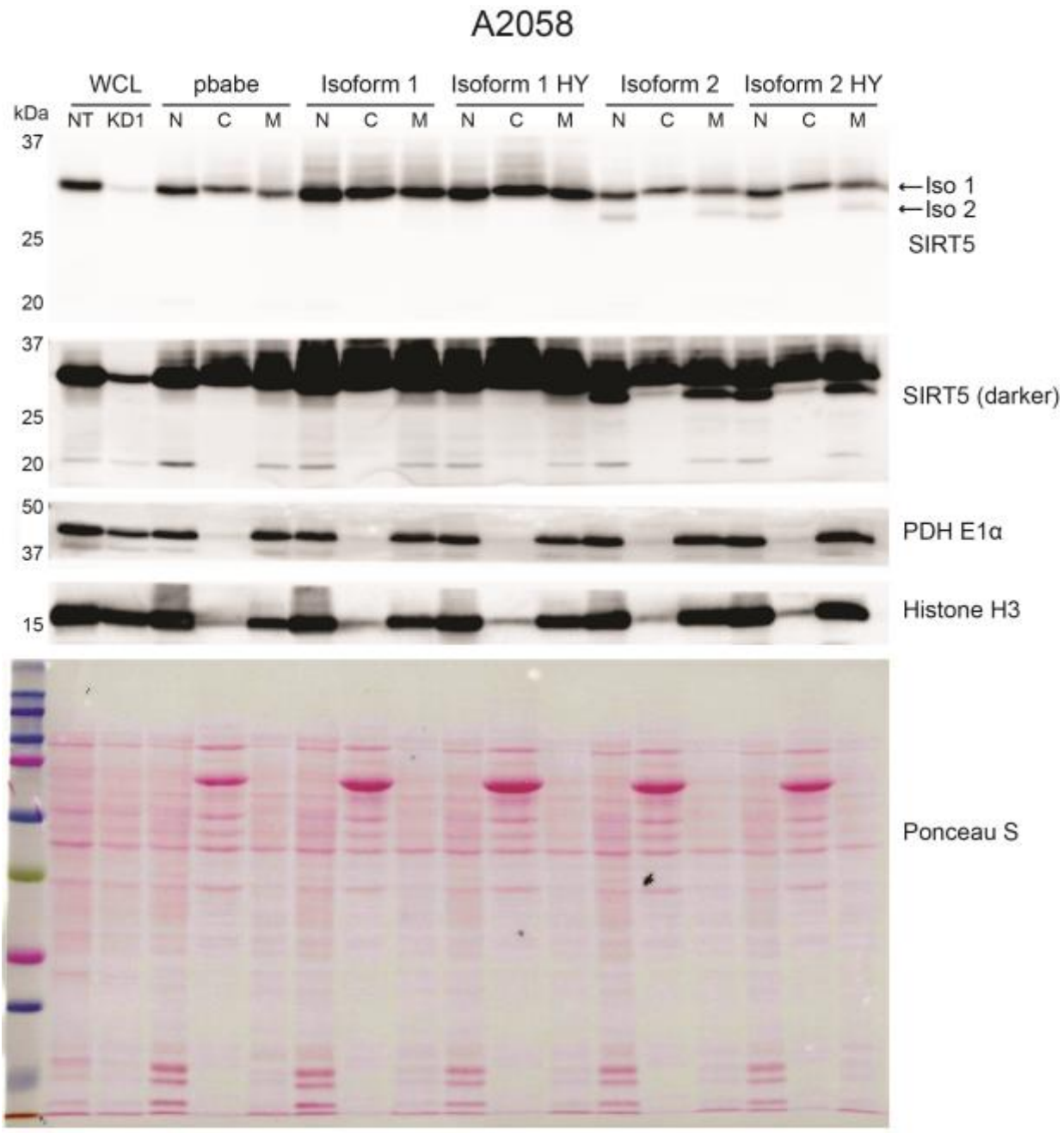

Figure 3.11 SIRT5 is localized to the nucleus and mitochondria in A2058 cells. A. Subcellular fractionation of SIRT5 from pbabe (mock)-infected control cells or cells overexpressing Isoform 1, Isoform 2 or the associated H159Y-mutant confirms SIRT5 isoform 1 and 2 overexpression and reveal that SIRT5 is resident in the nucleus (N), cytoplasm (C) and mitochondria (M). Immunoblot for PDH E1a (mitochondrial) and Histone H3 (nuclear) are used to assess purity of the associated fractions. Ponceau S total protein stain is illustrated below.

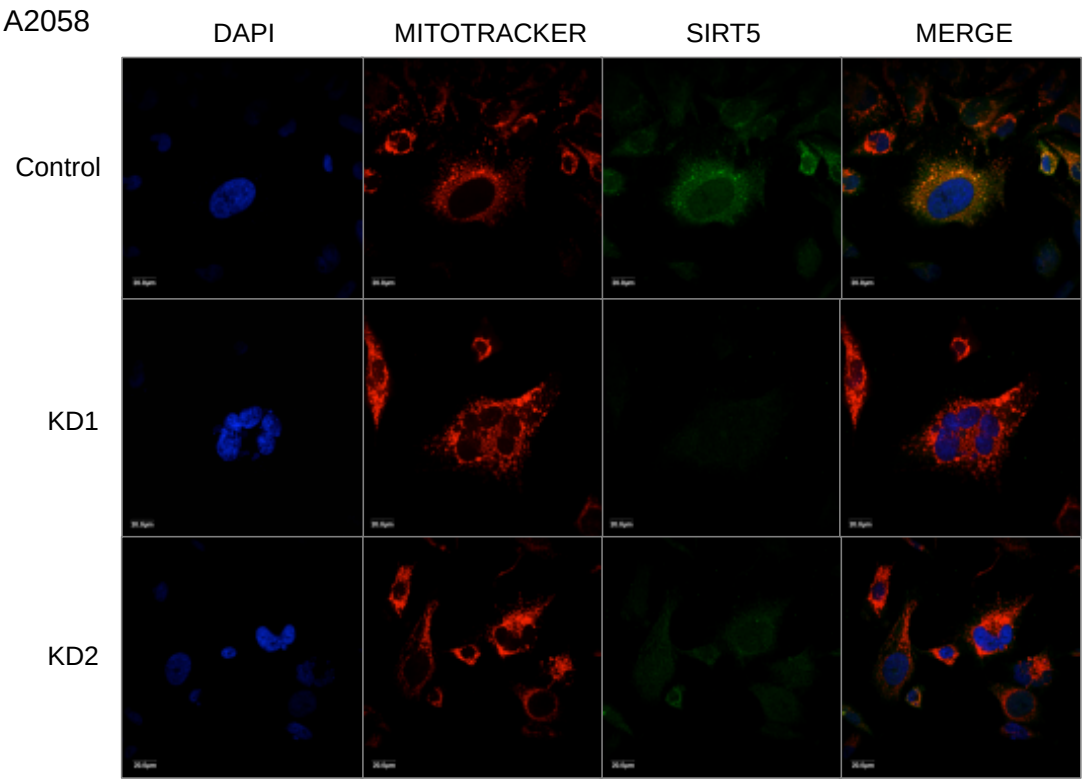

Figure 3.12 Immunofluorescent analysis of SIRT5 localization. Immunofluorescent analysis of A2058 cells 96 hours after SIRT5 shRNA-mediated knockdown reveals loss of SIRT5 antibody staining (compare Control to KD1 and KD2). SIRT5 (green) co-localizes with mitotracker-stained mitochondria (red) as well as to extra-mitochondrial cellular compartments.

results in an increase in apoptosis. As a positive control, A2058 and SK-MEL-102 cells were treated or mock-treated with the pro-apoptotic agent staurospoirne (1µm for 30 minutes). A 4-5 fold increase in Annexin V^+ cells was observed in treated cells when compared to cells treated with vehicle Figure 3.13 C.), indicating reliability of the assay.

To further investigate the role for SIRT5 in suppressing apoptosis in melanoma cells, we used RNAseq to determine global gene expression changes in A2058, SK-MEL-103 and A375 cells upon SIRT5 knockdown, with a focus on select genes encoding pro- or

anti-apoptotic proteins. Heatmaps of FPKM values, shown in Figure 3.14 A., B. and C., highlight perturbations in both the pro- and anti-apoptotic regulatory pathways. Interestingly, decreases in expression of several genes important for the anti-apoptotic response were noted (Figure 3.14, top panel). Surprisingly, RNAseq analysis reveals only a small number of genes, common to A2058, A375 and SK-MEL103 cells, are significantly ($p<0.05$) downregulated or upregulated 96 hours after SIRT5 depletion (Figure 3.14 D.). The pathways in which these genes act and their potential in modulating melanoma cell death requires further investigation. Upon closer examination, several of the anti-apoptotic BCL2 family members were often significantly ($p<0.05$) downregulated in both KD1 and KD2 in each cell lines (Figure 3.15 A.). Consistent with these data, expression of several pro-apoptotic genes is increased, though several inconsistencies between cell lines are noted (Figure 3.15 B.). Based on these data, we then proposed the model that SIRT5 impacts the anti-apoptotic response in part by downregulating BCL2 upon SIRT5 loss, leading to melanoma cell death.

To test this hypothesis, we generated A2058 cells that stably overexpress BCL2 (BCL2 OE), using an empty vector as a control (Vector) (Figure 3.16 A.). BCL2 is readily detected and increased in abundance compared to the vector control. As expected, upon SIRT5 knockdown, a reduction in the pro-apoptotic marker, caspase 3 cleavage is reduced. Using the WST-1 viability assay, A2058 cells lacking SIRT5, but overexpress BCL2, were found to have enhanced growth over those that did not overexpress BCL2 (Figure 3.16 B.). Importantly, BCL2 itself does not promote human melanoma cell growth in the presence of SIRT5 (Figure 3.16 B., Vector vs. BCL2 OE; Day 5 control).

Thus, expression of anti-apoptotic BCL2 is sufficient to partially rescue SIRT5-mediated cell death in A2058 cells.

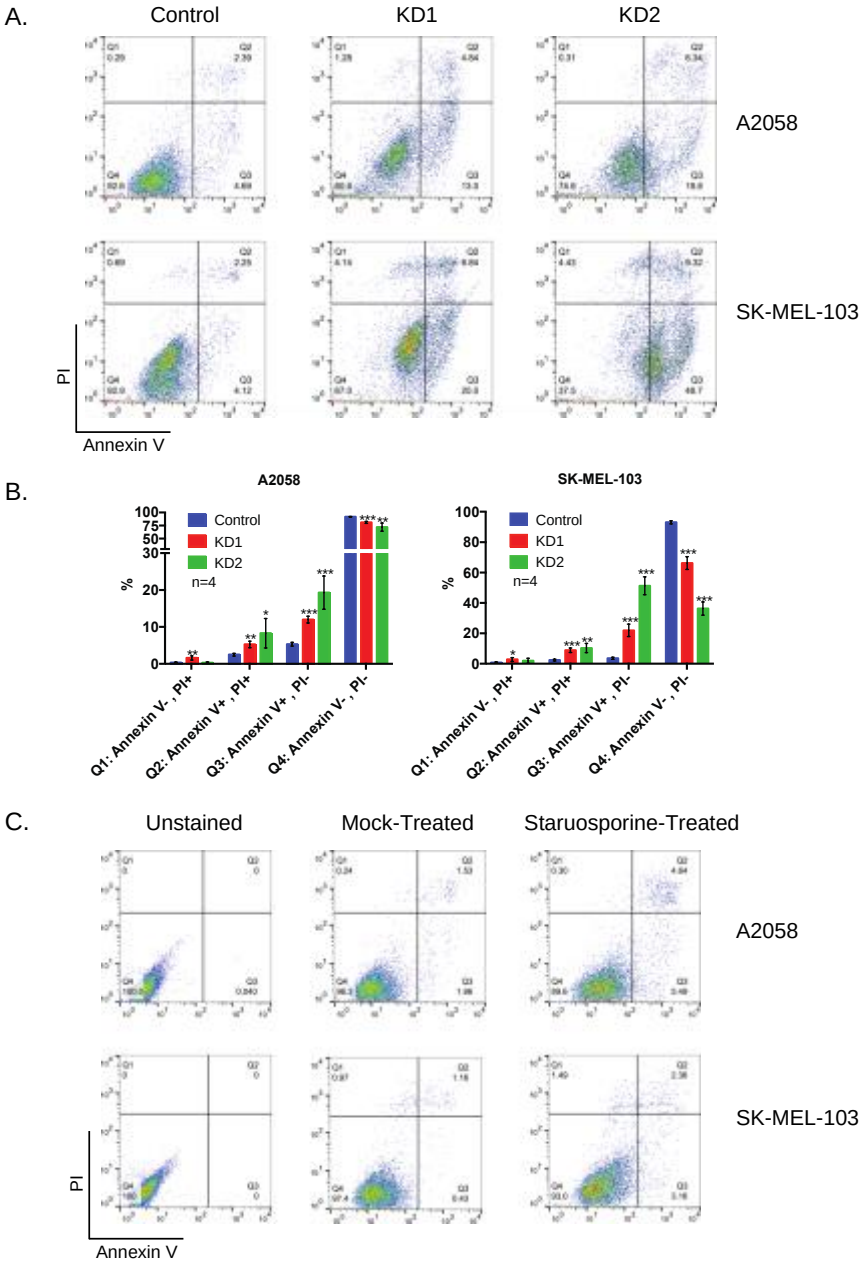

Figure 3.13 SIRT5 knockdown induces apoptosis in melanoma cell lines. A. Flow cytometric analysis of A2058 and SK-MEL103 cells show an increased percentage of Annexin V-stained cells 96 hours after SIRT5 knockdown. Representative plots are shown. **B**. Quantification of each quadrant in n=4 samples reveals a statistically significant increase in Annexin V^+ staining (Q2 and Q3) in both KD1 and KD2 in both cell lines. *p<0.05, **p<0.01, ***p<0.001 **C**. Staurosporine treatment induces apoptosis as measured by Annexin V staining in A2058 and SK-MEL103 cells lines, used as a positive control.

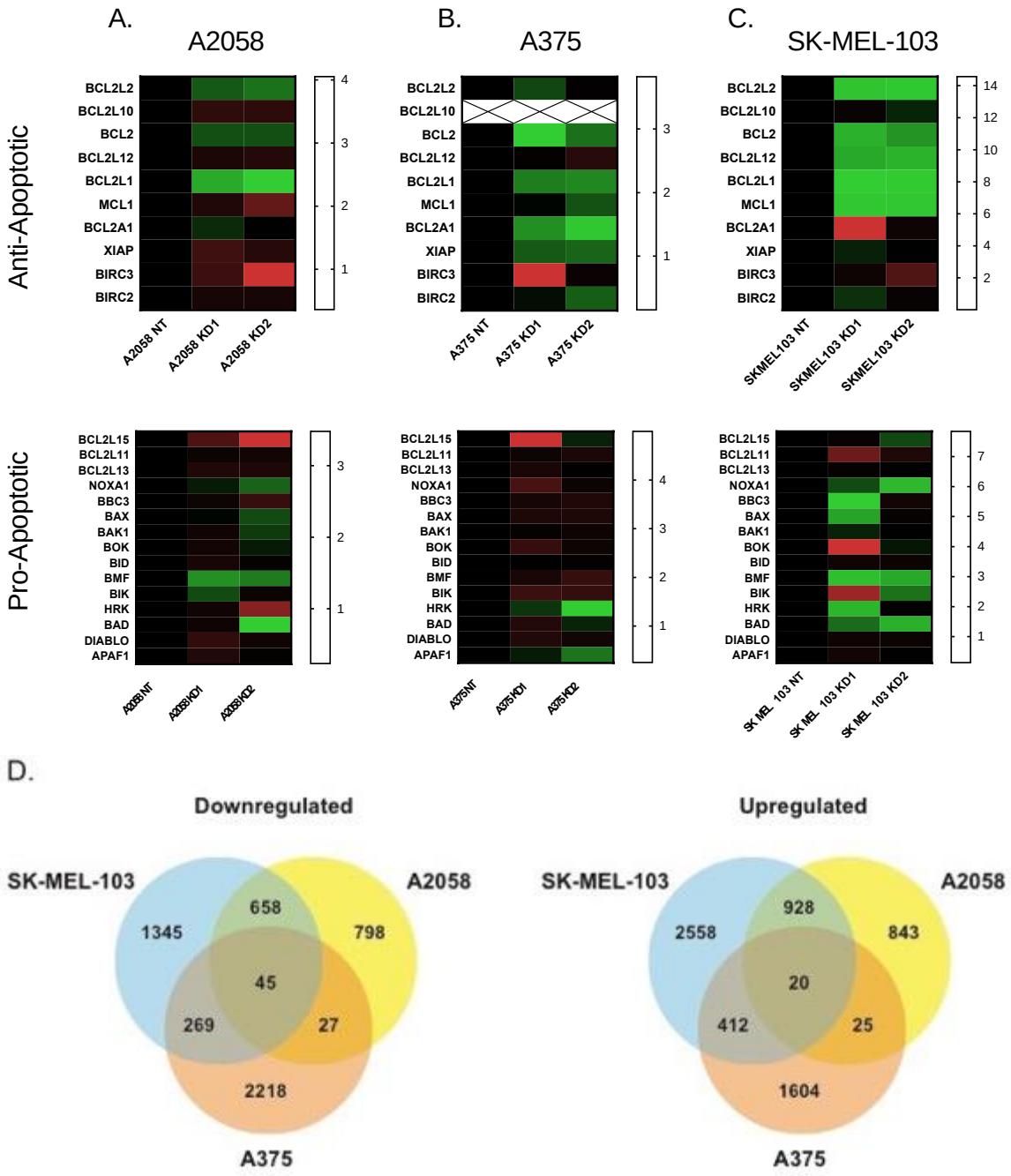

Figure 3.14 Apoptotic gene expression is altered upon SIRT5 knockdown. Heatmap of FPKM values calculated from RNAseq data of **A**. A2058, **B**. A375 and **C**. SK-MEL-103 cells. Expression profiles of selected pro- and anti-apoptotic genes are illustrated. Values for each non-targeting (NT) control sample are set to 1, relative differences for each knockdown are illustrated in red (increased expression) or green (decreased expression). Statistical significance is not calculated (see Figure 3.15). **D.** Venn diagrams of numbers of significantly ($p<0.05$) downregulated or upregulated gene expression changes from RNAseq analysis unique or common to the indicated cell lines upon SIRT5 knockdown (comparing NT control to changes common to both knockdowns).

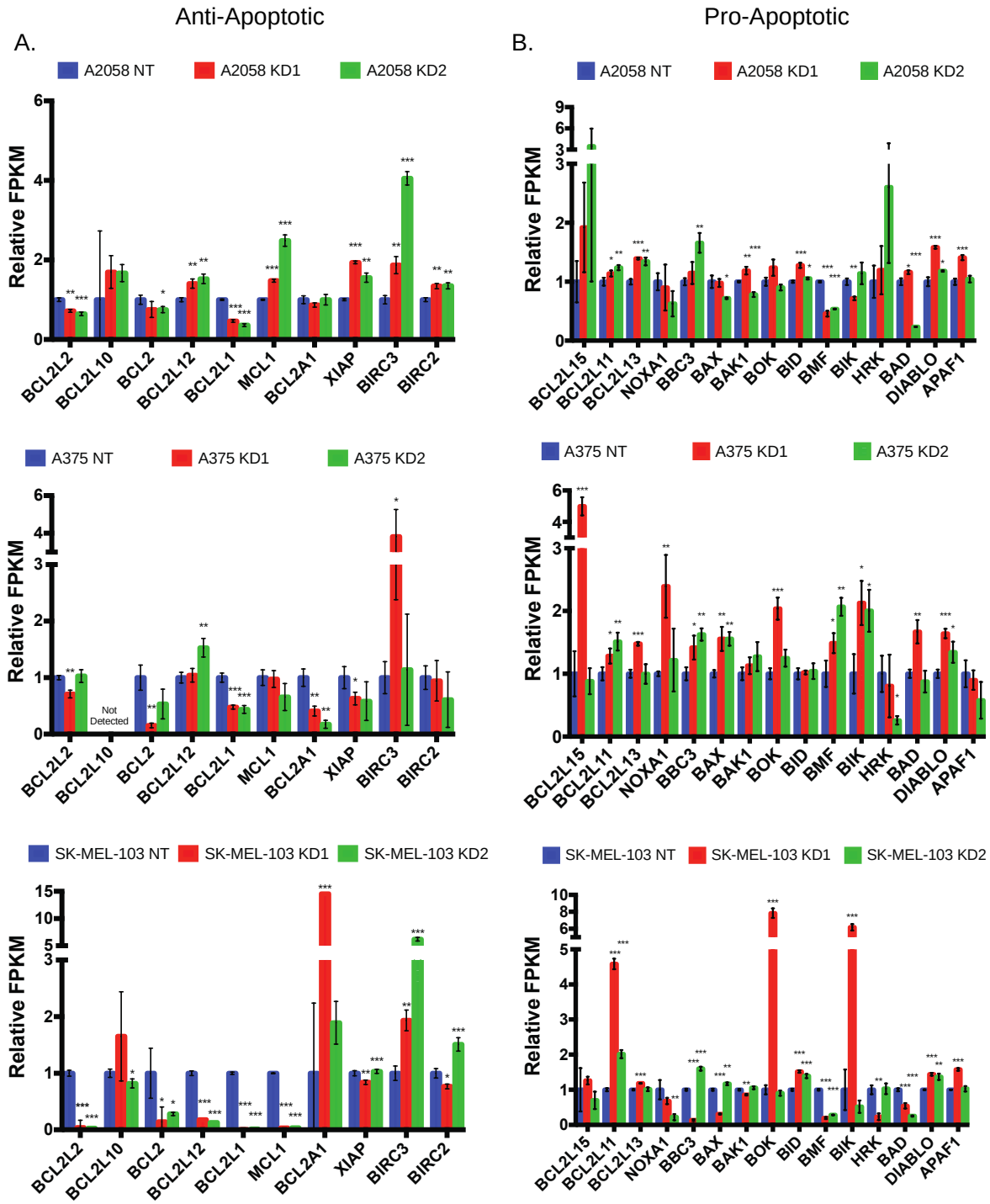

Figure 3.15 Significant pro- and anti-apoptotic gene expression changes upon SIRT5 knockdown. Relative FPKM values of selected anti-apoptotic (**A**.) and pro-apoptotic (**B**.) genes in non-targeting control (NT) compared to KD1 and KD2 in A2058, A375 and SK-MEL-103 cells lines, 96 hours post-lentiviral transduction. *p<0.05, **p<0.01, ***p<0.001, n=3

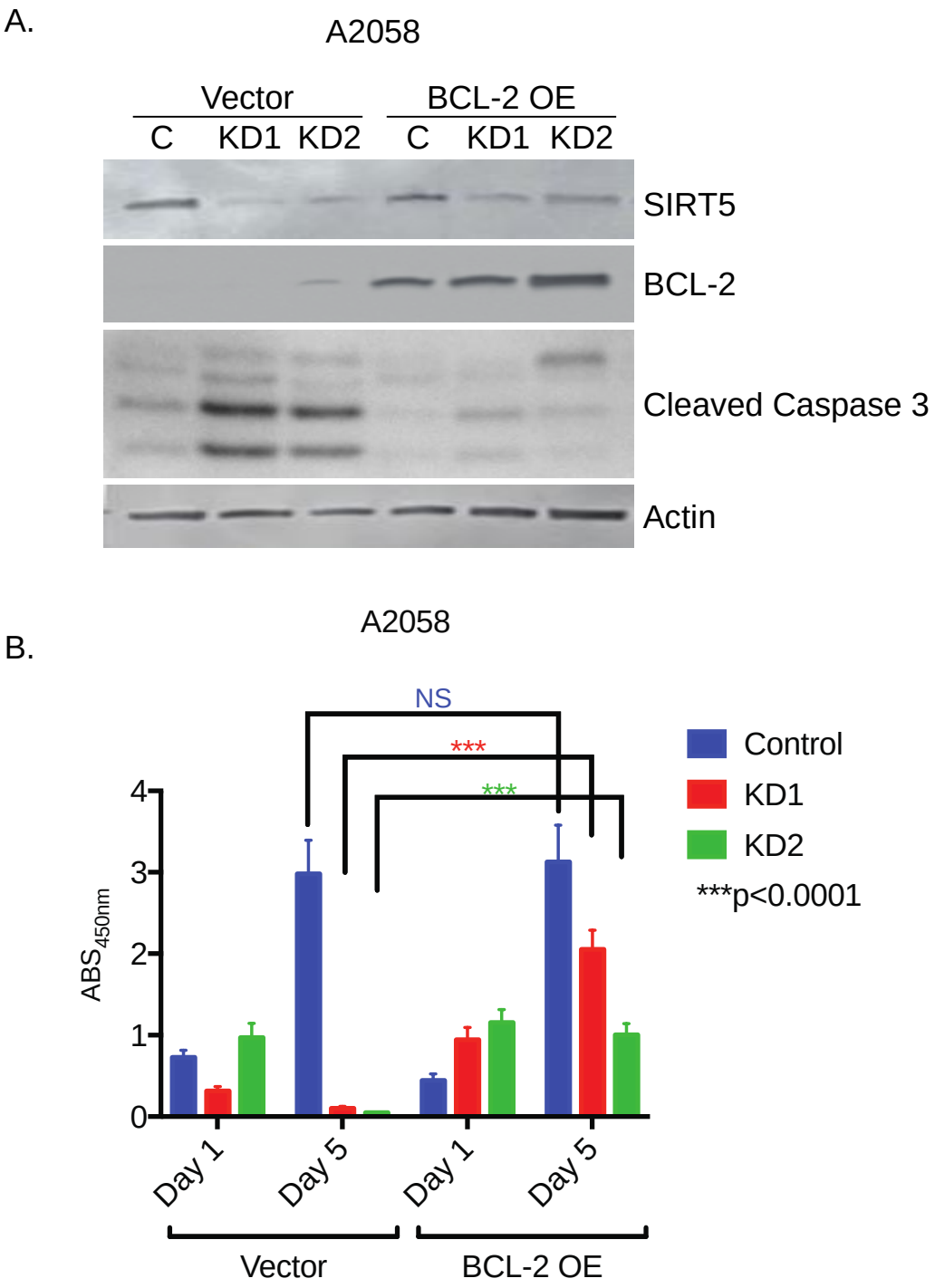

Figure 3.16 BCL-2 overexpression partially rescues SIRT5-dependent cell death in A2058 cells. **A**. Immunoblotting of A2058 cells overexpressing the anti-apoptotic BCL-2 (vector vs. BCL-2 OE) have reduced levels of cleaved caspase 3 upon SIRT5 knockdown (C, control, compared to KD1 and KD2). **B**. WST-1 viability assay (as done in Figure 3.4) demonstrates that BCL-2 overexpression (BCL-2 OE) from a lentivirally-transduced cDNA partially rescues cellular growth and viability upon SIRT5 knockdown.

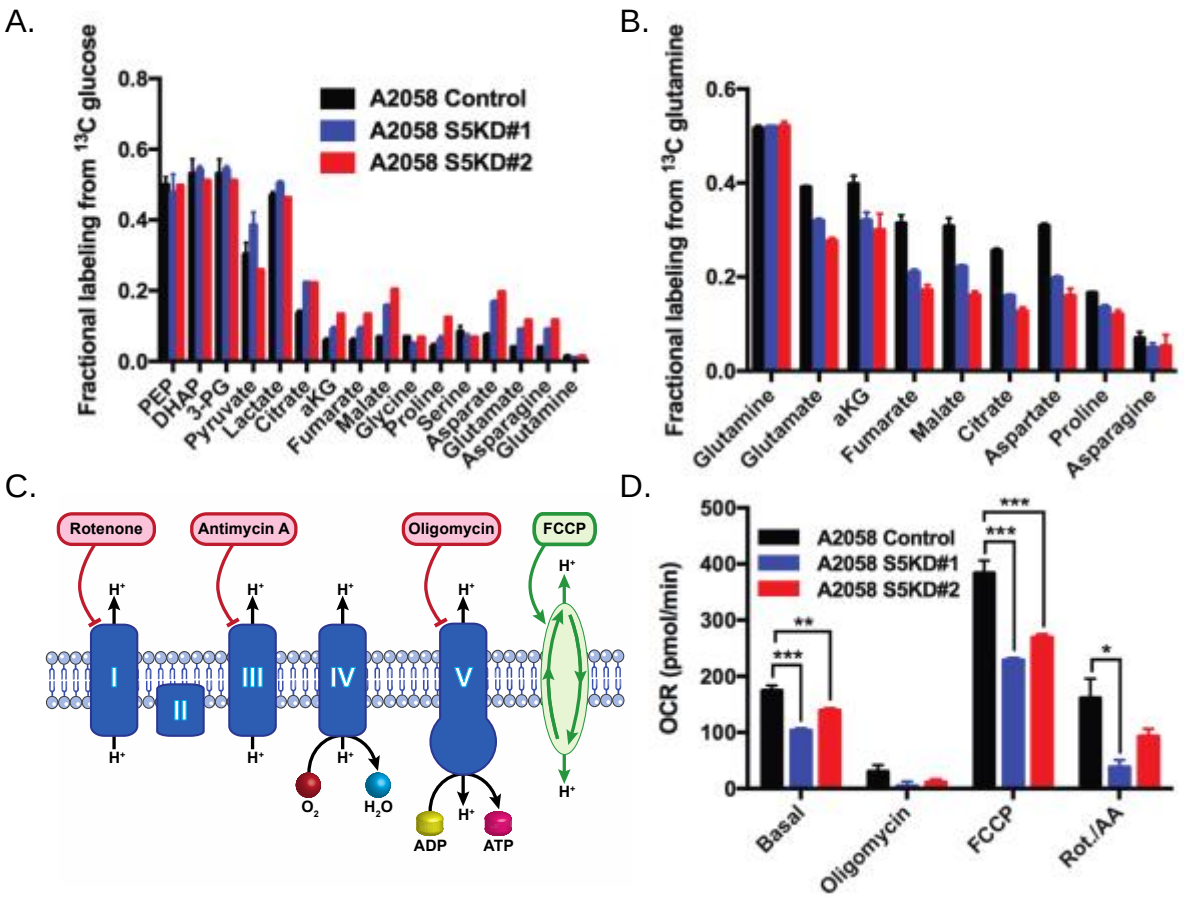

Figure 3.17 Loss of SIRT5 decreases glutamine-dependent metabolite labeling and glucose-dependent respiration. Fractionally-labeled, **A.** glucose-derived or **B.** glutamine-derived metabolite levels are quantified upon SIRT5 loss in A2058 cells. **C**. Schematic of the electron transport chain in mammalian mitochondria and the inhibitors of the associated complexes. The mitochondrial oxidative phosphorylation uncoupler, FCCP, carbonyl cyanide-*4*-(trifluoromethoxy)phenylhydrazone, disrupts ATP synthesis by allowing protons to cross the mitochondrial membrane, as indicated. **D**. Glucose-dependent oxygen-consumption rate (OCR), the measure of mitochondrial respiration, is decreased upon SIRT5 knockdown.

Metabolic alterations in SIRT5-deficient melanoma cells

Tumor cells are known to reconfigure metabolism in order to meet the anabolic demands of uncontrolled cellular proliferation (Ward and Thompson, 2012). Melanoma and other cancer cells perform robust aerobic glycolysis, described as Warburg

metabolism (Warburg, 1956), and glutamine-driven tricarboxylic acid (TCA) cycle filling (Filipp et al., 2012a; Filipp et al., 2012b; Ratnikov et al., 2015; Scott et al., 2011). Reports that inhibiting glycolysis or glutamine metabolism sensitizes melanoma cells to induction of cell death prompted us to further investigate the role of SIRT5 in promoting melanoma survival (Qin et al., 2010a, b). Therefore, considering the striking sensitivity of melanoma cells to SIRT5 depletion, we asked if a reduction of SIRT5 in melanoma would result in metabolic alterations. Culturing A2058 cells in medium containing stable isotopes of [$^{13}C_6$]-glucose or [$^{13}C_5$]-glutamine in the presence of SIRT5 knockdown, we are able to accurately quantify glucose and glutamine-derived metabolites using mass spectrometry. Upon SIRT5 knockdown, glucose-dependent metabolites were generally increased compared to controls (Figure 3.17 A.), indicating an increased contribution of [$^{13}C_6$]-glucose-derived carbon to the TCA cycle. Similarly, in control cells, glutamine is converted into each of the glutamine-derived metabolites evaluated: glutamate, proline, aspartate, asparagine, and the TCA cycle metabolites alpha-ketoglutarate, citrate, fumarate, and malate (Figure 3.17 B.). However, SIRT5 loss reduced the levels of these metabolites in A2058 cells. Importantly, the level of glutamine in both knockdown samples is equivalent to the non-targeting control sample (Figure 3.17 B.), suggesting a SIRT5-dependent defect in glutamine metabolism.

Previous reports indicate that SIRT5, predominantly localized to the mitochondrial matrix, suppresses mitochondrial respiration through specific mitochondrial complexes (Park et al., 2013). SIRT5 regulates the TCA cycle, in part by desuccinylating and inactivating succinate dehydrogenase (a member of the electron transport chain,

complex II, Figure 3.17 C.), and the pyruvate dehydrogenase complex that converts pyruvate generated in glycolysis into acetyl-CoA. We, therefore, used an XFe96 extracellular flux analyzer to determine the effect of SIRT5 knockdown on mitochondrial respiration through oxygen consumption rate (OCR) measurements of melanoma cells. We found that upon exposure of A2058 cells to oligomycin (inhibitor of complex V), FCCP (uncouples electron transport and phosphorylation reactions) or antimycin A/rotenone (complex I/III inhibitors) decreased OCR was observed, as well as a significantly ($p<0.005$) reduced basal respiration rates upon SIRT5 knockdown compared to SIRT5-proficient control cells (Figure 3.17 C. and D.). Thus, loss of SIRT5 in melanoma cells results in metabolic perturbations, including increased glucose and decreased glutamine metabolism, and decreased mitochondrial respiration as evidenced by a reduction in the oxygen consumption rate.

Discussion

Most sirtuins have been described as either tumor suppressors or oncogenes, or in some contexts both. Surprisingly, despite recent reports that SIRT5 promotes chemoresistance in non-small cell lung carcinoma (Lu et al., 2014), and suppresses ROS to promote growth of lung cancer cells (Lin et al., 2013), SIRT5 has yet to be clearly implicated in cancer. SIRT5, a lysine deacylase with desuccinyl, demalonyl, and deglutaryl activities, impacts the enzymatic functions regulating mitochondrial metabolism: amino acid degradation, TCA cycle, and fatty acid metabolism. We have previously described SIRT5-dependent regulation of two substrates, PDC and

Succinate Dehydrogenase (SDH). SIRT5 inhibits biochemical activities of both complexes, and suppressed overall mitochondrial respiration (Park et al., 2013).

In melanoma and other cancer types, metabolism is reconfigured to meet the anabolic demands of uncontrolled cellular proliferation (Theodosakis et al., 2014). Reversal of this metabolic reprogramming can induce senescence and cell death in melanoma (Kaplon et al., 2013); however, little research has focused on developing clinically-relevant therapeutics in this regard. These findings combined with the attention cancer metabolism as a potential therapeutic target has received (Zwaans and Lombard, 2014), we propose that SIRT5 may represent a useful means to modulate oncogenesis.

In this chapter, we define a role for SIRT5 in maintaining melanoma cell survival and in vivo tumor growth, through suppression of apoptosis and potentially through the regulation of metabolism. In 10/10 human melanoma cell lines, either harboring BRAF or NRAS mutations, SIRT5 knockdown results in rapid loss of proliferative potential and cell death. Surprisingly, reintroduction of RNAi-resistant SIRT5 does not rescue the cell death phenotype. One possibility for this is that exogenously expressed SIRT5 is not localized to the cellular compartment required for melanoma survival. Another explanation is that the SIRT5 cDNA sequence used to generate the exogenously expression protein does not match that required for survival of melanoma cell lines.

Overexpression of anti-apoptotic BCL2 thwarts the cell death phenotype induced upon SIRT5 depletion. Although our original hypothesis focused on regulation of metabolic

reprogramming in melanoma, these data point toward a role for SIRT5 in modulating apoptosis. It is not clear if overexpression of BCL2 is simply overriding the pro-apoptotic signal occurring upon SIRT5 loss. Whether SIRT5 directly interacts with and regulates the activity of apoptotic proteins or whether this is a secondary effect of metabolic derangement or other phenotypes is still unclear.

Furthermore, targeted metabolomics and respirometry demonstrates that SIRT5 regulates glucose and glutamine metabolism in melanoma to promote metabolic reprogramming. Although the impact of this reprogramming on melanoma survival has yet to be clearly described, and requires more careful examination (see Future Directions).

Based on these data, and our ability to identify SIRT5 inhibitors, our current goal is to elucidate roles for SIRT5 in regulating melanoma cellular metabolism, and to develop, optimize, and evaluate SIRT5 inhibitors. It is unclear if targeting SIRT5 in other cancers that depend on similar oncogenes or oncogenic pathway would result in the same sensitivity as described for melanoma; though, SIRT5 depletion is compatible with normal growth in many other cell types, such as 293T and MEFs, among others. Also, *Sirt5* knockout mice are grossly unremarkable, fertile, and healthy, with minimal metabolic phenotypes elicited in response to prolonged fasting. These mild phenotypes in normal cells and tissues, coupled with the dramatic, rapid lethality we observe upon SIRT5 depletion in melanoma, raise key questions about SIRT5 function in the melanocytic lineage.

Materials and Methods

Analysis of *SIRT5* gene amplification, mRNA and protein expression in melanoma

Copy number analysis of melanoma cell lines was performed by high density SNP array of 8 primary, 72 stage III, 51 stage IV and 8 stage III/IV ('metastatic' disease) melanoma cell lines, as previously described (Stark et al and Dutton-Regester et al). Data was analyzed using Nexus Copy Number (BioDiscovery) for copy gain, copy loss and loss of heterozygosity of genes and chromosomal regions. Data from the TCGA was used via cBioPortal to further investigate *SIRT5* in melanoma (n=278; Cancer Genome Atlas Network), including copy number (by GISTIC 2.0) and expression data (by RNAseq) and the correlation with clinical attribute, including the Clark Level at diagnosis of the melanoma. Analysis of mRNA expression data from a publically available dataset (Talantov et al; GEO accession ID: GDS1375) was carried out to investigate the potential correlation between *SIRT5* mRNA expression and melanoma, benign nevi and normal skin samples. These expression data were ascertained using the Human Genome U133A Array (Affymetrix), which analyzes expression using a number of probes that make up a 'Probe Set'. There is only one fully informative Probe Set in which all the individual probes bind to the *SIRT5* mRNA (219185_at), which was therefore used for the analysis.

Cell Culture

Melanoma cell lines harboring mutations in either *NRAS* or *BRAF* (Table 3.1): A375, A2058, SK-MEL-2, SK-MEL-28, VMM15, and VMM917 were purchased from ATCC; SK-MEL-19 and SK-MEL103 were generously provided by Dr. Monique Verhaegen; C8161were generously provided by Dr. Zaneta Nikolovska-Coleska; and SK-MEL-293 were generously provided by Dr. Emily Bernstein. Unless otherwise noted, A375, A2058, SK-MEL-19 and SK-MEL-103 cell lines were grown in DMEM (Gibco) containing 4.5g/L glucose, 110mg/L sodium pyruvate, 4mM L-glutamine, 10units/mL penicillin, 10µg/mL streptomycin and 10% heat-inactivated FBS. SK-MEL-2 and SK-MEL-28 cell lines were grown in EMEM (ATCC) containing 4.5g/L glucose, 110mg/L sodium pyruvate, 4mM L-glutamine, 10units/mL penicillin, 10µg/mL streptomycin and 10% heat-inactivated FBS. VMM15, VMM917, and SK-MEL-293 cell lines were grown in RPMI (Gibco) containing 4.5g/L glucose, 110mg/L sodium pyruvate, 4mM L-glutamine, 10units/mL penicillin, 10µg/mL streptomycin and 10% heat-inactivated FBS. The C8161 cell line was grown in DMEM/F12 (1:1) (Gibco) containing 1.2mM L-glutamine, 1% non-essential amino acids, 10units/mL penicillin, 10µg/mL streptomycin and 5% heat-inactivated FBS. All cell lines were routinely confirmed to be free of mycoplasma contamination and were grown in a humidified chamber at 37°C containing 5% CO_2.

Cell Line	Catalog Number	BRAF	NRAS	CDKN2A	p53	Tumor in Mice?	Age	Sex	Basal Growth Medium
A375	ATCC CRL-1619	V600E	WT	E61*, E69*	WT	Yes	54	F	DMEM
A2058	ATCC CRL-11147	V600E	WT	WT	V274F	Yes	43	M	DMEM
SK-MEL-28	ATCC HTB-72	V600E	WT	WT	L145R	Yes	51	M	EMEM
SK-MEL-19		V600E	WT	R58*	WT				DMEM
VMM15	ATCC CRL-3227	V600E	WT	WT	WT		39	M	RPMI
SK-MEL-239		V600E							RPMI
SK-MEL-2	ATCC HTB-68	WT	Q61R	WT		Yes	60	M	EMEM
VMM917	ATCC CRL-3232	WT	Q61L Q61R	R80			57	M	RPMI
SK-MEL-103		WT	Q61R	P114L	WT	Yes	66	M	DMEM
C8161		WT	Q61R			Yes			DMEM:F12

Table 3.1 Cell lines used in this chapter

Lentiviral Transduction for *SIRT5* Knockdown

Lentiviral plasmids containing a non-silencing shRNA (Control) (Addgene) or one of two shRNAs targeting human *SIRT5* (KD1: Dharmacon Clone TRCN0000018546, KD2: TRCN0000018547) in the pLKO.1 backbone, encoding puromycin *N*-acetyl-transferase, were used to generate lentiviral particles (UM Vector Core). Lentiviral transduction was carried out in the presence of 8µg/ml polybrene in complete growth medium for 24 hours, after which, virus-containing medium was replaced with fresh complete growth medium. Unless otherwise noted, 1µg/ml puromycin was added 48 hours post-infection to select for positive transductants. Successful SIRT5 knockdown was routinely confirmed by western blotting 48-96 hours post-infection.

Immunobloting

Whole-cell protein extracts were prepared in Laemmli sample buffer (62.5mM Tris pH 6.8, 2% SDS, 10% glycerol), supplemented with 710mM β-mercaptoethanol. Lysates were sonicated for 30 seconds using a Branson Sonifier set to output "2." Lysates were then clarified by centrifugation at 15 000rcf for 30 minutes at 4ºC. Protein concentrations were determined using the DC Protein Assay (Bio Rad). Equivalent amounts (10-100µg) of total protein were fractionated by SDS-PAGE on a 10% or 12% polyacrylamide gel, electrophoretically transferred to PVDF, and probed with antibodies diluted in 5% nonfat milk in 1XTBS-0.1% Tween-20 as indicated in Table 3.1. Probed membranes were imaged on an ImageQuant LAS 4000 Scanner (GE Healthcare) after application of Immobilon Western HRP Substrate (Millipore).

Antibody	**Company**	**Clone/Cat#**	**Dilution**	**~kDa**
α-Tubulin	Santa Cruz	B-5-1-2	1:5-10K	55
Cleaved Caspase 3	Cell Signaling	9664L	1:2K	17, 19
GAPDH	Santa Cruz	6C5	1:5-10K	37
PDH E1α	Abcam	ab67592	1:2K	43
BCL-2	Cell Signaling	4223	1:1K	26
β-Actin	Sigma	A5441	1:1K	42
SIRT5 (IF)	Sigma	HPA022002	1µg/ml	--
SIRT5 (western)	Cell Signaling	D8C3	1:2K	30
Pan-succinyllysine	PTM Biolabs	PTM-401	1:1K	Various
MCL1	Thermofisher	RC13	1:500	40

Table 3.2 Antibodies used in this chapter

Flow Cytometry

A2058 and SK-MEL-103 cells were plated at a density of $0.5x10^6$ per well of two six-well plates per cell line. Four wells of each cell line were transduced with either a lentivirus expressing a non-silencing shRNA (control) or one of two shRNAs targeting *SIRT5* (KD1 or KD2). Ninety-six hours after transduction, puromycin-unselected cells were harvested and stained for 30 minutes at room temperature with Annexin V (BD Biosciences) and propidium iodide (Sigma), according to BD Biosciences staining protocol. Cells were analyzed by flow cytometry using a BD FACSCalibur and results were graphed using FlowJo 10.2 analysis software.

Colony Formation

Two million A2058 or SK-MEL-103 melanoma cell lines were lentivirally transduced in a 10-cm dish with a non-silencing shRNA or one of two shRNAs targeting human *SIRT5*. Forty-eight hours post-infection 5×10^4 cells were plated into each of four wells of a six-well dish as previously described. Twelve days after transduction, puromycin-selected cells were stained with 0.25% (w/v) crystal violet (Sigma) in 20% ethanol for 30 minutes according to standard protocols. Visible colonies were counted and graphed.

Cellular Proliferation

Forty-eight hours after lentiviral transduction, 5×10^3 cells were plated into 96-well plates in the presence of 1µg/ml puromycin. Twenty-four hours after plating, relative

cell mass was assessed using WST-1 Cell Proliferation Reagent (Clontech) per manufacturer's instruction. After addition of WST-1, plates were incubated at 37ºC for 2 hours before being reading the optical density at 450nm. OD_{450nm} was assessed every 24 hours as indicated and graphed. In parallel, representative brightfield micrographs were obtained 96 hours post-infection using an inverted Olympus light microscope.

Xenograft Models

A2058 and SK-MEL-103 puromycin-unselected cells were harvested 72 hours post-transduction with pLKO control, pLKO *SIRT5* KD1, or pLKO *SIRT5* KD2. Subcutaneous tumor growth was initiated by injection of $1x10^6$ cells of each cell line, resuspended in 1:1 DMEM:Matrigel Matrix (Corning), into the flanks of 11-13 week old NOD.Cg-*Prkdc*^{scid}*Hr*^{hr}/NCrHsd female mice (Envigo). Each experimental group contained 5 mice. Tumor size was measured in millimeters (mm) using Vernier calipers at the timepoints indicated. Tumor volume was calculated according to the formula:

$$V = \frac{X(Y^2)}{2}$$

where V is tumor volume in mm^3, X is the longest length of the tumor, and Y is the shorted length of the tumor, perpendicular to X. All mice were euthanized when a tumor ulcerated or reached $2000mm^3$. All mice were housed at the Biomedical Science Research Building (UM). Experiments were approved by and performed in accordance with the regulations of the University Committee on Use and Care of Animals.

RNAseq

A2058, A375 and SK-MEL-103 cells were plated at a density of $0.5x10^6$ per well of two six-well plates per cell line. Four wells of each cell line were transduced with either a lentivirus expressing a non-silencing shRNA (control) or one of two shRNAs targeting *SIRT5* (KD1 or KD2). Total RNA was TRIzol (Invitrogen) extracted 96 hours post-infection from three wells, and treated with RNAse-free DNAse I (Roche) for 1 hour at 37ºC, according to manufacturer's instructions. RNAs (n=3 for each of 3 cell lines for each knockdown condition, totaling 27 samples) were submitted to the University of Michigan Sequencing Core for sample processing and Illumina HiSeq-4000 50nt paired-end sequencing. The remaining well was harvested for protein to confirm by immunoblot SIRT5 knockdown. Differential sequencing analysis (DEseq) and Fragments Per Kilobase of transcript per Million mapped reads (FPKM) calculations were done by Dr. Miguel Rivera and Sowmya Iyer of Harvard Medical School. DEseq analysis of gene expression changes, comparing control to changes common to both knockdowns, was used to generate the Venn diagrams in Figure 3.14. Calculated p-values after adjusting for multiple comparisons less than 0.05 were considered significant.

[$^{13}C_6$] Glucose and [$^{13}C_5$] Glutamine Labelling for Metabolic Flux

[$^{13}C_6$] Glucose and [$^{13}C_5$] Glutamine labelling was carried out as described in Scott et al., JBC, 2011 (Scott et al., 2011). Briefly, 72 hours after transduction with pLKO control, pLKO *SIRT5* KD1, or pLKO *SIRT5* KD2, cells were trypsinized and plated in

triplicate in 6-well dishes at a density of 1 x 10^6 cells per well. Culture medium was replaced with [$^{13}C_6$] Glucose or [$^{13}C_5$] Glutamine labelling medium for 6 hours. Glucose labeling medium consisted of: MEM (Invitrogen 11090-081: 1 g/L glucose) supplemented with 1 g/L [U-$^{13}C_6$] glucose (Sigma-Aldrich), 10% v/v fetal bovine serum, 2 mM L-glutamine, 1% v/v pen/strep solution, and 1% MEM non-essential amino acids. Glutamine labeling medium was prepared as the glucose labeling medium, except an additional 1 g/L of unlabeled glucose, 1 mM unlabeled, and 1 mM [U-$^{13}C_5$] glutamine (Sigma-Aldrich) was added. After 6 hours, cells were washed with cold PBS, then 0.45 ml of 50% methanol:50% water containing the internal standard, 20 µM L-norvaline (Sigma N7627) was added to each well. Plates were frozen on dry ice for 30 minutes, and thawed on ice for 10 minutes. The cell suspension was transferred to a microfuge tube followed by the addition of 0.225 ml chloroform. Samples were vortexed centrifuged for 5 min at 20,000 rcf at 4°C. The top layer was transferred to a fresh tube and dried in a speedvac. Samples were then sent to the Sanford-Burnham Medical Research Institute for GC/MS-based metabolic profiling.

Immunofluorescence

A2058 were plated at a density of 0.5x10^6 per well of six-well plates contained glass coverslips. Twenty-four hours later, cells were transduced with either a lentivirus expressing a non-silencing shRNA (control) or one of two shRNAs targeting *SIRT5* (KD1 or KD2). Ninety-six hours after transduction, puromycin-selected cells were incubated with 100mM Mitotracker (BD Biosciences) for 30 minutes at 37ºC, washed

with PBS, and fixed in 3.7% formaldehyde. After permeabilization in 0.3% Triton X-100 for 10 minutes at room temperature, cells were blocked with 5% normal goat serum in 0.2% Triton X-100 in PBS for one hour. Cells were incubated in SIRT5 (Sigma) primary antibody diluted to 1µg/ml in 5% bovine serum albumin in 0.2% Triton X-100 in PBS overnight at 4ºC. Cells were then washed 3 times in 1X PBS and incubated in Alexa 488 anti-rabbit (Invitrogen) diluted 1:1000 in 5% bovine serum albumin in 0.2% Triton X-100 in PBS for 1 hour at room temperature. Cells were wash washed 2 times in 1X PBS, and 1X with PBS supplemented with 0.01µg/ml DAPI. Cells were mounted with prolong gold antifade reagent (Thermo Fisher) and imaged on an Olympus FV 500 Confocal microscope.

Generation of SIRT5 and BCL-2 Overexpressing Cell Lines

A2058 or SK-MEL-103 cells were transduced with a vector-only control lentivirus or a lentivirus expressing either full-length SIRT5 isoform 1 (NM_012241.4; NP_036373.1) or full-length SIRT5 isoform 2 (NM_031244.3; NP_112534.1). Stable transductants were hygromycin selected in 100µg/ml hygromycin for 12 days. BCL-2 overexpressing cell lines were generated via transduction with a vector-only control lentivirus or a lentivirus expressing full-length BCL-2. Stable transductants were puromycin selected in 1µg/ml puromycin until complete cell death of the mock-infected cells was observed. Lentiviral particles were generated at the UM Vector Core, using plasmids pbabe-hygro (Addgene), SIRT5 isoform 1 or 2 cDNA cloned into pbabe-hygro, pCDH-puro and pCDH-puro-BCL2 (Addgene). Lentiviral transduction was carried out in the presence of

8µg/ml polybrene in complete growth medium for 24 hours, after which, virus-containing medium was replaced with fresh complete growth medium.

Oxygen Consumption Rate Measurement

The oxygen consumption rate [OCR (pmol/min)] in A2058 cells were measured using the Seahorse XF96 Extracellular Flux Analyzer (Seahorse Bioscience, Billerica, MA). Briefly, forty thousand A2058 cells (control, KD1 and KD2) were plated into each well of a 96-well plate and centrifuged at 200g for 1 minute. Cells were then incubated in 5% CO_2 at 37^{o}C for 6 hours. After incubation, cells were washed and analyzed in XF Running Buffer (XF base medium, supplemented with 25mM glucose and 1mM sodium pyruvate), pH 7.4 at 37^{o}C per the manufacturer's instructions to obtain real-time measurements of OCR. Where indicated, OCR was analyzed in response to 2 µM oligomycin, 1µM fluoro-carbonyl cyanide phenylhydrazone (FCCP) and 0.5 µM rotenone plus 0.5 µM antimycin A (all Sigma-Aldrich).

Statistical Analysis

All statistical analyses were performed using Prism 7 graphing software. Unless otherwise noted, $p<0.05$ produced from an unpaired student's t-test was considered significant.

Acknowledgments

I thank members of the Lombard lab for thoughtful discussions of these data. Dr. Zaneta Nikolovska-Coleska (UM) provided the C8161 cell line. Dr. Monique Verhaegen (UM) provided the SK-MEL-103 and SK-MEL-19 cell lines. Dr. Emily Bernstein (Mt. Sinai Health System, NY) provided the SK-MEL-239 cell line. Dr. Lauren Rodenbarger (UM) generated the BCL-2 overexpressing cell lines, and performed the viability and immunoblotting analysis presented in Figure 3.16. Dr. Surinder Kumar (UM) performed immunoblotting analysis in Figure 3.9. Dr. Antonia Prichard (Royal Brisbane Hospital, Australia) analyzed *SIRT5* copy number and RNA expression in melanoma samples in Figure 3.1, and Dr. David Lombard for TCGA data mining graphed in Figure 3.2. Drs. Miguel Rivera (Harvard) and Sowmya Iyer (Harvard) generated FPKM and differential gene expression analyses of RNAseq data (used in Figure 3.14 and 3.15). I thank Michelle Azar (UM) for help with immunoblotting analysis and immunofluorescence. I thank Dr. David Scott of Sanford-Burnham Medical Research Institute for metabolomics flux profiling analyses.

CHAPTER 4

Future Directions

Overview

In this thesis, I have investigated the roles for SIRT1 and SIRT5 in maintaining mammalian lifespan and healthspan, specifically maintenance of chromatin integrity and modulation of melanoma survival. In Chapter 1, I provide a comprehensive review of the current knowledge of sirtuin biology, including a historical narrative regarding the first description of sirtuin-mediated lifespan extension. I then focus on the current state of the field regarding sirtuin-mediated lifespan extension, and then describe the roles for each sirtuin in promoting variable aspects of mammalian healthspan. I then conclude with a discussion of efforts to regulate sirtuin activity in hopes of extending human healthspan. In Chapter 2, I present a 25-year-old observation of age-associated epigenetic dysfunction and undertake an investigation of its molecular underpinnings and implicate SIRT1 as the cause, in part, of this observation. Chapter 3 describes a striking phenotype wherein SIRT5 loss efficiently and reliably kills human melanoma cells in culture and inhibits in vivo tumor growth. While the exact mechanism is not known, these initial studies set the framework for future investigation, with a focus on regulation of apoptosis and metabolic reprograming. In this chapter I discuss the future directions associated with each of the previous two chapters.

Future Directions

In Chapter 2, I demonstrate that MSR expression is increased in aged mouse heart. If these regions are progressively becoming less heterochromatinized in an age-dependent fashion to allow access to the DNA by the cellular transcription machinery, then an assessment of chromatin structure at pericentromeric regions in aged mouse tissues is warranted. Digestion by micrococcal nuclease, followed by MSR Southern blot, would liberate nucleosomes positioned within MSR loci of purified nuclei at a greater rate in aged mouse tissues compared to young. In a complementary analysis, ATAC-seq, Assay for Transposase-Accessible Chromatin with high throughput sequencing, will be used to assess the accessibility of chromatin genome-wide to gain insight into the extent of age-associated loss of heterochromatin.

Data presented in this chapter generally focuses on global changes in histone PTMs and DNA methylation; however, nothing is known about the epigenetic state specifically at the MSR loci. In order to fully determine the effect of age-associated epigenetic decline at the MSRs, methylated DNA immunoprecipitation and chromatin immunoprecipitation must be performed for SIRT1 and its histone targets, H3K9ac and H4K16ac. Although the repressive H3K9me3 and H3K56me3 PTMs are not altered at the global level in heart tissue, it is possible that a redistribution of these marks away from the MSR loci occurs with age, allowing for an increase in MSR expression. Similarly, SIRT1 expression is unchanged between young and old mouse hearts,

indicating that either SIRT1 activity or localization at the MSRs is altered with age. Chromatin immunoprecipitation for each of the described activating and repressive PTMs as well as SIRT1 would be informative in this regard. One caveat to this approach is that some cells within the same tissue sample may be enriched for activating marks while others will have intact repressive marks – a phenomenon known as cellular mosaicism. To address this, a comparison of the distribution of histone PTMs in young and old heart tissues will then be done via immunofluorescence. The hypothesis that the SIRT1 expression pattern within the heart tissue changes as a function of age will be similarly tested.

Genetic or pharmacologic enhancement of NAD^+ levels should be more carefully assessed to rescue MSR derepression during aging. If SIRT1 activity indeed declines with age, augmentation of cellular NAD^+ levels in aged mice ought to suppress MSR expression. We have yet to reconstitute NAD^+ levels in aged mice to rigorously test this hypothesis. Treatment with NMN or another NAD^+ precursor, nicotinamide riboside, with a higher dose for a longer timecourse ought to bolster NAD^+ in the mouse heart. It should be noted that an increase in NAD^+ pools would presumably activate all NAD^+-dependent enzymes, particularly the other sirtuins. Given then loss of SIRT2, SIRT6 and SIRT7 in mouse hearts does not have an appreciable effect on MSR expression, this impact is not expected to confound this analysis. The impact of these rescue strategies on MSR structure and expression will be tested using northern blot, ChIP, and micrococcal nuclease studies. It is of great interest to confirm several of the histone PTM alterations discovered by mass spectrometry. In particular, assessment of

the role of H3K36me3 in modulating MSR transcription, and PTM changes on H2A.X, which would suggest a DNA damage model.

In Chapter 3, I demonstrate that SIRT5 depletion in melanoma cells results in rapid cell death, irrespective of genetic driver. It is unknown whether SIRT5 protein is overexpressed in melanoma cell lines compared to healthy melanocytes. To address this, immunoblotting for SIRT5 in these cell lines will be done. Given the variability in SIRT5 expression in melanoma cells, there is likely a threshold for SIRT5 expression required for melanomagenesis. Interestingly, melanoma cells with low SIRT5 protein expression exhibit a longer latency in an in vivo xenograft tumor formation assay compared to cells with a higher SIRT5 content. How well healthy melanocytes can tolerate SIRT5 loss has yet to be rigorously tested: This is critical for implicating SIRT5 as a pro-survival factor in cancer. While *Sirt5* germline knockout mice are fertile and generally healthy until at least 18 months of age (Lombard et al., 2007), though present with mild cardiac defects upon aging (Sadhukhan et al., 2016), a close examination of the impact of SIRT5 loss in healthy human melanocytes must be done. This can be accomplished using the same shRNA system described in this chapter in human melanocytes. Also, testing the ability of SIRT5 to transform pre-malignant melanocytes to metastatic melanoma, using both in vivo and ex vivo models, would strengthen the argument that SIRT5 is required for melanoma growth. In this regard, we are using a previously described melanoma mouse model developed by the Bosenberg group (Yale) (Dankort et al., 2009) to genetically modulate SIRT5 protein expression and ascertain melanoma formation and aggressiveness in this context. This model will also

be useful in testing and designing SIRT5 inhibitors to begin to define clinically relevant interventions for melanoma treatment.

Furthermore, since reintroduction of SIRT5 into the shRNA knockdown system failed to rescue cell death, it is important to verify the SIRT5 transcript sequence. If melanoma cells harbor mutations in SIRT5, reconstitution of the wild-type sequence would not be expected to rescue the phenotype presented in the chapter. To this end, we are preparing cDNA libraries in an effort to sequence the entire "SIRT5 transcriptome" in healthy human melanocytes and in a panel of melanoma cell lines. A second possibility is that exogenously expressed SIRT5 does not recapitulate the SIRT5 subcellular localization of the cell lines we have tested. To this end, we will alter the mitochondrial localization signal to allow for maximal efficiency in targeting SIRT5 to the mitochondrial matrix. Also, an orthogonal approach for deleting SIRT5 in melanoma (i.e. CRISPR) is critical in addressing the issue of potential off-targets effects of the shRNA lentiviral system.

If indeed SIRT5 loss induces apoptosis specifically in melanoma cells, pretreatment with inhibitors of apoptosis are expected to rescue cell death and recapitulate the BCL2 overexpression phenotype (Figure 3.16). Modulation of other anti-apoptosis related proteins, as informed by RNAseq data, genetically and pharmacologically will be an important next step to clarify the mechanism of SIRT5-mediated cell death. Also, a careful pathway analysis of the RNAseq data will be done, which may reveal previously undescribed SIRT5-mediated pathways important for modulating melanoma cell

survival. Data for A375 (BRAF mutant), A2058 (BRAF mutant), and SK-MEL-103 (NRAS mutant) cell lines have been collected (Figure 3.14), and a fourth cell line SK-MEL-2 (NRAS mutant) is currently being analyzed. Once collected, pathway analyses will be performed on all datasets.

Metabolic alterations are observed upon SIRT5 knockdown. We have focused specifically on glucose- and glutamine derived species at one timepoint, using a stable isotope labeling approach. It would be interesting to understand the broad metabolic changes that occur over time upon SIRT5 depletion, which would inform future cell-death rescue strategies and therapeutic development. Using an untargeted mass spectrometry approach in collaboration with the Lyssiotis group (UM), we are interested in visualizing, among several timepoints, SIRT5-dependent changes in potential key metabolites that may be critical for melanoma growth.

Summary

This thesis contributes to the growing body of knowledge regarding sirtuin biology as it relates to extending the number of years a person can live disease-free, known as healthspan. Sirtuins are NAD^+-dependent lysine deacylates that modulate many aspects of human health and disease, and in the case of two, SIRT1 and SIRT6, prolong lifespan. Little research has focused on the molecular mechanisms of SIRT1-mediated lifespan extension; one report focuses on regulating hypothalamic function to modulate this phenotype. The work presented in this thesis suggests the hypothesis

that SIRT1 regulates genome stability in an age-dependent manner. It is tempting to speculate that regulation of SIRT1 activity or localization would preserve genome stability and promote mammalian healthspan.

This thesis also focuses on the mitochondrial sirtuin, SIRT5, and its role in promoting melanoma cell survival. SIRT5 regulates various aspects of mitochondrial metabolism, and represents an attractive target for metabolic-directed therapies. Unexpectedly, we found that SIRT5 loss correlates with reductions in anti-apoptotic gene expression, suggesting a novel role for SIRT5 in allowing cancer cells to evade apoptosis. Metabolic alterations that occur in melanoma cells upon SIRT5 loss may potentiate this phenotype. While we have yet to discern the exact mechanism, these data highlight the importance of a previously underappreciated sirtuin in modulating human healthspan.

REFERENCES

Ahuja, N., Schwer, B., Carobbio, S., Waltregny, D., North, B.J., Castronovo, V., Maechler, P., and Verdin, E. (2007). Regulation of insulin secretion by SIRT4, a mitochondrial ADP-ribosyltransferase. J Biol Chem *282*, 33583-33592.

Alcendor, R.R., Gao, S., Zhai, P., Zablocki, D., Holle, E., Yu, X., Tian, B., Wagner, T., Vatner, S.F., and Sadoshima, J. (2007). Sirt1 regulates aging and resistance to oxidative stress in the heart. Circ Res *100*, 1512-1521.

Alhazzazi, T.Y., Kamarajan, P., Joo, N., Huang, J.Y., Verdin, E., D'Silva, N.J., and Kapila, Y.L. (2011). Sirtuin-3 (SIRT3), a novel potential therapeutic target for oral cancer. Cancer *117*, 1670-1678.

Ashraf, N., Zino, S., Macintyre, A., Kingsmore, D., Payne, A.P., George, W.D., and Shiels, P.G. (2006). Altered sirtuin expression is associated with node-positive breast cancer. British journal of cancer *95*, 1056-1061.

Aury-Landas, J., Bougeard, G., Castel, H., Hernandez-Vargas, H., Drouet, A., Latouche, J.B., Schouft, M.T., Ferec, C., Leroux, D., Lasset, C*., et al.* (2013). Germline copy number variation of genes involved in chromatin remodelling in families suggestive of Li-Fraumeni syndrome with brain tumours. Eur J Hum Genet, 1-8.

Bai, P., Canto, C., Brunyanszki, A., Huber, A., Szanto, M., Cen, Y., Yamamoto, H., Houten, S.M., Kiss, B., Oudart, H*., et al.* (2011a). PARP-2 regulates SIRT1 expression and whole-body energy expenditure. Cell Metab *13*, 450-460.

Bai, P., Canto, C., Oudart, H., Brunyanszki, A., Cen, Y., Thomas, C., Yamamoto, H., Huber, A., Kiss, B., Houtkooper, R.H*., et al.* (2011b). PARP-1 inhibition increases mitochondrial metabolism through SIRT1 activation. Cell Metab *13*, 461-468.

Baker, D.J., Dawlaty, M.M., Wijshake, T., Jeganathan, K.B., Malureanu, L., van Ree, J.H., Crespo-Diaz, R., Reyes, S., Seaburg, L., Shapiro, V*., et al.* (2012). Increased expression of BubR1 protects against aneuploidy and cancer and extends healthy lifespan. Nature cell biology *15*, 96-102.

Baker, D.J., Dawlaty, M.M., Wijshake, T., Jeganathan, K.B., Malureanu, L., van Ree, J.H., Crespo-Diaz, R., Reyes, S., Seaburg, L., Shapiro, V*., et al.* (2013). Increased expression of BubR1 protects against aneuploidy and cancer and extends healthy lifespan. Nat Cell Biol *15*, 96-102.

Baker, D.J., Jeganathan, K.B., Cameron, J.D., Thompson, M., Juneja, S., Kopecka, A., Kumar, R., Jenkins, R.B., de Groen, P.C., Roche, P.*, et al.* (2004). BubR1 insufficiency causes early onset of aging-associated phenotypes and infertility in mice. Nat Genet *36*, 744-749.

Banerjee, K.K., Ayyub, C., Ali, S.Z., Mandot, V., Prasad, N.G., and Kolthur-Seetharam, U. (2012). dSir2 in the adult fat body, but not in muscles, regulates life span in a diet-dependent manner. Cell Rep *2*, 1485-1491.

Banks, A.S., Kon, N., Knight, C., Matsumoto, M., Gutierrez-Juarez, R., Rossetti, L., Gu, W., and Accili, D. (2008). SirT1 gain of function increases energy efficiency and prevents diabetes in mice. Cell Metab *8*, 333-341.

Barber, M.F., Michishita-Kioi, E., Xi, Y., Tasselli, L., Kioi, M., Moqtaderi, Z., Tennen, R.I., Paredes, S., Young, N.L., Chen, K.*, et al.* (2012). SIRT7 links H3K18 deacetylation to maintenance of oncogenic transformation. Nature *487*, 114-118.

Barbosa, M.T., Soares, S.M., Novak, C.M., Sinclair, D., Levine, J.A., Aksoy, P., and Chini, E.N. (2007). The enzyme CD38 (a NAD glycohydrolase, EC 3.2.2.5) is necessary for the development of diet-induced obesity. FASEB J *21*, 3629-3639.

Barger, J.L., Kayo, T., Pugh, T.D., Prolla, T.A., and Weindruch, R. (2008a). Short-term consumption of a resveratrol-containing nutraceutical mixture mimics gene expression of long-term caloric restriction in mouse heart. Exp Gerontol *43*, 859-866.

Barger, J.L., Kayo, T., Vann, J.M., Arias, E.B., Wang, J., Hacker, T.A., Wang, Y., Raederstorff, D., Morrow, J.D., Leeuwenburgh, C.*, et al.* (2008b). A low dose of dietary resveratrol partially mimics caloric restriction and retards aging parameters in mice. PLoS One *3*, e2264.

Barquera, S., Pedroza-Tobias, A., Medina, C., Hernandez-Barrera, L., Bibbins-Domingo, K., Lozano, R., and Moran, A.E. (2015). Global Overview of the Epidemiology of Atherosclerotic Cardiovascular Disease. Archives of medical research *46*, 328-338.

Bauer, J.H., Morris, S.N., Chang, C., Flatt, T., Wood, J.G., and Helfand, S.L. (2009). dSir2 and Dmp53 interact to mediate aspects of CR-dependent lifespan extension in D. melanogaster. Aging (Albany NY) *1*, 38-48.

Baur, J.A. (2010a). Biochemical effects of SIRT1 activators. Biochim Biophys Acta *1804*, 1626-1634.

Baur, J.A. (2010b). Resveratrol, sirtuins, and the promise of a DR mimetic. Mech Ageing Dev *131*, 261-269.

Baur, J.A., Pearson, K.J., Price, N.L., Jamieson, H.A., Lerin, C., Kalra, A., Prabhu, V.V., Allard, J.S., Lopez-Lluch, G., Lewis, K.*, et al.* (2006). Resveratrol improves health and survival of mice on a high-calorie diet. Nature *444*, 337-342.

Baur, J.A., and Sinclair, D.A. (2006). Therapeutic potential of resveratrol: the in vivo evidence. Nat Rev Drug Discov *5*, 493-506.

Bell, E.L., Emerling, B.M., Ricoult, S.J., and Guarente, L. (2011). SirT3 suppresses hypoxia inducible factor 1alpha and tumor growth by inhibiting mitochondrial ROS production. Oncogene *30*, 2986-2996.

Bell, S.P., Orr, N.M., Dodson, J.A., Rich, M.W., Wenger, N.K., Blum, K., Harold, J.G., Tinetti, M.E., Maurer, M.S., and Forman, D.E. (2015). What to Expect From the Evolving Field of Geriatric Cardiology. J Am Coll Cardiol *66*, 1286-1299.

Berdichevsky, A., Viswanathan, M., Horvitz, H.R., and Guarente, L. (2006). C. elegans SIR-2.1 interacts with 14-3-3 proteins to activate DAF-16 and extend life span. Cell *125*, 1165-1177.

Black, J.C., Mosley, A., Kitada, T., Washburn, M., and Carey, M. (2008). The SIRT2 deacetylase regulates autoacetylation of p300. Mol Cell *32*, 449-455.

Boily, G., He, X.H., Pearce, B., Jardine, K., and McBurney, M.W. (2009). SirT1-null mice develop tumors at normal rates but are poorly protected by resveratrol. Oncogene *28*, 2882-2893.

Boily, G., Seifert, E.L., Bevilacqua, L., He, X.H., Sabourin, G., Estey, C., Moffat, C., Crawford, S., Saliba, S., Jardine, K.*, et al.* (2008). SirT1 regulates energy metabolism and response to caloric restriction in mice. PLoS One *3*, e1759.

Bolanos-Garcia, V.M., and Blundell, T.L. (2011). BUB1 and BUBR1: multifaceted kinases of the cell cycle. Trends Biochem Sci *36*, 141-150.

Bordone, L., Cohen, D., Robinson, A., Motta, M.C., van Veen, E., Czopik, A., Steele, A.D., Crowe, H., Marmor, S., Luo, J.*, et al.* (2007). SIRT1 transgenic mice show phenotypes resembling calorie restriction. Aging Cell *6*, 759-767.

Bordone, L., and Guarente, L. (2005). Calorie restriction, SIRT1 and metabolism: understanding longevity. Nat Rev Mol Cell Biol *6*, 298-305.

Braidy, N., Guillemin, G.J., Mansour, H., Chan-Ling, T., Poljak, A., and Grant, R. (2011). Age related changes in NAD+ metabolism oxidative stress and Sirt1 activity in wistar rats. PLoS One *6*, e19194.

Braidy, N., Poljak, A., Grant, R., Jayasena, T., Mansour, H., Chan-Ling, T., Guillemin, G.J., Smythe, G., and Sachdev, P. (2014). Mapping NAD(+) metabolism in the brain of ageing Wistar rats: potential targets for influencing brain senescence. Biogerontology *15*, 177-198.

Brandes, R.P., Fleming, I., and Busse, R. (2005). Endothelial aging. Cardiovasc Res *66*, 286-294.

Brenmoehl, J., and Hoeflich, A. (2013). Dual control of mitochondrial biogenesis by sirtuin 1 and sirtuin 3. Mitochondrion *13*, 755-761.

Bulut-Karslioglu, A., Perrera, V., Scaranaro, M., de la Rosa-Velazquez, I.A., van de Nobelen, S., Shukeir, N., Popow, J., Gerle, B., Opravil, S., Pagani, M.*, et al.* (2012). A transcription factor-based mechanism for mouse heterochromatin formation. Nat Struct Mol Biol *19*, 1023-1030.

Burnett, C., Valentini, S., Cabreiro, F., Goss, M., Somogyvari, M., Piper, M.D., Hoddinott, M., Sutphin, G.L., Leko, V., McElwee, J.J.*, et al.* (2011). Absence of effects of Sir2 overexpression on lifespan in C. elegans and Drosophila. Nature *477*, 482-485.

Byles, V., Chmilewski, L.K., Wang, J., Zhu, L., Forman, L.W., Faller, D.V., and Dai, Y. (2010). Aberrant cytoplasm localization and protein stability of SIRT1 is regulated by PI3K/IGF-1R signaling in human cancer cells. Int J Biol Sci *6*, 599-612.

Callier, P., Faivre, L., Cusin, V., Marle, N., Thauvin-Robinet, C., Sandre, D., Rousseau, T., Sagot, P., Lacombe, E., Faber, V.*, et al.* (2005). Microcephaly is not mandatory for the diagnosis of mosaic variegated aneuploidy syndrome. American journal of medical genetics Part A *137*, 204-207.

Canto, C., Houtkooper, R.H., Pirinen, E., Youn, D.Y., Oosterveer, M.H., Cen, Y., Fernandez-Marcos, P.J., Yamamoto, H., Andreux, P.A., Cettour-Rose, P.*, et al.* (2012a). The NAD(+) precursor nicotinamide riboside enhances oxidative metabolism and protects against high-fat diet-induced obesity. Cell metabolism *15*, 838-847.

Canto, C., Houtkooper, R.H., Pirinen, E., Youn, D.Y., Oosterveer, M.H., Cen, Y., Fernandez-Marcos, P.J., Yamamoto, H., Andreux, P.A., Cettour-Rose, P.*, et al.* (2012b). The NAD(+) precursor nicotinamide riboside enhances oxidative metabolism and protects against high-fat diet-induced obesity. Cell Metab *15*, 838-847.

Canto, C., Jiang, L.Q., Deshmukh, A.S., Mataki, C., Coste, A., Lagouge, M., Zierath, J.R., and Auwerx, J. (2010). Interdependence of AMPK and SIRT1 for metabolic adaptation to fasting and exercise in skeletal muscle. Cell Metab *11*, 213-219.

Canto, C., Sauve, A.A., and Bai, P. (2013). Crosstalk between poly(ADP-ribose) polymerase and sirtuin enzymes. Mol Aspects Med *34*, 1168-1201.

Chachay, V.S., Macdonald, G.A., Martin, J.H., Whitehead, J.P., O'Moore-Sullivan, T.M., Lee, P., Franklin, M., Klein, K., Taylor, P.J., Ferguson, M.*, et al.* (2014). Resveratrol Does Not Benefit Patients With Nonalcoholic Fatty Liver Disease. Clinical gastroenterology and hepatology : the official clinical practice journal of the American Gastroenterological Association, 1-35.

Chang, H.C., and Guarente, L. (2013). SIRT1 mediates central circadian control in the SCN by a mechanism that decays with aging. Cell *153*, 1448-1460.

Chen, D., Bruno, J., Easlon, E., Lin, S.J., Cheng, H.L., Alt, F.W., and Guarente, L. (2008). Tissue-specific regulation of SIRT1 by calorie restriction. Genes Dev *22*, 1753-1757.

Chen, D., Steele, A.D., Lindquist, S., and Guarente, L. (2005). Increase in activity during calorie restriction requires Sirt1. Science *310*, 1641.

Chen, I.C., Chiang, W.F., Liu, S.Y., Chen, P.F., and Chiang, H.C. (2013). Role of SIRT3 in the regulation of redox balance during oral carcinogenesis. Molecular cancer *12*, 68.

Cheng, H.L., Mostoslavsky, R., Saito, S., Manis, J.P., Gu, Y., Patel, P., Bronson, R., Appella, E., Alt, F.W., and Chua, K.F. (2003). Developmental defects and p53 hyperacetylation in Sir2 homolog (SIRT1)-deficient mice. Proc Natl Acad Sci U S A *100*, 10794-10799.

Chiang, W.C., Tishkoff, D.X., Yang, B., Wilson-Grady, J., Yu, X., Mazer, T., Eckersdorff, M., Gygi, S.P., Lombard, D.B., and Hsu, A.L. (2012). C. elegans SIRT6/7 homolog SIR-2.4 promotes DAF-16 relocalization and function during stress. PLoS Genet *8*, e1002948.

Chien, S. (2008). Effects of disturbed flow on endothelial cells. Annals of biomedical engineering *36*, 554-562.

Cohen, D.E., Supinski, A.M., Bonkowski, M.S., Donmez, G., and Guarente, L.P. (2009). Neuronal SIRT1 regulates endocrine and behavioral responses to calorie restriction. Genes Dev *23*, 2812-2817.

Cohen, H.Y., Miller, C., Bitterman, K.J., Wall, N.R., Hekking, B., Kessler, B., Howitz, K.T., Gorospe, M., de Cabo, R., and Sinclair, D.A. (2004). Calorie restriction promotes mammalian cell survival by inducing the SIRT1 deacetylase. Science *305*, 390-392.

Colombo, S.L., Palacios-Callender, M., Frakich, N., Carcamo, S., Kovacs, I., Tudzarova, S., and Moncada, S. (2011). Molecular basis for the differential use of glucose and glutamine in cell proliferation as revealed by synchronized HeLa cells. Proc Natl Acad Sci U S A *108*, 21069-21074.

Condorelli, G., Drusco, A., Stassi, G., Bellacosa, A., Roncarati, R., Iaccarino, G., Russo, M.A., Gu, Y., Dalton, N., Chung, C.*, et al.* (2002). Akt induces enhanced myocardial contractility and cell size in vivo in transgenic mice. Proc Natl Acad Sci U S A *99*, 12333-12338.

Csibi, A., Fendt, S.M., Li, C., Poulogiannis, G., Choo, A.Y., Chapski, D.J., Jeong, S.M., Dempsey, J.M., Parkhitko, A., Morrison, T.*, et al.* (2013). The mTORC1 pathway stimulates glutamine metabolism and cell proliferation by repressing SIRT4. Cell *153*, 840-854.

Csiszar, A., Labinskyy, N., Podlutsky, A., Kaminski, P.M., Wolin, M.S., Zhang, C., Mukhopadhyay, P., Pacher, P., Hu, F., de Cabo, R.*, et al.* (2008). Vasoprotective effects

of resveratrol and SIRT1: attenuation of cigarette smoke-induced oxidative stress and proinflammatory phenotypic alterations. Am J Physiol Heart Circ Physiol *294*, H2721-2735.

Dang, W., Steffen, K.K., Perry, R., Dorsey, J.A., Johnson, F.B., Shilatifard, A., Kaeberlein, M., Kennedy, B.K., and Berger, S.L. (2009). Histone H4 lysine 16 acetylation regulates cellular lifespan. Nature *459*, 802-807.

Dankort, D., Curley, D.P., Cartlidge, R.A., Nelson, B., Karnezis, A.N., Damsky, W.E., Jr., You, M.J., DePinho, R.A., McMahon, M., and Bosenberg, M. (2009). Braf(V600E) cooperates with Pten loss to induce metastatic melanoma. Nat Genet *41*, 544-552.

David, G., Dannenberg, J.H., Simpson, N., Finnerty, P.M., Miao, L., Turner, G.M., Ding, Z., Carrasco, R., and Depinho, R.A. (2006). Haploinsufficiency of the mSds3 chromatin regulator promotes chromosomal instability and cancer only upon complete neutralization of p53. Oncogene *25*, 7354-7360.

David, G., Turner, G.M., Yao, Y., Protopopov, A., and DePinho, R.A. (2003). mSin3-associated protein, mSds3, is essential for pericentric heterochromatin formation and chromosome segregation in mammalian cells. Genes Dev *17*, 2396-2405.

De Cecco, M., Criscione, S.W., Peterson, A.L., Neretti, N., Sedivy, J.M., and Kreiling, J.A. (2013a). Transposable elements become active and mobile in the genomes of aging mammalian somatic tissues. Aging (Albany NY).

De Cecco, M., Criscione, S.W., Peterson, A.L., Neretti, N., Sedivy, J.M., and Kreiling, J.A. (2013b). Transposable elements become active and mobile in the genomes of aging mammalian somatic tissues. Aging (Albany NY) *5*, 867-883.

Defossez, P.A., Prusty, R., Kaeberlein, M., Lin, S.J., Ferrigno, P., Silver, P.A., Keil, R.L., and Guarente, L. (1999). Elimination of replication block protein Fob1 extends the life span of yeast mother cells. Mol Cell *3*, 447-455.

Desouki, M.M., Doubinskaia, I., Gius, D., and Abdulkadir, S.A. (2014). Decreased mitochondrial SIRT3 expression is a potential molecular biomarker associated with poor outcome in breast cancer. Hum Pathol *45*, 1071-1077.

Dominy, J.E., Jr., Lee, Y., Jedrychowski, M.P., Chim, H., Jurczak, M.J., Camporez, J.P., Ruan, H.B., Feldman, J., Pierce, K., Mostoslavsky, R.*, et al.* (2012). The deacetylase Sirt6 activates the acetyltransferase GCN5 and suppresses hepatic gluconeogenesis. Mol Cell *48*, 900-913.

Dryden, S.C., Nahhas, F.A., Nowak, J.E., Goustin, A.S., and Tainsky, M.A. (2003). Role for human SIRT2 NAD-dependent deacetylase activity in control of mitotic exit in the cell cycle. Mol Cell Biol *23*, 3173-3185.

Du, J., Zhou, Y., Su, X., Yu, J.J., Khan, S., Jiang, H., Kim, J., Woo, J., Kim, J.H., Choi, B.H.*, et al.* (2011). Sirt5 is a NAD-dependent protein lysine demalonylase and desuccinylase. Science *334*, 806-809.

Du, X.J. (2004). Gender modulates cardiac phenotype development in genetically modified mice. Cardiovasc Res *63*, 510-519.

Elhanati, S., Kanfi, Y., Varvak, A., Roichman, A., Carmel-Gross, I., Barth, S., Gibor, G., and Cohen, H.Y. (2013). Multiple regulatory layers of SREBP1/2 by SIRT6. Cell Rep *4*, 905-912.

Elmore, S. (2007). Apoptosis: a review of programmed cell death. Toxicol Pathol *35*, 495-516.

Elowe, S. (2011). Bub1 and BubR1: at the interface between chromosome attachment and the spindle checkpoint. Mol Cell Biol *31*, 3085-3093.

Etchegaray, J.P., Chavez, L., Huang, Y., Ross, K.N., Choi, J., Martinez-Pastor, B., Walsh, R.M., Sommer, C.A., Lienhard, M., Gladden, A.*, et al.* (2015). The histone deacetylase SIRT6 controls embryonic stem cell fate via TET-mediated production of 5-hydroxymethylcytosine. Nat Cell Biol *17*, 545-557.

Fan, J., Shan, C., Kang, H.B., Elf, S., Xie, J., Tucker, M., Gu, T.L., Aguiar, M., Lonning, S., Chen, H.*, et al.* (2014). Tyr Phosphorylation of PDP1 Toggles Recruitment between ACAT1 and SIRT3 to Regulate the Pyruvate Dehydrogenase Complex. Mol Cell *53*, 534-548.

Feldman, J.L., Baeza, J., and Denu, J.M. (2013). Activation of the protein deacetylase SIRT6 by long-chain fatty acids and widespread deacylation by mammalian sirtuins. J Biol Chem *288*, 31350-31356.

Filipp, F.V., Ratnikov, B., De Ingeniis, J., Smith, J.W., Osterman, A.L., and Scott, D.A. (2012a). Glutamine-fueled mitochondrial metabolism is decoupled from glycolysis in melanoma. Pigment cell & melanoma research *25*, 732-739.

Filipp, F.V., Scott, D.A., Ronai, Z.A., Osterman, A.L., and Smith, J.W. (2012b). Reverse TCA cycle flux through isocitrate dehydrogenases 1 and 2 is required for lipogenesis in hypoxic melanoma cells. Pigment cell & melanoma research *25*, 375-383.

Finkel, T., Deng, C.X., and Mostoslavsky, R. (2009). Recent progress in the biology and physiology of sirtuins. Nature *460*, 587-591.

Finley, L.W., Carracedo, A., Lee, J., Souza, A., Egia, A., Zhang, J., Teruya-Feldstein, J., Moreira, P.I., Cardoso, S.M., Clish, C.B.*, et al.* (2011). SIRT3 Opposes Reprogramming of Cancer Cell Metabolism through HIF1alpha Destabilization. Cancer Cell *19*, 416-428.

Firestein, R., Blander, G., Michan, S., Oberdoerffer, P., Ogino, S., Campbell, J., Bhimavarapu, A., Luikenhuis, S., de Cabo, R., Fuchs, C.*, et al.* (2008). The SIRT1

deacetylase suppresses intestinal tumorigenesis and colon cancer growth. PLoS One *3*, e2020.

Fontana, L., Partridge, L., and Longo, V.D. (2010). Extending healthy life span--from yeast to humans. Science *328*, 321-326.

Ford, E., Voit, R., Liszt, G., Magin, C., Grummt, I., and Guarente, L. (2006). Mammalian Sir2 homolog SIRT7 is an activator of RNA polymerase I transcription. Genes Dev *20*, 1075-1080.

Frederick, D.W., Davis, J.G., Davila, A., Jr., Agarwal, B., Michan, S., Puchowicz, M.A., Nakamaru-Ogiso, E., and Baur, J.A. (2015). Increasing NAD synthesis in muscle via nicotinamide phosphoribosyltransferase is not sufficient to promote oxidative metabolism. J Biol Chem *290*, 1546-1558.

Frye, R.A. (2000). Phylogenetic classification of prokaryotic and eukaryotic Sir2-like proteins. Biochem Biophys Res Commun *273*, 793-798.

Garagna, S., Zuccotti, M., Capanna, E., and Redi, C.A. (2002). High-resolution organization of mouse telomeric and pericentromeric DNA. Cytogenetic and genome research *96*, 125-129.

Garcia-Castillo, H., Vasquez-Velasquez, A.I., Rivera, H., and Barros-Nunez, P. (2008). Clinical and genetic heterogeneity in patients with mosaic variegated aneuploidy: delineation of clinical subtypes. American journal of medical genetics Part A *146A*, 1687-1695.

Gaubatz, J.W., and Cutler, R.G. (1990). Mouse satellite DNA is transcribed in senescent cardiac muscle. J Biol Chem *265*, 17753-17758.

Gems, D. (2011). Tragedy and delight: the ethics of decelerated ageing. Philosophical transactions of the Royal Society of London Series B, Biological sciences *366*, 108-112.

Go, A.S., Mozaffarian, D., Roger, V.L., Benjamin, E.J., Berry, J.D., Blaha, M.J., Dai, S., Ford, E.S., Fox, C.S., Franco, S.*, et al.* (2014). Heart disease and stroke statistics--2014 update: a report from the American Heart Association. Circulation *129*, e28-e292.

Gomes, A.P., Price, N.L., Ling, A.J., Moslehi, J.J., Montgomery, M.K., Rajman, L., White, J.P., Teodoro, J.S., Wrann, C.D., Hubbard, B.P.*, et al.* (2013). Declining NAD(+) Induces a Pseudohypoxic State Disrupting Nuclear-Mitochondrial Communication during Aging. Cell *155*, 1624-1638.

Greer, E.L., and Brunet, A. (2009). Different dietary restriction regimens extend lifespan by both independent and overlapping genetic pathways in C. elegans. Aging Cell *8*, 113-127.

Guarani, V., Deflorian, G., Franco, C.A., Kruger, M., Phng, L.K., Bentley, K., Toussaint, L., Dequiedt, F., Mostoslavsky, R., Schmidt, M.H.*, et al.* (2011). Acetylation-dependent

regulation of endothelial Notch signalling by the SIRT1 deacetylase. Nature *473*, 234-238.

Guarente, L. (2000). Sir2 links chromatin silencing, metabolism, and aging. Genes Dev *14*, 1021-1026.

Guarente, L. (2013). Calorie restriction and sirtuins revisited. Genes Dev *27*, 2072-2085.

Guarente, L., and Kenyon, C. (2000). Genetic pathways that regulate ageing in model organisms. Nature *408*, 255-262.

Guibert, S., and Weber, M. (2013). Functions of DNA methylation and hydroxymethylation in mammalian development. Current topics in developmental biology *104*, 47-83.

Haber, J.E., and George, J.P. (1979). A mutation that permits the expression of normally silent copies of mating-type information in Saccharomyces cerevisiae. Genetics *93*, 13-35.

Hafner, A.V., Dai, J., Gomes, A.P., Xiao, C.Y., Palmeira, C.M., Rosenzweig, A., and Sinclair, D.A. (2010). Regulation of the mPTP by SIRT3-mediated deacetylation of CypD at lysine 166 suppresses age-related cardiac hypertrophy. Aging (Albany NY) *2*, 914-923.

Haigis, M.C., Mostoslavsky, R., Haigis, K.M., Fahie, K., Christodoulou, D.C., Murphy, A.J., Valenzuela, D.M., Yancopoulos, G.D., Karow, M., Blander, G.*, et al.* (2006). SIRT4 inhibits glutamate dehydrogenase and opposes the effects of calorie restriction in pancreatic beta cells. Cell *126*, 941-954.

Hallows, W.C., Yu, W., Smith, B.C., Devries, M.K., Ellinger, J.J., Someya, S., Shortreed, M.R., Prolla, T., Markley, J.L., Smith, L.M.*, et al.* (2011). Sirt3 promotes the urea cycle and fatty acid oxidation during dietary restriction. Mol Cell *41*, 139-149.

Hanahan, D., and Weinberg, R.A. (2011). Hallmarks of cancer: the next generation. Cell *144*, 646-674.

Hansen, M., Taubert, S., Crawford, D., Libina, N., Lee, S.J., and Kenyon, C. (2007). Lifespan extension by conditions that inhibit translation in Caenorhabditis elegans. Aging Cell *6*, 95-110.

Harrison, D.E., Strong, R., Sharp, Z.D., Nelson, J.F., Astle, C.M., Flurkey, K., Nadon, N.L., Wilkinson, J.E., Frenkel, K., Carter, C.S.*, et al.* (2009). Rapamycin fed late in life extends lifespan in genetically heterogeneous mice. Nature *460*, 392-395.

Harting, K., and Knoll, B. (2010). SIRT2-mediated protein deacetylation: An emerging key regulator in brain physiology and pathology. Eur J Cell Biol *89*, 262-269.

Hartman, T.K., Wengenack, T.M., Poduslo, J.F., and van Deursen, J.M. (2007). Mutant mice with small amounts of BubR1 display accelerated age-related gliosis. Neurobiol Aging *28*, 921-927.

Hashimoto, T., Horikawa, M., Nomura, T., and Sakamoto, K. (2010). Nicotinamide adenine dinucleotide extends the lifespan of Caenorhabditis elegans mediated by sir-2.1 and daf-16. Biogerontology *11*, 31-43.

Hebert, A.S., Dittenhafer-Reed, K.E., Yu, W., Bailey, D.J., Selen, E.S., Boersma, M.D., Carson, J.J., Tonelli, M., Balloon, A.J., Higbee, A.J.*, et al.* (2013). Calorie restriction and SIRT3 trigger global reprogramming of the mitochondrial protein acetylome. Mol Cell *49*, 186-199.

Herranz, D., Munoz-Martin, M., Canamero, M., Mulero, F., Martinez-Pastor, B., Fernandez-Capetillo, O., and Serrano, M. (2010). Sirt1 improves healthy ageing and protects from metabolic syndrome-associated cancer. Nat Commun *1*, 3.

Heydari, A.R., Unnikrishnan, A., Lucente, L.V., and Richardson, A. (2007). Caloric restriction and genomic stability. Nucleic Acids Res *35*, 7485-7496.

Higuchi, R., Vevea, J.D., Swayne, T.C., Chojnowski, R., Hill, V., Boldogh, I.R., and Pon, L.A. (2013). Actin dynamics affect mitochondrial quality control and aging in budding yeast. Curr Biol *23*, 2417-2422.

Hirschey, M.D., Shimazu, T., Goetzman, E., Jing, E., Schwer, B., Lombard, D.B., Grueter, C.A., Harris, C., Biddinger, S., Ilkayeva, O.R.*, et al.* (2010). SIRT3 regulates mitochondrial fatty-acid oxidation by reversible enzyme deacetylation. Nature *464*, 121-125.

Hisahara, S., Chiba, S., Matsumoto, H., Tanno, M., Yagi, H., Shimohama, S., Sato, M., and Horio, Y. (2008). Histone deacetylase SIRT1 modulates neuronal differentiation by its nuclear translocation. Proc Natl Acad Sci U S A *105*, 15599-15604.

Hodis, E., Watson, I.R., Kryukov, G.V., Arold, S.T., Imielinski, M., Theurillat, J.P., Nickerson, E., Auclair, D., Li, L., Place, C.*, et al.* (2012). A landscape of driver mutations in melanoma. Cell *150*, 251-263.

Hoffmann, J., Romey, R., Fink, C., Yong, L., and Roeder, T. (2013). Overexpression of Sir2 in the adult fat body is sufficient to extend lifespan of male and female Drosophila. Aging (Albany NY) *5*, 315-327.

Hong, S., Zhao, B., Lombard, D.B., Fingar, D.C., and Inoki, K. (2014). Cross-talk between sirtuin and mammalian target of rapamycin complex 1 (mTORC1) signaling in the regulation of S6 kinase 1 (S6K1) phosphorylation. J Biol Chem *289*, 13132-13141.

Howitz, K.T., Bitterman, K.J., Cohen, H.Y., Lamming, D.W., Lavu, S., Wood, J.G., Zipkin, R.E., Chung, P., Kisielewski, A., Zhang, L.L.*, et al.* (2003). Small molecule activators of sirtuins extend Saccharomyces cerevisiae lifespan. Nature *425*, 191-196.

Huang, Y., and Rao, A. (2014). Connections between TET proteins and aberrant DNA modification in cancer. Trends in genetics : TIG.

Hubbard, B.P., Gomes, A.P., Dai, H., Li, J., Case, A.W., Considine, T., Riera, T.V., Lee, J.E., E, S.Y., Lamming, D.W*., et al.* (2013). Evidence for a common mechanism of SIRT1 regulation by allosteric activators. Science *339*, 1216-1219.

Hubbard, B.P., and Sinclair, D.A. (2014). Small molecule SIRT1 activators for the treatment of aging and age-related diseases. Trends Pharmacol Sci *35*, 146-154.

Imai, S. (2009). SIRT1 and caloric restriction: an insight into possible trade-offs between robustness and frailty. Curr Opin Clin Nutr Metab Care *12*, 350-356.

Imai, S., Armstrong, C.M., Kaeberlein, M., and Guarente, L. (2000). Transcriptional silencing and longevity protein Sir2 is an NAD-dependent histone deacetylase. Nature *403*, 795-800.

Imai, S., and Guarente, L. (2014). NAD+ and sirtuins in aging and disease. Trends Cell Biol *24*, 464-471.

Imai, S., and Kitano, H. (1998). Heterochromatin islands and their dynamic reorganization: a hypothesis for three distinctive features of cellular aging. Exp Gerontol *33*, 555-570.

Inoue, T., Hiratsuka, M., Osaki, M., Yamada, H., Kishimoto, I., Yamaguchi, S., Nakano, S., Katoh, M., Ito, H., and Oshimura, M. (2007). SIRT2, a tubulin deacetylase, acts to block the entry to chromosome condensation in response to mitotic stress. Oncogene *26*, 945-957.

Inoue, T., Nakayama, Y., Yamada, H., Li, Y.C., Yamaguchi, S., Osaki, M., Kurimasa, A., Hiratsuka, M., Katoh, M., and Oshimura, M. (2009). SIRT2 downregulation confers resistance to microtubule inhibitors by prolonging chronic mitotic arrest. Cell Cycle *8*, 1279-1291.

Jack, A.P., Bussemer, S., Hahn, M., Punzeler, S., Snyder, M., Wells, M., Csankovszki, G., Solovei, I., Schotta, G., and Hake, S.B. (2013). H3K56me3 is a novel, conserved heterochromatic mark that largely but not completely overlaps with H3K9me3 in both regulation and localization. PLoS One *8*, e51765.

Janssen, A., van der Burg, M., Szuhai, K., Kops, G.J., and Medema, R.H. (2011). Chromosome segregation errors as a cause of DNA damage and structural chromosome aberrations. Science *333*, 1895-1898.

Jedrusik-Bode, M., Studencka, M., Smolka, C., Baumann, T., Schmidt, H., Kampf, J., Paap, F., Martin, S., Tazi, J., Muller, K.M*., et al.* (2013). The sirtuin SIRT6 regulates stress granule formation in C. elegans and mammals. J Cell Sci *126*, 5166-5177.

Jeong, H., Cohen, D.E., Cui, L., Supinski, A., Savas, J.N., Mazzulli, J.R., Yates, J.R., 3rd, Bordone, L., Guarente, L., and Krainc, D. (2012). Sirt1 mediates neuroprotection from mutant huntingtin by activation of the TORC1 and CREB transcriptional pathway. Nat Med *18*, 159-165.

Jeong, S.M., Lee, A., Lee, J., and Haigis, M.C. (2014a). SIRT4 protein suppresses tumor formation in genetic models of Myc-induced B cell lymphoma. J Biol Chem *289*, 4135-4144.

Jeong, S.M., Lee, J., Finley, L.W., Schmidt, P.J., Fleming, M.D., and Haigis, M.C. (2014b). SIRT3 regulates cellular iron metabolism and cancer growth by repressing iron regulatory protein 1. Oncogene.

Jeong, S.M., Xiao, C., Finley, L.W., Lahusen, T., Souza, A.L., Pierce, K., Li, Y.H., Wang, X., Laurent, G., German, N.J.*, et al.* (2013a). SIRT4 has tumor-suppressive activity and regulates the cellular metabolic response to DNA damage by inhibiting mitochondrial glutamine metabolism. Cancer Cell *23*, 450-463.

Jeong, Seung M., Xiao, C., Finley, Lydia W.S., Lahusen, T., Souza, Amanda L., Pierce, K., Li, Y.-H., Wang, X., Laurent, G., German, Natalie J.*, et al.* (2013b). SIRT4 Has Tumor-Suppressive Activity and Regulates the Cellular Metabolic Response to DNA Damage by Inhibiting Mitochondrial Glutamine Metabolism. Cancer Cell *23*, 450-463.

Jiang, H., Khan, S., Wang, Y., Charron, G., He, B., Sebastian, C., Du, J., Kim, R., Ge, E., Mostoslavsky, R.*, et al.* (2013). SIRT6 regulates TNF-α secretion through hydrolysis of long-chain fatty acyl lysine. Nature *496*, 110-113.

Jin, Q., Yan, T., Ge, X., Sun, C., Shi, X., and Zhai, Q. (2007). Cytoplasm-localized SIRT1 enhances apoptosis. Journal of cellular physiology *213*, 88-97.

Jing, E., O'Neill, B.T., Rardin, M.J., Kleinridders, A., Ilkeyeva, O.R., Ussar, S., Bain, J.R., Lee, K.Y., Verdin, E.M., Newgard, C.B.*, et al.* (2013). Sirt3 regulates metabolic flexibility of skeletal muscle through reversible enzymatic deacetylation. Diabetes *62*, 3404-3417.

Kaeberlein, M., McDonagh, T., Heltweg, B., Hixon, J., Westman, E.A., Caldwell, S.D., Napper, A., Curtis, R., DiStefano, P.S., Fields, S.*, et al.* (2005). Substrate-specific activation of sirtuins by resveratrol. J Biol Chem *280*, 17038-17045.

Kaeberlein, M., McVey, M., and Guarente, L. (1999). The SIR2/3/4 complex and SIR2 alone promote longevity in Saccharomyces cerevisiae by two different mechanisms. Genes Dev *13*, 2570-2580.

Kaeberlein, M., and Powers, R.W., 3rd (2007). Sir2 and calorie restriction in yeast: a skeptical perspective. Ageing Res Rev *6*, 128-140.

Kaeberlein, T.L., Smith, E.D., Tsuchiya, M., Welton, K.L., Thomas, J.H., Fields, S., Kennedy, B.K., and Kaeberlein, M. (2006). Lifespan extension in Caenorhabditis elegans by complete removal of food. Aging Cell *5*, 487-494.

Kaidi, A., Weinert, B.T., Choudhary, C., and Jackson, S.P. (2010). Human SIRT6 promotes DNA end resection through CtIP deacetylation. Science *329*, 1348-1353.

Kanfi, Y., Naiman, S., Amir, G., Peshti, V., Zinman, G., Nahum, L., Bar-Joseph, Z., and Cohen, H.Y. (2012). The sirtuin SIRT6 regulates lifespan in male mice. Nature *483*, 218-221.

Kanfi, Y., Shalman, R., Peshti, V., Pilosof, S.N., Gozlan, Y.M., Pearson, K.J., Lerrer, B., Moazed, D., Marine, J.C., de Cabo, R.*, et al.* (2008). Regulation of SIRT6 protein levels by nutrient availability. FEBS Lett *582*, 543-548.

Kaplon, J., Zheng, L., Meissl, K., Chaneton, B., Selivanov, V.A., Mackay, G., van der Burg, S.H., Verdegaal, E.M., Cascante, M., Shlomi, T.*, et al.* (2013). A key role for mitochondrial gatekeeper pyruvate dehydrogenase in oncogene-induced senescence. Nature *498*, 109-112.

Kennedy, B.K., Austriaco, N.R., Jr., Zhang, J., and Guarente, L. (1995). Mutation in the silencing gene SIR4 can delay aging in S. cerevisiae. Cell *80*, 485-496.

Kennedy, B.K., Gotta, M., Sinclair, D.A., Mills, K., McNabb, D.S., Murthy, M., Pak, S.M., Laroche, T., Gasser, S.M., and Guarente, L. (1997). Redistribution of silencing proteins from telomeres to the nucleolus is associated with extension of life span in S. cerevisiae. Cell *89*, 381-391.

Kim, H.J., Kim, J.H., Noh, S., Hur, H.J., Sung, M.J., Hwang, J.T., Park, J.H., Yang, H.J., Kim, M.S., Kwon, D.Y.*, et al.* (2011a). Metabolomic analysis of livers and serum from high-fat diet induced obese mice. Journal of proteome research *10*, 722-731.

Kim, H.S., Patel, K., Muldoon-Jacobs, K., Bisht, K.S., Aykin-Burns, N., Pennington, J.D., van der Meer, R., Nguyen, P., Savage, J., Owens, K.M.*, et al.* (2010a). SIRT3 is a mitochondria-localized tumor suppressor required for maintenance of mitochondrial integrity and metabolism during stress. Cancer Cell *17*, 41-52.

Kim, H.S., Vassilopoulos, A., Wang, R.H., Lahusen, T., Xiao, Z., Xu, X., Li, C., Veenstra, T.D., Li, B., Yu, H.*, et al.* (2011b). SIRT2 maintains genome integrity and suppresses tumorigenesis through regulating APC/C activity. Cancer Cell *20*, 487-499.

Kim, H.S., Xiao, C., Wang, R.H., Lahusen, T., Xu, X., Vassilopoulos, A., Vazquez-Ortiz, G., Jeong, W.I., Park, O., Ki, S.H.*, et al.* (2010b). Hepatic-specific disruption of SIRT6 in mice results in fatty liver formation due to enhanced glycolysis and triglyceride synthesis. Cell Metab *12*, 224-236.

Klar, A.J., Fogel, S., and Macleod, K. (1979). MAR1-a Regulator of the HMa and HMalpha Loci in SACCHAROMYCES CEREVISIAE. Genetics *93*, 37-50.

Kolwicz, S.C., Jr., and Tian, R. (2011). Glucose metabolism and cardiac hypertrophy. Cardiovasc Res *90*, 194-201.

Kueng, S., Oppikofer, M., and Gasser, S.M. (2013). SIR proteins and the assembly of silent chromatin in budding yeast. Annual review of genetics *47*, 275-306.

Kume, S., Uzu, T., Horiike, K., Chin-Kanasaki, M., Isshiki, K., Araki, S., Sugimoto, T., Haneda, M., Kashiwagi, A., and Koya, D. (2010). Calorie restriction enhances cell adaptation to hypoxia through Sirt1-dependent mitochondrial autophagy in mouse aged kidney. The Journal of clinical investigation *120*, 1043-1055.

Laemmle, A., Lechleiter, A., Roh, V., Schwarz, C., Portmann, S., Furer, C., Keogh, A., Tschan, M.P., Candinas, D., Vorburger, S.A.*, et al.* (2012). Inhibition of SIRT1 impairs the accumulation and transcriptional activity of HIF-1alpha protein under hypoxic conditions. PLoS One *7*, e33433.

Lain, S., Hollick, J.J., Campbell, J., Staples, O.D., Higgins, M., Aoubala, M., McCarthy, A., Appleyard, V., Murray, K.E., Baker, L.*, et al.* (2008). Discovery, in vivo activity, and mechanism of action of a small-molecule p53 activator. Cancer Cell *13*, 454-463.

Lakatta, E.G., and Levy, D. (2003). Arterial and cardiac aging: major shareholders in cardiovascular disease enterprises: Part II: the aging heart in health: links to heart disease. Circulation *107*, 346-354.

Lamming, D.W., Latorre-Esteves, M., Medvedik, O., Wong, S.N., Tsang, F.A., Wang, C., Lin, S.J., and Sinclair, D.A. (2005). HST2 mediates SIR2-independent life-span extension by calorie restriction. Science *309*, 1861-1864.

Langley, E., Pearson, M., Faretta, M., Bauer, U.M., Frye, R.A., Minucci, S., Pelicci, P.G., and Kouzarides, T. (2002). Human SIR2 deacetylates p53 and antagonizes PML/p53-induced cellular senescence. EMBO J *21*, 2383-2396.

Laurent, G., German, N.J., Saha, A.K., de Boer, V.C., Davies, M., Koves, T.R., Dephoure, N., Fischer, F., Boanca, G., Vaitheesvaran, B.*, et al.* (2013). SIRT4 Coordinates the Balance between Lipid Synthesis and Catabolism by Repressing Malonyl CoA Decarboxylase. Mol Cell *50*, 686-698.

Lee, G.D., Wilson, M.A., Zhu, M., Wolkow, C.A., de Cabo, R., Ingram, D.K., and Zou, S. (2006). Dietary deprivation extends lifespan in Caenorhabditis elegans. Aging Cell *5*, 515-524.

Lehnertz, B., Ueda, Y., Derijck, A.A., Braunschweig, U., Perez-Burgos, L., Kubicek, S., Chen, T., Li, E., Jenuwein, T., and Peters, A.H. (2003a). Suv39h-mediated histone H3 lysine 9 methylation directs DNA methylation to major satellite repeats at pericentric heterochromatin. Curr Biol *13*, 1192-1200.

Lehnertz, B., Ueda, Y., Derijck, A.A.H.A., Braunschweig, U., Perez-Burgos, L., Kubicek, S., Chen, T., Li, E., Jenuwein, T., and Peters, A.H.F.M. (2003b). Suv39h-Mediated

Histone H3 Lysine 9 Methylation Directs DNA Methylation to Major Satellite Repeats at Pericentric Heterochromatin. Current Biology *13*, 1192-1200.

Leko, V., Park, G.J., Lao, U., Simon, J.A., and Bedalov, A. (2013). Enterocyte-specific inactivation of SIRT1 reduces tumor load in the APC(+/min) mouse model. PLoS One *8*, e66283.

Li, S., Banck, M., Mujtaba, S., Zhou, M.M., Sugrue, M.M., and Walsh, M.J. (2010). p53-induced growth arrest is regulated by the mitochondrial SirT3 deacetylase. PLoS One *5*, e10486.

Li, Y., Xu, W., McBurney, M.W., and Longo, V.D. (2008). SirT1 inhibition reduces IGF-I/IRS-2/Ras/ERK1/2 signaling and protects neurons. Cell Metab *8*, 38-48.

Lim, J.H., Lee, Y.M., Chun, Y.S., Chen, J., Kim, J.E., and Park, J.W. (2010). Sirtuin 1 modulates cellular responses to hypoxia by deacetylating hypoxia-inducible factor 1alpha. Mol Cell *38*, 864-878.

Lin, S., and Garcia, B.A. (2012). Examining histone posttranslational modification patterns by high-resolution mass spectrometry. Methods Enzymol *512*, 3-28.

Lin, S.J., Defossez, P.A., and Guarente, L. (2000). Requirement of NAD and SIR2 for life-span extension by calorie restriction in Saccharomyces cerevisiae. Science *289*, 2126-2128.

Lin, Y.Y., Lu, J.Y., Zhang, J., Walter, W., Dang, W., Wan, J., Tao, S.C., Qian, J., Zhao, Y., Boeke, J.D.*, et al.* (2009). Protein acetylation microarray reveals that NuA4 controls key metabolic target regulating gluconeogenesis. Cell *136*, 1073-1084.

Lin, Z.F., Xu, H.B., Wang, J.Y., Lin, Q., Ruan, Z., Liu, F.B., Jin, W., Huang, H.H., and Chen, X. (2013). SIRT5 desuccinylates and activates SOD1 to eliminate ROS. Biochem Biophys Res Commun *441*, 191-195.

Liou, G.Y., and Storz, P. (2010). Reactive oxygen species in cancer. Free radical research *44*, 479-496.

Liu, B., Larsson, L., Caballero, A., Hao, X., Oling, D., Grantham, J., and Nystrom, T. (2010). The polarisome is required for segregation and retrograde transport of protein aggregates. Cell *140*, 257-267.

Lombard, D.B., Alt, F.W., Cheng, H.L., Bunkenborg, J., Streeper, R.S., Mostoslavsky, R., Kim, J., Yancopoulos, G., Valenzuela, D., Murphy, A.*, et al.* (2007). Mammalian Sir2 homolog SIRT3 regulates global mitochondrial lysine acetylation. Mol Cell Biol *27*, 8807-8814.

Lombard, D.B., and Miller, R.A. (2014). Aging, Disease, and Longevity in Mice. Annual Review of Gerontology and Geriatrics *34*, 93-138.

Lombard, D.B., and Zwaans, B.M. (2014). SIRT3: As Simple As It Seems? Gerontology *60*, 56-64.

Longo, V.D., and Kennedy, B.K. (2006). Sirtuins in aging and age-related disease. Cell *126*, 257-268.

Lopez-Otin, C., Blasco, M.A., Partridge, L., Serrano, M., and Kroemer, G. (2013). The hallmarks of aging. Cell *153*, 1194-1217.

Lu, M., Sarruf, D.A., Li, P., Osborn, O., Sanchez-Alavez, M., Talukdar, S., Chen, A., Bandyopadhyay, G., Xu, J., Morinaga, H.*, et al.* (2013). Neuronal Sirt1 deficiency increases insulin sensitivity in both brain and peripheral tissues. The Journal of biological chemistry *288*, 10722-10735.

Lu, W., Zuo, Y., Feng, Y., and Zhang, M. (2014). SIRT5 facilitates cancer cell growth and drug resistance in non-small cell lung cancer. Tumour biology : the journal of the International Society for Oncodevelopmental Biology and Medicine.

Ludewig, A.H., Izrayelit, Y., Park, D., Malik, R.U., Zimmermann, A., Mahanti, P., Fox, B.W., Bethke, A., Doering, F., Riddle, D.L.*, et al.* (2013). Pheromone sensing regulates Caenorhabditis elegans lifespan and stress resistance via the deacetylase SIR-2.1. Proc Natl Acad Sci U S A *110*, 5522-5527.

Luo, J., Li, M., Tang, Y., Laszkowska, M., Roeder, R.G., and Gu, W. (2004). Acetylation of p53 augments its site-specific DNA binding both in vitro and in vivo. Proc Natl Acad Sci U S A *101*, 2259-2264.

Luo, J., Nikolaev, A.Y., Imai, S., Chen, D., Su, F., Shiloh, A., Guarente, L., and Gu, W. (2001). Negative control of p53 by Sir2alpha promotes cell survival under stress. Cell *107*, 137-148.

Mair, W., Panowski, S.H., Shaw, R.J., and Dillin, A. (2009). Optimizing dietary restriction for genetic epistasis analysis and gene discovery in C. elegans. PLoS ONE *4*, e4535.

Manning, B.D., and Cantley, L.C. (2007). AKT/PKB signaling: navigating downstream. Cell *129*, 1261-1274.

Mao, B., Zhao, G., Lv, X., Chen, H.Z., Xue, Z., Yang, B., Liu, D.P., and Liang, C.C. (2011a). Sirt1 deacetylates c-Myc and promotes c-Myc/Max association. Int J Biochem Cell Biol *43*, 1573-1581.

Mao, Z., Hine, C., Tian, X., Van Meter, M., Au, M., Vaidya, A., Seluanov, A., and Gorbunova, V. (2011b). SIRT6 promotes DNA repair under stress by activating PARP1. Science *332*, 1443-1446.

Masri, S., Rigor, P., Cervantes, M., Ceglia, N., Sebastian, C., Xiao, C., Roqueta-Rivera, M., Deng, C., Osborne, T.F., Mostoslavsky, R.*, et al.* (2014). Partitioning Circadian

Transcription by SIRT6 Leads to Segregated Control of Cellular Metabolism. Cell *158*, 659-672.

Masri, S., and Sassone-Corsi, P. (2014). Sirtuins and the circadian clock: bridging chromatin and metabolism. Sci Signal *7*, re6.

Massudi, H., Grant, R., Braidy, N., Guest, J., Farnsworth, B., and Guillemin, G.J. (2012). Age-associated changes in oxidative stress and NAD+ metabolism in human tissue. PLoS One *7*, e42357.

Matsumoto, T., Baker, D.J., d'Uscio, L.V., Mozammel, G., Katusic, Z.S., and van Deursen, J.M. (2007). Aging-associated vascular phenotype in mutant mice with low levels of BubR1. Stroke; a journal of cerebral circulation *38*, 1050-1056.

Matsushita, N., Yonashiro, R., Ogata, Y., Sugiura, A., Nagashima, S., Fukuda, T., Inatome, R., and Yanagi, S. (2011). Distinct regulation of mitochondrial localization and stability of two human Sirt5 isoforms. Genes to cells : devoted to molecular & cellular mechanisms *16*, 190-202.

Mattagajasingh, I., Kim, C.S., Naqvi, A., Yamamori, T., Hoffman, T.A., Jung, S.B., DeRicco, J., Kasuno, K., and Irani, K. (2007). SIRT1 promotes endothelium-dependent vascular relaxation by activating endothelial nitric oxide synthase. Proc Natl Acad Sci U S A *104*, 14855-14860.

McBurney, M.W., Yang, X., Jardine, K., Hixon, M., Boekelheide, K., Webb, J.R., Lansdorp, P.M., and Lemieux, M. (2003). The mammalian SIR2alpha protein has a role in embryogenesis and gametogenesis. Mol Cell Biol *23*, 38-54.

McCarthy, A.R., Hollick, J.J., and Westwood, N.J. (2010). The discovery of nongenotoxic activators of p53: building on a cell-based high-throughput screen. Seminars in cancer biology *20*, 40-45.

McCarthy, A.R., Pirrie, L., Hollick, J.J., Ronseaux, S., Campbell, J., Higgins, M., Staples, O.D., Tran, F., Slawin, A.M., Lain, S.*, et al.* (2012). Synthesis and biological characterisation of sirtuin inhibitors based on the tenovins. Bioorg Med Chem *20*, 1779-1793.

Menssen, A., Hydbring, P., Kapelle, K., Vervoorts, J., Diebold, J., Luscher, B., Larsson, L.G., and Hermeking, H. (2012). The c-MYC oncoprotein, the NAMPT enzyme, the SIRT1-inhibitor DBC1, and the SIRT1 deacetylase form a positive feedback loop. Proc Natl Acad Sci U S A *109*, E187-196.

Mercken, E.M., Hu, J., Krzysik-Walker, S., Wei, M., Li, Y., McBurney, M.W., de Cabo, R., and Longo, V.D. (2014a). SIRT1 but not its increased expression is essential for lifespan extension in caloric-restricted mice. Aging Cell *13*, 193-196.

Mercken, E.M., Mitchell, S.J., Martin-Montalvo, A., Minor, R.K., Almeida, M., Gomes, A.P., Scheibye-Knudsen, M., Palacios, H.H., Licata, J.J., Zhang, Y.*, et al.* (2014b).

SRT2104 extends survival of male mice on a standard diet and preserves bone and muscle mass. Aging Cell *13*, 787-796.

Michishita, E., McCord, R.A., Berber, E., Kioi, M., Padilla-Nash, H., Damian, M., Cheung, P., Kusumoto, R., Kawahara, T.L., Barrett, J.C.*, et al.* (2008). SIRT6 is a histone H3 lysine 9 deacetylase that modulates telomeric chromatin. Nature *452*, 492-496.

Michishita, E., McCord, R.A., Boxer, L.D., Barber, M.F., Hong, T., Gozani, O., and Chua, K.F. (2009). Cell cycle-dependent deacetylation of telomeric histone H3 lysine K56 by human SIRT6. Cell Cycle *8*, 2664-2666.

Michishita, E., Park, J.Y., Burneskis, J.M., Barrett, J.C., and Horikawa, I. (2005). Evolutionarily conserved and nonconserved cellular localizations and functions of human SIRT proteins. Mol Biol Cell *16*, 4623-4635.

Miller, R.A., Buehner, G., Chang, Y., Harper, J.M., Sigler, R., and Smith-Wheelock, M. (2005). Methionine-deficient diet extends mouse lifespan, slows immune and lens aging, alters glucose, T4, IGF-I and insulin levels, and increases hepatocyte MIF levels and stress resistance. Aging Cell *4*, 119-125.

Miller, R.A., Harrison, D.E., Astle, C.M., Baur, J.A., Boyd, A.R., de Cabo, R., Fernandez, E., Flurkey, K., Javors, M.A., Nelson, J.F.*, et al.* (2011). Rapamycin, but not resveratrol or simvastatin, extends life span of genetically heterogeneous mice. J Gerontol A Biol Sci Med Sci *66*, 191-201.

Ming, M., Qiang, L., Zhao, B., and He, Y.Y. (2014). Mammalian SIRT2 inhibits keratin 19 expression and is a tumor suppressor in skin. Exp Dermatol *23*, 207-209.

Minor, R.K., Baur, J.A., Gomes, A.P., Ward, T.M., Csiszar, A., Mercken, E.M., Abdelmohsen, K., Shin, Y.K., Canto, C., Scheibye-Knudsen, M.*, et al.* (2011). SRT1720 improves survival and healthspan of obese mice. Sci Rep *1*, 70.

Mitchell, S.J., Martin-Montalvo, A., Mercken, E.M., Palacios, H.H., Ward, T.M., Abulwerdi, G., Minor, R.K., Vlasuk, G.P., Ellis, J.L., Sinclair, D.A.*, et al.* (2014). The SIRT1 activator SRT1720 extends lifespan and improves health of mice fed a standard diet. Cell Rep *6*, 836-843.

Moreno-Sanchez, R., Rodriguez-Enriquez, S., Marin-Hernandez, A., and Saavedra, E. (2007). Energy metabolism in tumor cells. FEBS J *274*, 1393-1418.

Mostoslavsky, R., Chua, K.F., Lombard, D.B., Pang, W.W., Fischer, M.R., Gellon, L., Liu, P., Mostoslavsky, G., Franco, S., Murphy, M.M.*, et al.* (2006). Genomic instability and aging-like phenotype in the absence of mammalian SIRT6. Cell *124*, 315-329.

Mouchiroud, L., Houtkooper, R.H., Moullan, N., Katsyuba, E., Ryu, D., Canto, C., Mottis, A., Jo, Y.S., Viswanathan, M., Schoonjans, K.*, et al.* (2013). The NAD(+)/Sirtuin

Pathway Modulates Longevity through Activation of Mitochondrial UPR and FOXO Signaling. Cell *154*, 430-441.

Nakagawa, T., Lomb, D.J., Haigis, M.C., and Guarente, L. (2009). SIRT5 Deacetylates carbamoyl phosphate synthetase 1 and regulates the urea cycle. Cell *137*, 560-570.

Nakamura, Y., Ogura, M., Ogura, K., Tanaka, D., and Inagaki, N. (2012). SIRT5 deacetylates and activates urate oxidase in liver mitochondria of mice. FEBS Lett *586*, 4076-4081.

North, B.J., Marshall, B.L., Borra, M.T., Denu, J.M., and Verdin, E. (2003). The human Sir2 ortholog, SIRT2, is an NAD+-dependent tubulin deacetylase. Mol Cell *11*, 437-444.

North, B.J., Rosenberg, M.A., Jeganathan, K.B., Hafner, A.V., Michan, S., Dai, J., Baker, D.J., Cen, Y., Wu, L.E., Sauve, A.A.*, et al.* (2014). SIRT2 induces the checkpoint kinase BubR1 to increase lifespan. EMBO J *33*, 1438-1453.

North, B.J., and Verdin, E. (2007). Mitotic regulation of SIRT2 by cyclin-dependent kinase 1-dependent phosphorylation. J Biol Chem *282*, 19546-19555.

Oberdoerffer, P., Michan, S., McVay, M., Mostoslavsky, R., Vann, J., Park, S.K., Hartlerode, A., Stegmuller, J., Hafner, A., Loerch, P.*, et al.* (2008). SIRT1 redistribution on chromatin promotes genomic stability but alters gene expression during aging. Cell *135*, 907-918.

Oellerich, M.F., and Potente, M. (2012). FOXOs and sirtuins in vascular growth, maintenance, and aging. Circ Res *110*, 1238-1251.

Ogura, M., Nakamura, Y., Tanaka, D., Zhuang, X., Fujita, Y., Obara, A., Hamasaki, A., Hosokawa, M., and Inagaki, N. (2010a). Overexpression of SIRT5 confirms its involvement in deacetylation and activation of carbamoyl phosphate synthetase 1. Biochemical and biophysical research communications *393*, 73-78.

Ogura, M., Nakamura, Y., Tanaka, D., Zhuang, X., Fujita, Y., Obara, A., Hamasaki, A., Hosokawa, M., and Inagaki, N. (2010b). Overexpression of SIRT5 confirms its involvement in deacetylation and activation of carbamoyl phosphate synthetase 1. Biochem Biophys Res Commun *393*, 73-78.

Oka, S., Alcendor, R., Zhai, P., Park, J.Y., Shao, D., Cho, J., Yamamoto, T., Tian, B., and Sadoshima, J. (2011). PPARalpha-Sirt1 complex mediates cardiac hypertrophy and failure through suppression of the ERR transcriptional pathway. Cell Metab *14*, 598-611.

Pacholec, M., Bleasdale, J.E., Chrunyk, B., Cunningham, D., Flynn, D., Garofalo, R.S., Griffith, D., Griffor, M., Loulakis, P., Pabst, B.*, et al.* (2010). SRT1720, SRT2183, SRT1460, and resveratrol are not direct activators of SIRT1. J Biol Chem *285*, 8340-8351.

Paik, J.H. (2006). FOXOs in the maintenance of vascular homoeostasis. Biochem Soc Trans *34*, 731-734.

Paik, J.H., Kollipara, R., Chu, G., Ji, H., Xiao, Y., Ding, Z., Miao, L., Tothova, Z., Horner, J.W., Carrasco, D.R.*, et al.* (2007). FoxOs are lineage-restricted redundant tumor suppressors and regulate endothelial cell homeostasis. Cell *128*, 309-323.

Palacios, O.M., Carmona, J.J., Michan, S., Chen, K.Y., Manabe, Y., Ward, J.L., 3rd, Goodyear, L.J., and Tong, Q. (2009). Diet and exercise signals regulate SIRT3 and activate AMPK and PGC-1alpha in skeletal muscle. Aging (Albany NY) *1*, 771-783.

Pallos, J., Bodai, L., Lukacsovich, T., Purcell, J.M., Steffan, J.S., Thompson, L.M., and Marsh, J.L. (2008). Inhibition of specific HDACs and sirtuins suppresses pathogenesis in a Drosophila model of Huntington's disease. Hum Mol Genet *17*, 3767-3775.

Pandithage, R., Lilischkis, R., Harting, K., Wolf, A., Jedamzik, B., Luscher-Firzlaff, J., Vervoorts, J., Lasonder, E., Kremmer, E., Knoll, B.*, et al.* (2008). The regulation of SIRT2 function by cyclin-dependent kinases affects cell motility. J Cell Biol *180*, 915-929.

Pardue, M.L., and Gall, J.G. (1970). Chromosomal localization of mouse satellite DNA. Science *168*, 1356-1358.

Park, J., Chen, Y., Tishkoff, D.X., Peng, C., Tan, M., Dai, L., Xie, Z., Zhang, Y., Zwaans, B.M., Skinner, M.E.*, et al.* (2013). SIRT5-mediated lysine desuccinylation impacts diverse metabolic pathways. Mol Cell *50*, 919-930.

Park, S.J., Ahmad, F., Philp, A., Baar, K., Williams, T., Luo, H., Ke, H., Rehmann, H., Taussig, R., Brown, A.L.*, et al.* (2012). Resveratrol ameliorates aging-related metabolic phenotypes by inhibiting cAMP phosphodiesterases. Cell *148*, 421-433.

Pearson, K.J., Baur, J.A., Lewis, K.N., Peshkin, L., Price, N.L., Labinskyy, N., Swindell, W.R., Kamara, D., Minor, R.K., Perez, E.*, et al.* (2008). Resveratrol delays age-related deterioration and mimics transcriptional aspects of dietary restriction without extending life span. Cell Metab *8*, 157-168.

Peng, C., Lu, Z., Xie, Z., Cheng, Z., Chen, Y., Tan, M., Luo, H., Zhang, Y., He, W., Yang, K.*, et al.* (2011a). The first identification of lysine malonylation substrates and its regulatory enzyme. Mol Cell Proteomics *10*, M111 012658.

Peng, C., Lu, Z., Xie, Z., Cheng, Z., Chen, Y., Tan, M., Luo, H., Zhang, Y., He, W., Yang, K.*, et al.* (2011b). The first identification of lysine malonylation substrates and its regulatory enzyme. Mol Cell Proteomics *10*, M111 012658 012651-012612.

Perrone, C.E., Malloy, V.L., Orentreich, D.S., and Orentreich, N. (2013). Metabolic adaptations to methionine restriction that benefit health and lifespan in rodents. Exp Gerontol *48*, 654-660.

Peters, A.H., O'Carroll, D., Scherthan, H., Mechtler, K., Sauer, S., Schofer, C., Weipoltshammer, K., Pagani, M., Lachner, M., Kohlmaier, A.*, et al.* (2001). Loss of the Suv39h histone methyltransferases impairs mammalian heterochromatin and genome stability. Cell *107*, 323-337.

Pfluger, P.T., Herranz, D., Velasco-Miguel, S., Serrano, M., and Tschop, M.H. (2008). Sirt1 protects against high-fat diet-induced metabolic damage. Proc Natl Acad Sci U S A *105*, 9793-9798.

Phng, L.K., and Gerhardt, H. (2009). Angiogenesis: a team effort coordinated by notch. Dev Cell *16*, 196-208.

Pillai, V.B., Sundaresan, N.R., Kim, G., Gupta, M., Rajamohan, S.B., Pillai, J.B., Samant, S., Ravindra, P.V., Isbatan, A., and Gupta, M.P. (2010). Exogenous NAD blocks cardiac hypertrophic response via activation of the SIRT3-LKB1-AMP-activated kinase pathway. J Biol Chem *285*, 3133-3144.

Planavila, A., Iglesias, R., Giralt, M., and Villarroya, F. (2011). Sirt1 acts in association with PPARalpha to protect the heart from hypertrophy, metabolic dysregulation, and inflammation. Cardiovasc Res *90*, 276-284.

Polletta, L., Vernucci, E., Carnevale, I., Arcangeli, T., Rotili, D., Palmerio, S., Steegborn, C., Nowak, T., Schutkowski, M., Pellegrini, L.*, et al.* (2015). SIRT5 regulation of ammonia-induced autophagy and mitophagy. Autophagy, 0.

Porter, G.A., Urciuoli, W.R., Brookes, P.S., and Nadtochiy, S.M. (2014). SIRT3 deficiency exacerbates ischemia-reperfusion injury: implication for aged hearts. Am J Physiol Heart Circ Physiol *306*, H1602-1609.

Postepska-Igielska, A., Krunic, D., Schmitt, N., Greulich-Bode, K.M., Boukamp, P., and Grummt, I. (2013). The chromatin remodelling complex NoRC safeguards genome stability by heterochromatin formation at telomeres and centromeres. EMBO reports.

Potente, M., and Dimmeler, S. (2008). Emerging roles of SIRT1 in vascular endothelial homeostasis. Cell Cycle *7*, 2117-2122.

Potente, M., Ghaeni, L., Baldessari, D., Mostoslavsky, R., Rossig, L., Dequiedt, F., Haendeler, J., Mione, M., Dejana, E., Alt, F.W.*, et al.* (2007). SIRT1 controls endothelial angiogenic functions during vascular growth. Genes Dev *21*, 2644-2658.

Potente, M., Urbich, C., Sasaki, K., Hofmann, W.K., Heeschen, C., Aicher, A., Kollipara, R., DePinho, R.A., Zeiher, A.M., and Dimmeler, S. (2005). Involvement of Foxo transcription factors in angiogenesis and postnatal neovascularization. J Clin Invest *115*, 2382-2392.

Prashad, N., and Cutler, R.G. (1976). Percent satellite DNA as a function of tissue and age of mice. Biochim Biophys Acta *418*, 1-23.

Price, N.L., Gomes, A.P., Ling, A.J., Duarte, F.V., Martin-Montalvo, A., North, B.J., Agarwal, B., Ye, L., Ramadori, G., Teodoro, J.S.*, et al.* (2012). SIRT1 is required for AMPK activation and the beneficial effects of resveratrol on mitochondrial function. Cell Metab *15*, 675-690.

Qin, J.Z., Xin, H., and Nickoloff, B.J. (2010a). 2-deoxyglucose sensitizes melanoma cells to TRAIL-induced apoptosis which is reduced by mannose. Biochem Biophys Res Commun *401*, 293-299.

Qin, J.Z., Xin, H., and Nickoloff, B.J. (2010b). Targeting glutamine metabolism sensitizes melanoma cells to TRAIL-induced death. Biochem Biophys Res Commun *398*, 146-152.

Qiu, X., Brown, K., Hirschey, M.D., Verdin, E., and Chen, D. (2010). Calorie restriction reduces oxidative stress by SIRT3-mediated SOD2 activation. Cell Metab *12*, 662-667.

Rahman, S., and Islam, R. (2011). Mammalian Sirt1: insights on its biological functions. Cell Commun Signal *9*, 11.

Ramsey, K.M., Mills, K.F., Satoh, A., and Imai, S. (2008). Age-associated loss of Sirt1-mediated enhancement of glucose-stimulated insulin secretion in beta cell-specific Sirt1-overexpressing (BESTO) mice. Aging Cell *7*, 78-88.

Rando, T.A., and Chang, H.Y. (2012). Aging, rejuvenation, and epigenetic reprogramming: resetting the aging clock. Cell *148*, 46-57.

Rardin, M.J., He, W., Nishida, Y., Newman, J.C., Carrico, C., Danielson, S.R., Guo, A., Gut, P., Sahu, A.K., Li, B.*, et al.* (2013). SIRT5 regulates the mitochondrial lysine succinylome and metabolic networks. Cell Metab *18*, 920-933.

Ratnikov, B., Aza-Blanc, P., Ronai, Z.A., Smith, J.W., Osterman, A.L., and Scott, D.A. (2015). Glutamate and asparagine cataplerosis underlie glutamine addiction in melanoma. Oncotarget *6*, 7379-7389.

Richie, J.P., Jr., Leutzinger, Y., Parthasarathy, S., Malloy, V., Orentreich, N., and Zimmerman, J.A. (1994). Methionine restriction increases blood glutathione and longevity in F344 rats. FASEB J *8*, 1302-1307.

Rine, J., and Herskowitz, I. (1987). Four genes responsible for a position effect on expression from HML and HMR in Saccharomyces cerevisiae. Genetics *116*, 9-22.

Rine, J., Strathern, J.N., Hicks, J.B., and Herskowitz, I. (1979). A suppressor of mating-type locus mutations in Saccharomyces cerevisiae: evidence for and identification of cryptic mating-type loci. Genetics *93*, 877-901.

Rizki, G., Iwata, T.N., Li, J., Riedel, C.G., Picard, C.L., Jan, M., Murphy, C.T., and Lee, S.S. (2011). The evolutionarily conserved longevity determinants HCF-1 and SIR-2.1/SIRT1 collaborate to regulate DAF-16/FOXO. PLoS Genet *7*, e1002235.

Rogina, B., and Helfand, S.L. (2004). Sir2 mediates longevity in the fly through a pathway related to calorie restriction. Proc Natl Acad Sci U S A *101*, 15998-16003.

Ryu, D., Jo, Y.S., Lo Sasso, G., Stein, S., Zhang, H., Perino, A., Lee, J.U., Zeviani, M., Romand, R., Hottiger, M.O*., et al.* (2014). A SIRT7-Dependent Acetylation Switch of GABPbeta1 Controls Mitochondrial Function. Cell Metab.

Sadhukhan, S., Liu, X., Ryu, D., Nelson, O.D., Stupinski, J.A., Li, Z., Chen, W., Zhang, S., Weiss, R.S., Locasale, J.W*., et al.* (2016). Metabolomics-assisted proteomics identifies succinylation and SIRT5 as important regulators of cardiac function. Proc Natl Acad Sci U S A *113*, 4320-4325.

Saka, K., Ide, S., Ganley, A.R., and Kobayashi, T. (2013). Cellular senescence in yeast is regulated by rDNA noncoding transcription. Curr Biol *23*, 1794-1798.

Santos, G.C., Zielenska, M., Prasad, M., and Squire, J.A. (2007). Chromosome 6p amplification and cancer progression. J Clin Pathol *60*, 1-7.

Satoh, A., Brace, C.S., Ben-Josef, G., West, T., Wozniak, D.F., Holtzman, D.M., Herzog, E.D., and Imai, S. (2010). SIRT1 promotes the central adaptive response to diet restriction through activation of the dorsomedial and lateral nuclei of the hypothalamus. The Journal of neuroscience : the official journal of the Society for Neuroscience *30*, 10220-10232.

Satoh, A., Brace, C.S., Rensing, N., Cliften, P., Wozniak, D.F., Herzog, E.D., Yamada, K.A., and Imai, S. (2013). Sirt1 extends life span and delays aging in mice through the regulation of Nk2 homeobox 1 in the DMH and LH. Cell Metab *18*, 416-430.

Schenk, S., McCurdy, C.E., Philp, A., Chen, M.Z., Holliday, M.J., Bandyopadhyay, G.K., Osborn, O., Baar, K., and Olefsky, J.M. (2011). Sirt1 enhances skeletal muscle insulin sensitivity in mice during caloric restriction. The Journal of clinical investigation *121*, 4281-4288.

Schmeisser, K., Mansfeld, J., Kuhlow, D., Weimer, S., Priebe, S., Heiland, I., Birringer, M., Groth, M., Segref, A., Kanfi, Y*., et al.* (2013). Role of sirtuins in lifespan regulation is linked to methylation of nicotinamide. Nature chemical biology *9*, 693-700.

Schwer, B., Eckersdorff, M., Li, Y., Silva, J.C., Fermin, D., Kurtev, M.V., Giallourakis, C., Comb, M.J., Alt, F.W., and Lombard, D.B. (2009). Calorie restriction alters mitochondrial protein acetylation. Aging Cell *8*, 604-606.

Scott, D.A., Richardson, A.D., Filipp, F.V., Knutzen, C.A., Chiang, G.G., Ronai, Z.A., Osterman, A.L., and Smith, J.W. (2011). Comparative metabolic flux profiling of melanoma cell lines: beyond the Warburg effect. J Biol Chem *286*, 42626-42634.

Sen, P., Dang, W., Donahue, G., Dai, J., Dorsey, J., Cao, X., Liu, W., Cao, K., Perry, R., Lee, J.Y*., et al.* (2015). H3K36 methylation promotes longevity by enhancing transcriptional fidelity. Genes Dev *29*, 1362-1376.

Serrano, L., Martinez-Redondo, P., Marazuela-Duque, A., Vazquez, B.N., Dooley, S.J., Voigt, P., Beck, D.B., Kane-Goldsmith, N., Tong, Q., Rabanal, R.M.*, et al.* (2013a). The tumor suppressor SirT2 regulates cell cycle progression and genome stability by modulating the mitotic deposition of H4K20 methylation. Genes Dev *27*, 639-653.

Serrano, L., Martinez-Redondo, P., Marazuela-Duque, A., Vazquez, B.N., Dooley, S.J., Voigt, P., Beck, D.B., Kane-Goldsmith, N., Tong, Q., Rabanal, R.M.*, et al.* (2013b). The tumor suppressor SirT2 regulates cell cycle progression and genome stability by modulating the mitotic deposition of H4K20 methylation. Genes & Development *27*, 639-653.

Shi, T., Wang, F., Stieren, E., and Tong, Q. (2005). SIRT3, a mitochondrial sirtuin deacetylase, regulates mitochondrial function and thermogenesis in brown adipocytes. J Biol Chem *280*, 13560-13567.

Shin, J., He, M., Liu, Y., Paredes, S., Villanova, L., Brown, K., Qiu, X., Nabavi, N., Mohrin, M., Wojnoonski, K.*, et al.* (2013). SIRT7 represses Myc activity to suppress ER stress and prevent fatty liver disease. Cell Rep *5*, 654-665.

Shiojima, I., Yefremashvili, M., Luo, Z., Kureishi, Y., Takahashi, A., Tao, J., Rosenzweig, A., Kahn, C.R., Abel, E.D., and Walsh, K. (2002). Akt signaling mediates postnatal heart growth in response to insulin and nutritional status. J Biol Chem *277*, 37670-37677.

Shore, D., Squire, M., and Nasmyth, K.A. (1984). Characterization of two genes required for the position-effect control of yeast mating-type genes. EMBO J *3*, 2817-2823.

Siegel, R.L., Miller, K.D., and Jemal, A. (2015). Cancer statistics, 2015. CA Cancer J Clin *65*, 5-29.

Silberman, D.M., Ross, K., Sande, P.H., Kubota, S., Ramaswamy, S., Apte, R.S., and Mostoslavsky, R. (2014). SIRT6 is required for normal retinal function. PLoS One *9*, e98831.

Simeoni, F., Tasselli, L., Tanaka, S., Villanova, L., Hayashi, M., Kubota, K., Isono, F., Garcia, B.A., Michishita-Kioi, E., and Chua, K.F. (2013). Proteomic analysis of the SIRT6 interactome: novel links to genome maintenance and cellular stress signaling. Sci Rep *3*, 3085.

Sinclair, D.A., and Guarente, L. (1997). Extrachromosomal rDNA circles--a cause of aging in yeast. Cell *91*, 1033-1042.

Someya, S., Yu, W., Hallows, W.C., Xu, J., Vann, J.M., Leeuwenburgh, C., Tanokura, M., Denu, J.M., and Prolla, T.A. (2010). Sirt3 mediates reduction of oxidative damage and prevention of age-related hearing loss under caloric restriction. Cell *143*, 802-812.

Speakman, J.R., and Mitchell, S.E. (2011). Caloric restriction. Mol Aspects Med *32*, 159-221.

Srisuttee, R., Koh, S.S., Kim, S.J., Malilas, W., Boonying, W., Cho, I.R., Jhun, B.H., Ito, M., Horio, Y., Seto, E.*, et al.* (2012). Hepatitis B virus X (HBX) protein upregulates beta-catenin in a human hepatic cell line by sequestering SIRT1 deacetylase. Oncol Rep *28*, 276-282.

Stein, L.R., and Imai, S. (2014). Specific ablation of Nampt in adult neural stem cells recapitulates their functional defects during aging. EMBO J *33*, 1321-1340.

Strong, R., Miller, R.A., Astle, C.M., Floyd, R.A., Flurkey, K., Hensley, K.L., Javors, M.A., Leeuwenburgh, C., Nelson, J.F., Ongini, E.*, et al.* (2008). Nordihydroguaiaretic acid and aspirin increase lifespan of genetically heterogeneous male mice. Aging Cell *7*, 641-650.

Suka, N., Luo, K., and Grunstein, M. (2002). Sir2p and Sas2p opposingly regulate acetylation of yeast histone H4 lysine16 and spreading of heterochromatin. Nat Genet *32*, 378-383.

Sundaresan, N.R., Gupta, M., Kim, G., Rajamohan, S.B., Isbatan, A., and Gupta, M.P. (2009). Sirt3 blocks the cardiac hypertrophic response by augmenting Foxo3a-dependent antioxidant defense mechanisms in mice. J Clin Invest *119*, 2758-2771.

Sundaresan, N.R., Pillai, V.B., Wolfgeher, D., Samant, S., Vasudevan, P., Parekh, V., Raghuraman, H., Cunningham, J.M., Gupta, M., and Gupta, M.P. (2011). The deacetylase SIRT1 promotes membrane localization and activation of Akt and PDK1 during tumorigenesis and cardiac hypertrophy. Sci Signal *4*, ra46 41-13.

Sundaresan, N.R., Vasudevan, P., Zhong, L., Kim, G., Samant, S., Parekh, V., Pillai, V.B., Ravindra, P.V., Gupta, M., Jeevanandam, V.*, et al.* (2012). The sirtuin SIRT6 blocks IGF-Akt signaling and development of cardiac hypertrophy by targeting c-Jun. Nat Med *18*, 1643-1650.

Tan, M., Peng, C., Anderson, K.A., Chhoy, P., Xie, Z., Dai, L., Park, J., Chen, Y., Huang, H., Zhang, Y.*, et al.* (2014a). Lysine Glutarylation Is a Protein Posttranslational Modification Regulated by SIRT5. Cell Metab *19*, 605-617.

Tan, M., Peng, C., Anderson, Kristin A., Chhoy, P., Xie, Z., Dai, L., Park, J., Chen, Y., Huang, H., Zhang, Y.*, et al.* (2014b). Lysine Glutarylation Is a Protein Posttranslational Modification Regulated by SIRT5. Cell Metabolism *19*, 605-617.

Tanner, K.G., Landry, J., Sternglanz, R., and Denu, J.M. (2000). Silent information regulator 2 family of NAD- dependent histone/protein deacetylases generates a unique product, 1-O-acetyl-ADP-ribose. Proc Natl Acad Sci U S A *97*, 14178-14182.

Tanno, M., Sakamoto, J., Miura, T., Shimamoto, K., and Horio, Y. (2007). Nucleocytoplasmic shuttling of the NAD+-dependent histone deacetylase SIRT1. J Biol Chem *282*, 6823-6832.

Tao, R., Coleman, M.C., Pennington, J.D., Ozden, O., Park, S.H., Jiang, H., Kim, H.S., Flynn, C.R., Hill, S., Hayes McDonald, W*., et al.* (2010). Sirt3-mediated deacetylation of evolutionarily conserved lysine 122 regulates MnSOD activity in response to stress. Mol Cell *40*, 893-904.

Tao, R., Xiong, X., DePinho, R.A., Deng, C.X., and Dong, X.C. (2013). Hepatic SREBP-2 and cholesterol biosynthesis are regulated by FoxO3 and Sirt6. Journal of lipid research *54*, 2745-2753.

Tatar, M., Post, S., and Yu, K. (2014). Nutrient control of Drosophila longevity. Trends Endocrinol Metab, 1-9.

Theodosakis, N., Micevic, G., Kelly, D.P., and Bosenberg, M. (2014). Mitochondrial function in melanoma. Arch Biochem Biophys *563*, 56-59.

Tissenbaum, H.A., and Guarente, L. (2001). Increased dosage of a sir-2 gene extends lifespan in Caenorhabditis elegans. Nature *410*, 227-230.

Tissenbaum, H.A., and Guarente, L. (2002). Model organisms as a guide to mammalian aging. Dev Cell *2*, 9-19.

Ungvari, Z., Kaley, G., de Cabo, R., Sonntag, W.E., and Csiszar, A. (2010). Mechanisms of vascular aging: new perspectives. J Gerontol A Biol Sci Med Sci *65*, 1028-1041.

Vakhrusheva, O., Smolka, C., Gajawada, P., Kostin, S., Boettger, T., Kubin, T., Braun, T., and Bober, E. (2008). Sirt7 increases stress resistance of cardiomyocytes and prevents apoptosis and inflammatory cardiomyopathy in mice. Circ Res *102*, 703-710.

van Leeuwen, I.M., Higgins, M., Campbell, J., McCarthy, A.R., Sachweh, M.C., Navarro, A.M., and Lain, S. (2013). Modulation of p53 C-terminal acetylation by mdm2, p14ARF, and cytoplasmic SirT2. Mol Cancer Ther *12*, 471-480.

Vaquero, A., and Reinberg, D. (2009). Calorie restriction and the exercise of chromatin. Genes Dev *23*, 1849-1869.

Vaquero, A., Scher, M., Erdjument-Bromage, H., Tempst, P., Serrano, L., and Reinberg, D. (2007). SIRT1 regulates the histone methyl-transferase SUV39H1 during heterochromatin formation. Nature *450*, 440-444.

Vaquero, A., Scher, M., Lee, D., Erdjument-Bromage, H., Tempst, P., and Reinberg, D. (2004). Human SirT1 interacts with histone H1 and promotes formation of facultative heterochromatin. Mol Cell *16*, 93-105.

Vaquero, A., Scher, M.B., Lee, D.H., Sutton, A., Cheng, H.L., Alt, F.W., Serrano, L., Sternglanz, R., and Reinberg, D. (2006). SirT2 is a histone deacetylase with preference for histone H4 Lys 16 during mitosis. Genes Dev *20*, 1256-1261.

Vaziri, H., Dessain, S.K., Ng Eaton, E., Imai, S.I., Frye, R.A., Pandita, T.K., Guarente, L., and Weinberg, R.A. (2001). hSIR2(SIRT1) functions as an NAD-dependent p53 deacetylase. Cell *107*, 149-159.

Villeponteau, B. (1997). The heterochromatin loss model of aging. Exp Gerontol *32*, 383-394.

Vissel, B., and Choo, K.H. (1989). Mouse major (gamma) satellite DNA is highly conserved and organized into extremely long tandem arrays: implications for recombination between nonhomologous chromosomes. Genomics *5*, 407-414.

Viswanathan, M., and Guarente, L. (2011). Regulation of Caenorhabditis elegans lifespan by sir-2.1 transgenes. Nature *477*, E1-2.

Wang, F., Nguyen, M., Qin, F.X., and Tong, Q. (2007). SIRT2 deacetylates FOXO3a in response to oxidative stress and caloric restriction. Aging Cell *6*, 505-514.

Wang, R.H., Sengupta, K., Li, C., Kim, H.S., Cao, L., Xiao, C., Kim, S., Xu, X., Zheng, Y., Chilton, B.*, et al.* (2008). Impaired DNA damage response, genome instability, and tumorigenesis in SIRT1 mutant mice. Cancer Cell *14*, 312-323.

Wang, Y., and Tissenbaum, H.A. (2006). Overlapping and distinct functions for a Caenorhabditis elegans SIR2 and DAF-16/FOXO. Mech Ageing Dev *127*, 48-56.

Wang, Y.P., Zhou, L.S., Zhao, Y.Z., Wang, S.W., Chen, L.L., Liu, L.X., Ling, Z.Q., Hu, F.J., Sun, Y.P., Zhang, J.Y.*, et al.* (2014). Regulation of G6PD acetylation by SIRT2 and KAT9 modulates NADPH homeostasis and cell survival during oxidative stress. EMBO J *33*, 1304-1320.

Warburg, O. (1956). On the origin of cancer cells. Science *123*, 309-314.

Ward, P.S., and Thompson, C.B. (2012). Metabolic reprogramming: a cancer hallmark even warburg did not anticipate. Cancer Cell *21*, 297-308.

Waring, M., and Britten, R.J. (1966). Nucleotide sequence repetition: a rapidly reassociating fraction of mouse DNA. Science *154*, 791-794.

Wen, L., Chen, Z., Zhang, F., Cui, X., Sun, W., Geary, G.G., Wang, Y., Johnson, D.A., Zhu, Y., Chien, S.*, et al.* (2013). Ca2+/calmodulin-dependent protein kinase kinase beta phosphorylation of Sirtuin 1 in endothelium is atheroprotective. Proc Natl Acad Sci U S A *110*, E2420-2427.

Whitaker, R., Faulkner, S., Miyokawa, R., Burhenn, L., Henriksen, M., Wood, J.G., and Helfand, S.L. (2013). Increased expression of Drosophila Sir2 extends life span in a dose-dependent manner. Aging (Albany NY) *5*, 682-691.

White, A.T., Philp, A., Fridolfsson, H.N., Schilling, J.M., Murphy, A.N., Hamilton, D.L., McCurdy, C.E., Patel, H.H., and Schenk, S. (2014). High-fat diet-induced impairment of skeletal muscle insulin sensitivity is not prevented by SIRT1 overexpression. Am J Physiol Endocrinol Metab *307*, E764-772.

Wijshake, T., Malureanu, L.A., Baker, D.J., Jeganathan, K.B., van de Sluis, B., and van Deursen, J.M. (2012). Reduced life- and healthspan in mice carrying a mono-allelic BubR1 MVA mutation. PLoS Genet *8*, e1003138.

Xiao, C., Kim, H.S., Lahusen, T., Wang, R.H., Xu, X., Gavrilova, O., Jou, W., Gius, D., and Deng, C.X. (2010). SIRT6 deficiency results in severe hypoglycemia by enhancing both basal and insulin-stimulated glucose uptake in mice. J Biol Chem *285*, 36776-36784.

Xiong, X., Tao, R., DePinho, R.A., and Dong, X.C. (2013). Deletion of hepatic FoxO1/3/4 genes in mice significantly impacts on glucose metabolism through downregulation of gluconeogenesis and upregulation of glycolysis. PLoS One *8*, e74340.

Yang, B., Zwaans, B.M., Eckersdorff, M., and Lombard, D.B. (2009). The sirtuin SIRT6 deacetylates H3 K56Ac in vivo to promote genomic stability. Cell Cycle *8*, 2662-2663.

Yang, H., Yang, T., Baur, J.A., Perez, E., Matsui, T., Carmona, J.J., Lamming, D.W., Souza-Pinto, N.C., Bohr, V.A., Rosenzweig, A.*, et al.* (2007). Nutrient-sensitive mitochondrial NAD+ levels dictate cell survival. Cell *130*, 1095-1107.

Yeung, F., Hoberg, J.E., Ramsey, C.S., Keller, M.D., Jones, D.R., Frye, R.A., and Mayo, M.W. (2004). Modulation of NF-kappaB-dependent transcription and cell survival by the SIRT1 deacetylase. EMBO J *23*, 2369-2380.

Yoshino, J., Mills, K.F., Yoon, M.J., and Imai, S. (2011). Nicotinamide mononucleotide, a key NAD(+) intermediate, treats the pathophysiology of diet- and age-induced diabetes in mice. Cell Metab *14*, 528-536.

Yoshizawa, T., Karim, M.F., Sato, Y., Senokuchi, T., Miyata, K., Fukuda, T., Go, C., Tasaki, M., Uchimura, K., Kadomatsu, T.*, et al.* (2014). SIRT7 Controls Hepatic Lipid Metabolism by Regulating the Ubiquitin-Proteasome Pathway. Cell Metab *19*, 712-721.

Yu, J., Sadhukhan, S., Noriega, L.G., Moullan, N., He, B., Weiss, R.S., Lin, H., Schoonjans, K., and Auwerx, J. (2013). Metabolic characterization of a Sirt5 deficient mouse model. Sci Rep *3*, 2806.

Yuan, H., Su, L., and Chen, W.Y. (2013). The emerging and diverse roles of sirtuins in cancer: a clinical perspective. OncoTargets and therapy *6*, 1399-1416.

Yuan, J., Minter-Dykhouse, K., and Lou, Z. (2009). A c-Myc-SIRT1 feedback loop regulates cell growth and transformation. J Cell Biol *185*, 203-211.

Zhang, G., Li, J., Purkayastha, S., Tang, Y., Zhang, H., Yin, Y., Li, B., Liu, G., and Cai, D. (2013). Hypothalamic programming of systemic ageing involving IKK-beta, NF-kappaB and GnRH. Nature *497*, 211-216.

Zhu, Q., Pao, G.M., Huynh, A.M., Suh, H., Tonnu, N., Nederlof, P.M., Gage, F.H., and Verma, I.M. (2011a). BRCA1 tumour suppression occurs via heterochromatin-mediated silencing. Nature *477*, 179-184.

Zhu, Q., Pao, G.M., Huynh, A.M., Suh, H., Tonnu, N., Nederlof, P.M., Gage, F.H., and Verma, I.M. (2011b). BRCA1 tumour suppression occurs via heterochromatin-mediated silencing. Nature *477*, 179-184.

Zwaans, B.M., and Lombard, D.B. (2014). Interplay between sirtuins, MYC and hypoxia-inducible factor in cancer-associated metabolic reprogramming. Dis Model Mech *7*, 1023-1032.